이학박사 학위논문

Molecular mechanism of the vernalization-induced expression of *COOLAIR*, an Arabidopsis long noncoding RNA

애기장대 긴 비암호화 RNA *COOLAIR*의 춘화처리에 의한 발현 유도 기전 연구

2023년 2월

서울대학교 대학원

생명과학부

전 명 준

애기장대 긴 비암호화 RNA *COOLAIR*의 춘화처리에 의한 발현 유도 기전 연구

Molecular mechanism of the vernalization-induced expression of *COOLAIR*, an Arabidopsis long noncoding RNA

지도교수 이 일 하

이 논문을 이학박사 학위논문으로 제출함

2023년 1월

서울대학교 대학원

생명과학부

전 명 준

전명준의 이학박사 학위논문을 인준함

2023년 1월

위 원 장 최 연 희 (인)

부위원장 이 일 하 (인)

위 원 노 유 선 (인)

위 원 이 호 림 (인)

위 원 현 유 봉 (인)

Molecular mechanism of the vernalization-induced expression of *COOLAIR*, an Arabidopsis long noncoding RNA

A dissertation submitted in partial fulfillment of the requirement for the degree of

DOCTOR OF PHILOSOPHY

TO THE FACULTY of
THE SCHOOL of BIOLOGICAL SCIENCES
at
SEOUL NATIONAL UNIVERSITY
by

Myeongjune Jeon

Date approved
4th Jan. 2023

Chair	Yeonhee Choi	(Seal)
Vice Chair	Ilha Lee	(Seal)
Examiner	Yoo-Sun Noh	(Seal)
Examiner	Horim Lee	(Seal)
Examiner	Youbong Hyun	(Seal)

Abstract

Molecular mechanism of the vernalization-induced expression of *COOLAIR*, an Arabidopsis long noncoding RNA

Myeongjune Jeon
School of Biological Sciences
The Graduate School
Seoul National University

To synchronize flowering time with spring, many plants undergo vernalization, a floral-promotion process triggered by exposure to long-term winter cold. In *Arabidopsis thaliana*, this is achieved through cold-mediated epigenetic silencing of the floral repressor, *FLOWERING LOCUS C* (*FLC*). *COOLAIR*, a cold-induced antisense RNA transcribed from the *FLC* locus, has been proposed to facilitate *FLC* silencing. However, how cold induces *COOLAIR* expression has yet to be understood.

Here, I show that C-repeat (CRT)/dehydration-responsive elements (DREs) at the 3′-end of *FLC* and CRT/DRE-BINDING FACTORs (CBFs) are required for cold-mediated expression of *COOLAIR*. CBFs bound to CRT/DREs at the 3′-end of *FLC*, both *in vitro* and *in vivo*, and CBF levels increased gradually during vernalization. Cold-induced *COOLAIR* expression was severely impaired in *cbfs* mutants in which all *CBF* genes were knocked-out. Conversely, *CBF*-overexpressing plants showed increased *COOLAIR* levels even at warm temperatures. I show that *COOLAIR* is induced by CBFs during early stages of vernalization but *COOLAIR*

levels decrease in later phases as *FLC* chromatin transitions to an inactive state to which CBFs can no longer bind. I also demonstrate that *cbfs* and $FLC_{\Delta COOLAIR}$ mutants exhibit a normal vernalization response despite their inability to activate *COOLAIR* expression during cold, revealing that *COOLAIR* is not required for this process.

Keywords: *Arabidopsis thaliana*, Flowering, Vernalization, *COOLAIR*, *CBF*, *FLC*

Student Number: 2015-20445

Contents

Abstract i

Contents iii

List of Figures v

List of Tables ix

Abbreviations x

Chapter 1. Introduction 1

1.1. Winter-annual flowering habit of plants 2

1.2. Cold acclimation 5

1.3. Vernalization 8

1.4. Cold-induced lncRNAs in Arabidopsis 11

1.5. Aims of the thesis 15

Chapter 2. Materials and Methods 17

2.1. Plant materials and treatments 18

2.2. Generation of *FLC*$_{\Delta COOLAIR}$ lines by CRISPR-Cas9 19

2.3. Plasmid construction 19

2.4. EMSA 21

2.5. ChIP assay 23

2.6. Gene expression analysis 26

2.7. Immunoblotting 29

2.8. RNA-seq data analysis 29

2.9. Luciferase assay using Arabidopsis protoplast 30

2.10. Statistical analysis 30

Chapter 3. Results.....31

3.1. A CRT/DRE-binding factor, CBF3, directly binds to CRT/DREs at the 3′-end of the *FLC* 32

3.2. *COOLAIR* is one of the CBF regulons in Arabidopsis.....40

3.3. CBFs accumulate during vernalization 46

3.4. *CBFs* are involved in vernalization-induced *COOLAIR* expression..54

3.5. CRT/DREs at the 3′-end of *FLC* are necessary for CBFs-mediated induction of *COOLAIR* during vernalization 63

3.6. CBFs-mediated *COOLAIR* induction during vernalization is not required for *FLC* silencing 73

Chapter 4. Discussion 83

4.1. Molecular mechanisms behind the CBFs-mediated regulation of *COOLAIR* expression.....84

4.2. Relationship among *COOLAIR*-activating thermosensors.....85

4.3. Function of *COOLAIR* in vernalization 86

Chapter 5. Conclusion.....89

References.....91

Appendix 103

Abstract in Korean 국문초록 123

List of Figures

Figure 1. Winter-annual and rapid-cycling lifestyles of plants.....4

Figure 2. Signaling pathway of cold acclimation 7

Figure 3. Epigenetic silencing of *FLC* during vernalization 10

Figure 4. Characteristics of lncRNAs transcribed from the *FLC* locus.....13

Figure 5. Proposed model for the roles of *FLC*-derived lncRNAs in *FLC* silencing.....14

Figure 6. Comparison of sequences around the 3′-end of the *FLC* orthologs from Arabidopsis relatives.....34

Figure 7. DAP-seq results showing the binding of CBF proteins to the 3′-end region of *FLC* 35

Figure 8. Schematic showing the positions of six CRT/DRE-like sequences distributed on the *FLC* locus.....36

Figure 9. *In vitro* binding of CBF3 protein to the CRT/DREs at the *FLC*'s 3′-end.....37

Figure 10. Comparison of CBF3-binding affinity between the CRT/DREs at the 3′-end and first exon of *FLC*.....38

Figure 11. *In vivo* enrichment of CBF3 protein at the *FLC* locus during vernalization 39

Figure 12. Increased *COOLAIR* expression levels in *CBF3*-overexpressing plant 42

Figure 13. Different effects of *CBF1*-, *2*-, and *3*-overexpressions on *COOLAIR* variants.....43

Figure 14. Expression dynamics of total *COOLAIR* after short-term cold

treatment 44
Figure 15. Transcript levels of total *COOLAIR* and *COOLAIR* isoforms in the wild type and *cbfs* mutant before and after a day of cold treatment .45
Figure 16. Transcript levels of *CBF1*, *2*, and *3* under short-term cold exposure 48
Figure 17. Transcript levels of *CBF1*, *2*, and *3* during vernalization 49
Figure 18. Daily rhythms of *CBF1*, *2*, and *3* transcript levels in non-vernalized or vernalized plants 50
Figure 19. Daily rhythms of CBF3 protein levels in non-vernalized or vernalized plants 51
Figure 20. Dynamics of CBF3 protein abundance under short-term cold exposure 52
Figure 21. Increase in CBF3 protein level during the vernalization process 53
Figure 22. Expression dynamics of total *COOLAIR* in wild-type, *cbfs*, and $FLC_{\Delta COOLAIR\text{-}1}$ plants during vernalization 56
Figure 23. Expression dynamics of CBF regulons in wild-type, *cbfs*, and $FLC_{\Delta COOLAIR\text{-}1}$ plants during vernalization 57
Figure 24. Expression dynamics of total, proximal, and distal *COOLAIR* in the wild type and *cbfs* mutant upon short-term cold exposure, as determined by RNA-seq 58
Figure 25. Expression dynamics of total, proximal, and distal *COOLAIR* in the wild type and *cbfs* mutant during vernalization, as determined by RNA-seq 59
Figure 26. Expression dynamics of total *COOLAIR* in wild-type and *CBF3*-

overexpressing plants during vernalization 60

Figure 27. Effect of the first frost-mimicking treatment on the level of total *COOLAIR* in non-vernalized or vernalized wild type and *cbfs* 61

Figure 28. Effect of the first frost-mimicking treatment on the levels of *CBFs* 62

Figure 29. Arabidopsis protoplast transfection assay showing that CBF3 activates *COOLAIR* promoter through CRT/DREs 65

Figure 30. Transcript levels of total *COOLAIR* and *COOLAIR* variants in $FLC_{\Delta COOLAIR}$ lines.....66

Figure 31. Genomic sequences near the deleted regions in two *COOLAIR* promoter deletion lines, $FLC_{\Delta COOLAIR\text{-}3}$ and $FLC_{\Delta COOLAIR\text{-}4}$.....68

Figure 32. Transcript levels of *CAS* and unspliced *FLC* in $FLC_{\Delta COOLAIR}$ lines 70

Figure 33. Transcript levels of proximal *COOLAIR* isoform in wild-type, *cbfs*, and $FLC_{\Delta COOLAIR\text{-}1}$ plants during vernalization 71

Figure 34. Effect of *CBF3*-overexpression on proximal *COOLAIR* expression in wild-type or $FLC_{\Delta COOLAIR}$ background.....72

Figure 35. Histone modifications at the *FLC* chromatin in non-vernalized or vernalized wild type and *cbfs* mutant 75

Figure 36. Expression dynamics of *FLC* mRNA in the wild type, *cbfs*, and $FLC_{\Delta COOLAIR}$ lines during vernalization 77

Figure 37. Effect of the first frost-mimicking treatment on the *FLC* mRNA level in the wild type and *cbfs* after vernalization 78

Figure 38. Flowering times of non-vernalized or vernalized wild-type, *cbfs*, and $FLC_{\Delta COOLAIR\text{-}1}$ plants.....79

Figure 39. Flowering times of non-vernalized or vernalized wild type and *FLC*$_{\Delta COOLAIR}$ lines.....80

Figure 40. Schematic model describing the regulatory mechanism *COOLAIR* mediated by CBFs during vernalization 81

List of Tables

Table 1. Primers used for plasmid construction.....20

Table 2. Probes and competitors used for EMSA.....22

Table 3. Primers used for ChIP assay.....24

Table 4. Primers used for gene expression analysis.....27

Abbreviations

General abbreviations

3′	Three-prime end of nucleic acid molecule
35S	The cauliflower mosaic virus 35S promoter
5′	Five-prime end of nucleic acid molecule
Aa	*Arabis alpina*
Al	*Arabidopsis lyrata*
ANOVA	Analysis of variance
At	*Arabidopsis thaliana*
CAS	Convergent antisense transcript
cDNA	Complementary DNA
ChIP	Chromatin immunoprecipitation
ChIP-seq	ChIP sequencing
Col	Columbia
COR gene	Cold-regulated gene
Cr	*Capsella rubella*
CRISPR	Clustered regularly interspaced short palindromic repeats
CRT/DRE	C-repeat/dehydration-responsive element
Cy5	Cyanine 5
DAP-seq	DNA affinity purification sequencing
DTT	Dithiothreitol
EDTA	Ethylenediaminetetraacetic acid
EGTA	Egtazic acid
EMSA	Electrophoretic mobility shift assay

FP	Free probe
FPLC	Fast protein liquid chromatography
gDNA	Genomic DNA
H3K27me3	Trimethylation of lysine 27 on histone H3
H3K36me3	Trimethylation of lysine 36 on histone H3
H3K4me3	Trimethylation of lysine 4 on histone H3
H3K9me2	Dimethylation of lysine 9 on histone H3
IPTG	Isopropyl β-D-1-thiogalactopyranoside
LD	Long day
lncRNA	Long noncoding RNA
MES	2-Morpholinoethanesulfonic acid
mRNA	Messenger RNA
MS	Murashige and Skoog
NV	Non-vernalized
PCR	Polymerase chain reaction
PEG	Polyethylene glycol
PHD	Plant homeodomain
PIPES	1,4-Piperazinediethanesulfonic acid
PMSF	Phenylmethylsulfonyl fluoride
PRC2	Polycomb repressive complex 2
PVDF	Polyvinylidene difluoride
qPCR	Quantitative PCR
RNA-seq	RNA sequencing
RT-qPCR	Quantitative reverse transcription PCR
SD	Short day

SD	Standard deviation
SDS	Sodium dodecyl sulfate
SEM	Standard error of the mean
Sf	San Feliu
sgRNA	Single-guide RNA
SW	Sweden
T_2	The second transgenic generation
T_3	The third transgenic generation
T-DNA	Transfer DNA
Th	*Thellungiella halophila*
TPM	Transcript per million
TSS	Transcription start site
UTR	Untranslated region
Ws	Wassilewskija
ZT	Zeitgeber time

Abbreviations for nucleobases and amino acids

Nucleobases

A	Adenine
C	Cytosine
G	Guanine
T	Thymine

Amino acids

Lys	**K**	Lysine

Abbreviations for gene and protein names

AP2	APETALA 2
BTF3	BASIC TRANSCRIPTION FACTOR 3
BZR1	BRASSINAZOLE-RESISTANT 1
CAMTA	CALMODULIN-BINDING TRANSCRIPTION ACTIVATOR
Cas9	CRISPR-associated protein 9
CBF1–3	CRT/DRE-BINDING FACTOR 1–3
CCA1	CIRCADIAN CLOCK-ASSOCIATED 1
CES	CESTA
CLF	CURLY LEAF
COR15A	COLD-REGULATED 15A
FLC	FLOWERING LOCUS C
FRI	FRIGIDA
FT	FLOWERING LOCUS T
HD2C	HISTONE DEACETYLASE 2C
HRP	Horseradish peroxidase
IgG	Immunoglobulin G
LHP1	LIKE HETEROCHROMATIN PROTEIN 1
LHY	LATE-ELONGATED HYPOCOTYL
LUC	Luciferase
MBP	Maltose-binding protein
NTL8	NAC WITH TRANSMEMBRANE MOTIF 1-LIKE 8
PP2A	SERINE/THREONINE PROTEIN PHOSPHATASE 2A
RD29A	RESPONSIVE TO DESICCATION 29A
SOC1	SUPPRESSOR OF OVEREXPRESSION OF CO 1

TUB2 TUBULIN BETA CHAIN 2

UBC UBIQUITIN-CONJUGATING ENZYME 21

VAL1–2 VP1/ABI3-LIKE 1–2

VIN3 VERNALIZATION INSENSITIVE 3

Chapter 1

Introduction

1.1. Winter-annual flowering habit of plants

Plants pass through several developmental phases in their lifetime: embryonic, vegetative, and reproductive stages and senescence. They carry out different body plans by switching these phases to optimize their survival and reproduction.

Flowering is one way of transition from vegetative to reproductive growth, adopted by the dominant land plant group, angiosperms. During the floral transition, flowering plants' shoot apical meristem develops an inflorescence architecture required for sexual reproduction rather than producing more vegetative organs. The timely initiation of this process guarantees reproductive success. Hence, plants strictly determine when to flower by integrating various cues from the internal and external environments (Lang, 1952; Wada and Takeno, 2010; Srikanth and Schmid, 2011).

Of diverse determinants of flowering time, seasonal cues are the primary one, as plants cannot behaviorally decide their exposure to unfavorable conditions due to their sessile nature. Especially for plants adapted to temperate climates, successful reproduction heavily depends on the temperature continuously changing during the seasons. Cold temperatures during winter particularly have adverse effects on plant reproduction, such as reducing the activity of pollinators and disturbing the survival or growth of parental plants and their offspring. To overcome this, many temperate plant lineages, including some accessions of the model plant *Arabidopsis thaliana*, have evolved to germinate in fall and flower in spring after getting through the winter (**Figure 1**; Napp-Zinn, 1955; Chouard, 1960; Weinig and Schmitt, 2004).

Two adaptive responses of plants to low temperatures, cold acclimation and vernalization, ensure such a "winter-annual" habit (Napp-Zinn, 1955; Chouard, 1960; Weiser, 1970; Gilmour et al., 1988; Sung and Amasino, 2004a). Plants exquisitely monitor the surrounding temperature during winter and elicit these responses

through which they tolerate thermal stress and control the timing of flowering properly (Went, 1953; Penfield, 2008; Ding and Yang, 2022).

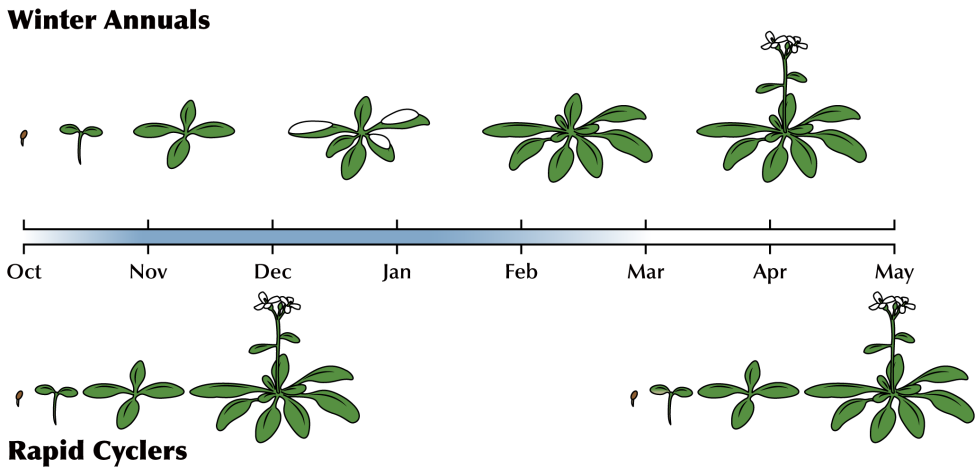

Figure 1. Winter-annual and rapid-cycling lifestyles of plants.

Adapted from Figure 2 in Weinig and Schmitt, 2004.

1.2. Cold acclimation

Cold acclimation is generally initiated by a short period of non-freezing cold exposure and increases the frost tolerance of plants (Weiser, 1970; Gilmour et al., 1988; Guy, 1990; Thomashow, 1999; Chinnusamy et al., 2007). The three C-REPEAT (CRT)/DEHYDRATION-RESPONSIVE ELEMENT (DRE) BINDING FACTORs (CBFs) and their encoding genes serve as signaling hubs for cold acclimation in *A. thaliana* (**Figure 2**; Stockinger et al., 1997; Medina et al., 1999; Thomashow, 2010; Ding et al., 2019). When exposed to low temperatures, the transcription of *CBFs* is rapidly promoted by a group of cold-signal transducers, including the Ca^{2+}/calmodulin-binding proteins, CALMODULIN-BINDING TRANSCRIPTION ACTIVATORs (CAMTAs) (Doherty et al., 2009; Kim et al., 2013; Kidokoro et al., 2017); the clock proteins, CIRCADIAN CLOCK-ASSOCIATED 1 (CCA1) and LATE-ELONGATED HYPOCOTYL (LHY) (Dong et al., 2011); and the brassinosteroid-responsive proteins, BRASSINAZOLE-RESISTANT 1 (BZR1) and CESTA (CES) (Eremina et al., 2016; Li et al., 2017). In addition, cold also enhances the stability or activity of CBF proteins. For example, cold facilitates the interaction between CBFs and BASIC TRANSCRIPTION FACTOR 3s (BTF3s), which promotes CBF stability (Ding et al., 2018), and it triggers the degradation of co-repressor, HISTONE DEACETYLASE 2C (HD2C), thereby allowing CBFs to activate their targets (Park et al., 2018a). Furthermore, cold reduces oxidized CBFs, which increases active CBF monomers (Lee et al., 2021).

Low temperature-induced CBFs, in turn, activate the expression of *co*ld-*r*egulated (*COR*) genes by binding to CRT/DREs in their promoters (Stockinger et al., 1997; Medina et al., 1999). Diverse arrays of cryoprotective proteins encoded by *COR* genes allow plants to overcome freezing stress (Gilmour et al., 1988; Hajela et

al., 1990; Thomashow et al., 1997; Shinozaki et al., 2003; Shi et al., 2018; Ding et al., 2019).

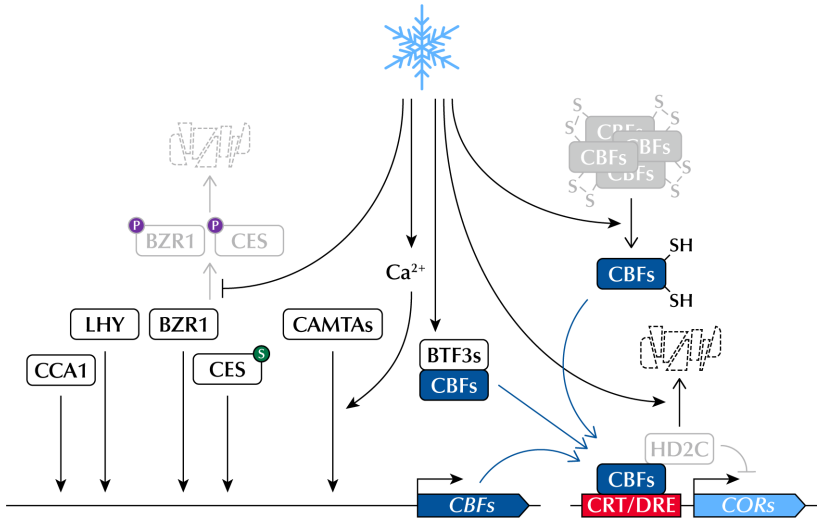

Figure 2. Signaling pathway of cold acclimation.

1.3. Vernalization

In contrast to cold acclimation, vernalization, a floral-promotion process that occurs during winter, requires an extended cold period (Napp-Zinn, 1955; Chouard, 1960; Michaels and Amasino, 2000). This allows plants to synchronize the timing of flowering with favorable spring conditions.

Vernalization in *A. thaliana* is mainly achieved by silencing the floral repressor gene, *FLOWERING LOCUS C* (*FLC*) (Michaels and Amasino, 1999; Sheldon et al., 1999; Sheldon et al., 2000; Michaels and Amasino, 2001). *FLC* encodes an MADS-box protein that represses the expression of floral activator genes, *SUPPRESSOR OF OVEREXPRESSION OF CO 1* (*SOC1*) and *FLOWERING LOCUS T* (*FT*), by directly binding to their promoter regions (Lee et al., 2000; Michaels et al., 2005; Helliwell et al., 2006). In Arabidopsis winter annuals, such as San Feliu-2 (Sf-2), Löv-1, and Sweden (SW) ecotypes, flowering is prevented by the high expression of *FLC* before exposure to winter cold (Lee et al., 1993; Shindo et al., 2005; Park et al., 2018b). This is caused by the strong transcriptional activation of *FLC* by the FRIGIDA (FRI) supercomplex, which recruits general transcription factors and several chromatin modifiers (Michaels and Amasino, 1999; Sheldon et al., 1999; Johanson et al., 2000; Choi et al., 2011; Li et al., 2018).

Prior to vernalization, *FLC* chromatin is highly enriched with active histone marks such as histone H3 acetylation and trimethylation of Lys4 or Lys36 at H3 (H3K4me3/H3K36me3) (**Figure 3**; Bastow et al., 2004; Yang et al., 2014). In contrast, prolonged cold exposure results in gradual deacetylation of *FLC* chromatin and concomitant removal of H3K4me3 and H3K36me3 from the *FLC* (Bastow et al., 2004; Yang et al., 2014; Nishio et al., 2016). Additionally, VP1/ABI3-LIKE 1 (VAL1) and VAL2 recruit Polycomb repressive complex 2 (PRC2) onto the *FLC* chromatin, thereby accumulating the repressive histone mark, H3 Lys27 trimethylation

(H3K27me3), in the nucleation region around the first exon and intron of *FLC* (Sung and Amasino, 2004b; Wood et al., 2006; De Lucia et al., 2008; Angel et al., 2011; Nishio et al., 2016; Qüesta et al., 2016; Yuan et al., 2016). Subsequently, upon returning to warm temperatures, H3K27me3 marks are spread over the entire *FLC* chromatin region by LIKE HETEROCHROMATIN PROTEIN 1 (LHP1), which ensures stable *FLC* suppression and renders plants competent to flower (Mylne et al., 2006; Sung et al., 2006; Yang et al., 2017).

Several long-term cold-induced factors have been shown to play crucial roles in the vernalization-triggered epigenetic silencing of *FLC*. *VERNALIZATION INSENSITIVE 3* (*VIN3*) family genes, which are upregulated by prolonged cold, encode plant homeodomain (PHD) proteins that recognize H3K9me2 enriched in *FLC* chromatin during vernalization (Sung and Amasino, 2004b; Kim and Sung, 2013, 2017a). These proteins mediate the recruitment of PRC2 and the subsequent deposition of H3K27me3 at the *FLC* nucleation region (Sung and Amasino, 2004b; De Lucia et al., 2008; Kim and Sung, 2013). In addition to *VIN3*, a group of long noncoding RNAs (lncRNAs) expressed from the *FLC* locus contribute to controlling the *FLC* chromatin environment.

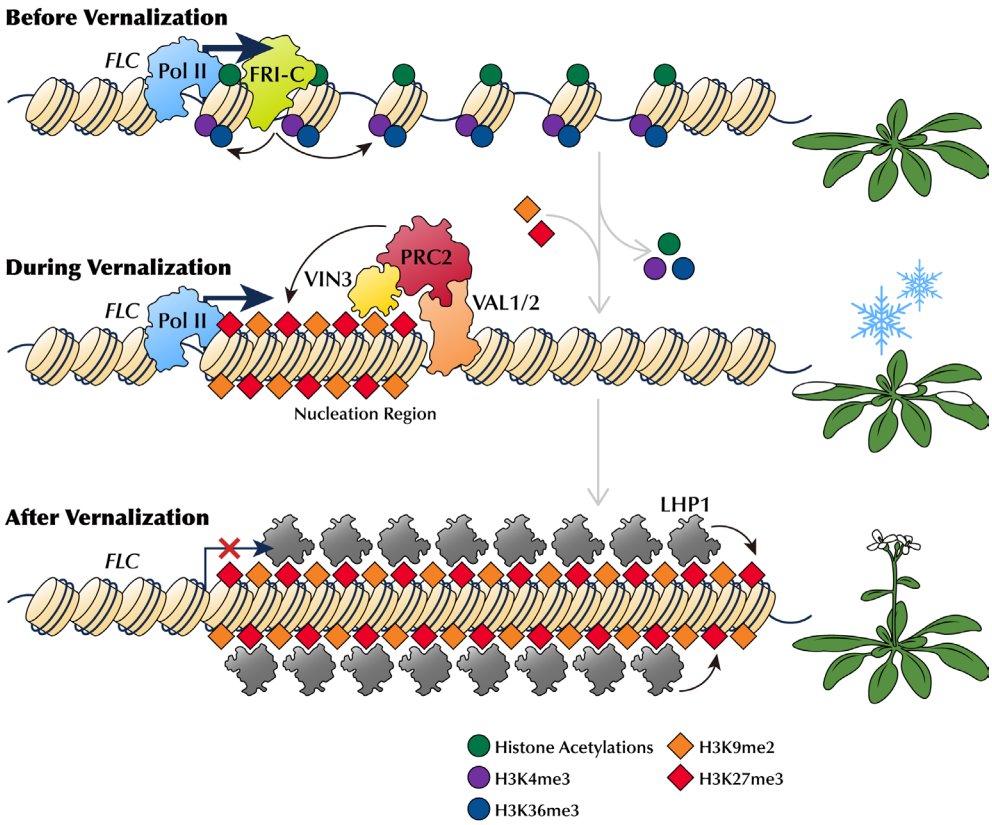

Figure 3. Epigenetic silencing of *FLC* during vernalization.

1.4. Cold-induced lncRNAs in Arabidopsis

COLDAIR and *COLDWRAP*, the two lncRNAs transcribed from the first intron and promoter region of *FLC*, respectively (**Figure 4A**), are required for H3K27me3 deposition in response to long-term cold (Heo and Sung, 2011; Kim and Sung, 2017b). They directly associate with the PRC2 component, CURLY LEAF (CLF), thereby recruiting PRC2 to the *FLC* locus (**Figure 5**). *COLDAIR* and *COLDWRAP* are also thought to affect the formation of the intragenic chromatin loop at the *FLC*, which may be a part of the *FLC* silencing mechanism (Kim and Sung, 2017b).

Unlike *COLDAIR* and *COLDWRAP*, which are transcribed in the sense direction of *FLC*, another lncRNA, *COOLAIR*, is an antisense transcript expressed from the 3′-end of *FLC* (**Figure 4A**; Swiezewski et al., 2009). The gradual accumulation of *COOLAIR* reaches a maximum within a few weeks of cold exposure, whereas *COLDAIR* and *COLDWRAP* show peaks at a later phase of vernalization (**Figure 4B**; Csorba et al., 2014; Kim and Sung, 2017b).

COOLAIR was reported to remove active histone marks from *FLC* chromatin (Liu et al., 2007; Csorba et al., 2014; Fang et al., 2020; Xu et al., 2021a; Zhu et al., 2021). Particularly, in summer annuals, phase-separated RNA-processing complexes favor co-transcriptional proximal polyadenylation of *COOLAIR* (Marquardt et al., 2014; Wang et al., 2014; Fang et al., 2019; Wu et al., 2020; Xu et al., 2021a). The *COOLAIR*-processing machinery exhibits transient and dynamic interactions with an H3K4 demethylation complex, leading to *FLC* suppression at warm temperatures (**Appendix**; Liu et al., 2007; Fang et al., 2020; Xu et al., 2021a; Kyung et al., 2022b). *COOLAIR* is also likely to be involved in reducing H3K36me3 at the *FLC* during the vernalization process (**Figure 5**; Csorba et al., 2014). *COOLAIR* was reported to promote the sequestration of the FRI complex from the *FLC* promoter by condensing it into phase-separated nuclear bodies (Zhu et al., 2021). This has been suggested to

cause the inactivation of *FLC,* which is probably accompanied by the silencing of *FLC* chromatin through the removal of H3K36me3. However, a previous study has raised the issue that *COOLAIR* appears not to be necessary for vernalization (Helliwell et al., 2011; Luo et al., 2019).

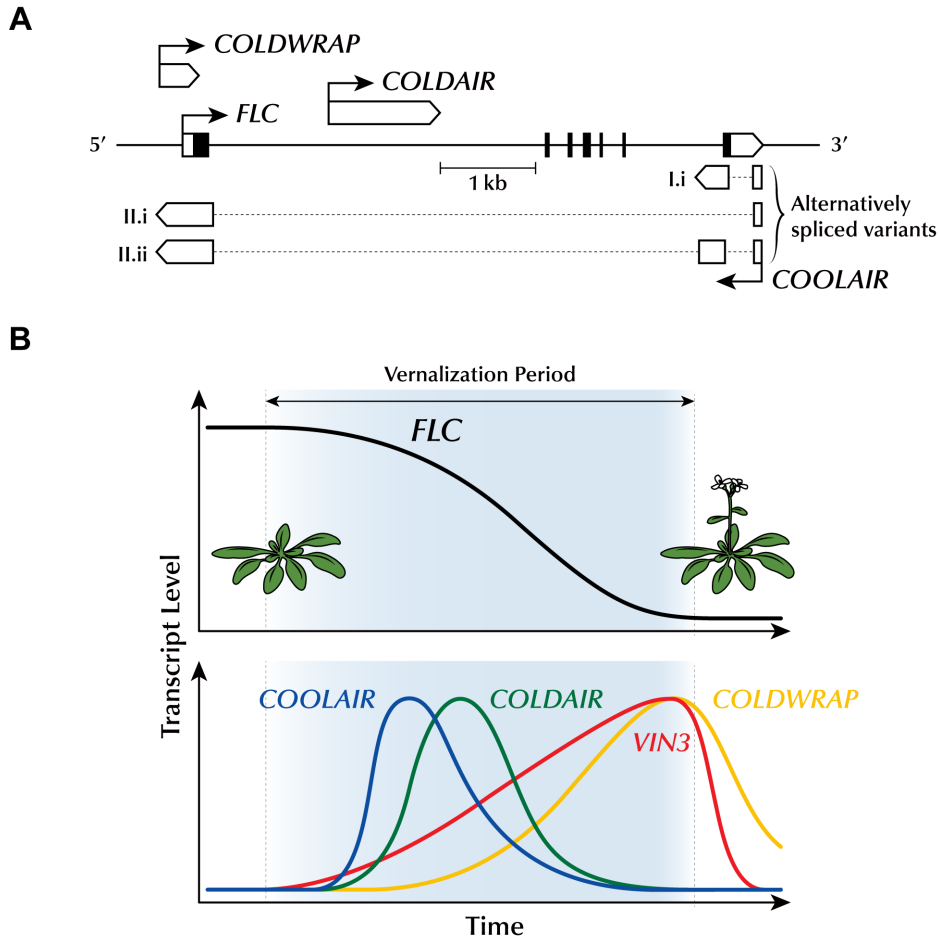

Figure 4. Characteristics of lncRNAs transcribed from the *FLC* locus.

(A) Gene structures of *A. thaliana FLC* and lncRNAs transcribed from the *FLC* locus: *COOLAIR*, *COLDAIR*, and *COLDWRAP*. For *FLC*, the black and white bars indicate protein-coding exons and untranslated regions (UTRs), respectively. For lncRNAs, the white bars indicate exons. The thin black arrows indicate the transcription start sites (TSSs).

(B) Expression patterns of *FLC*, *VIN3* and *FLC*-derived lncRNAs during the vernalization period.

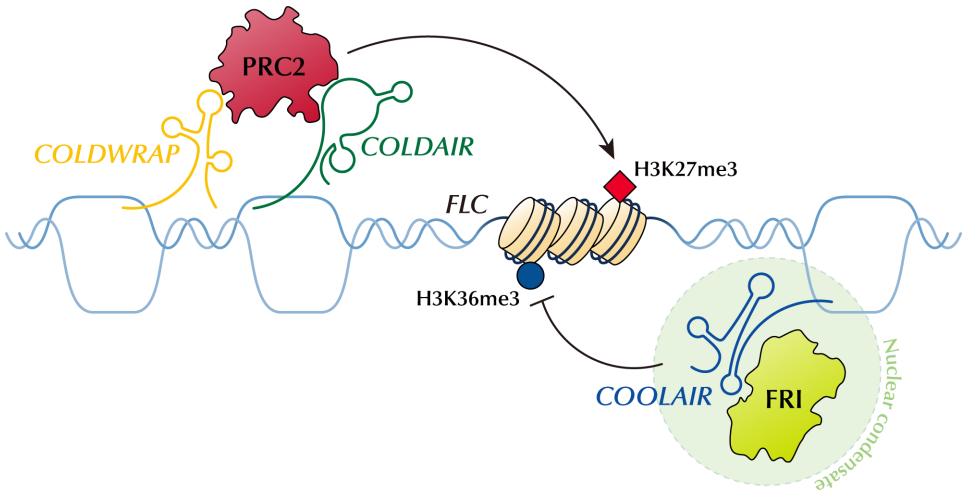

Figure 5. Proposed model for the roles of *FLC*-derived lncRNAs in *FLC* silencing.

1.5. Aims of the thesis

Compared with the signaling pathway of cold acclimation, how a long-term cold signal is transduced to trigger the induction of *VIN3* and lncRNAs needs to be better understood. It is marginally known that some chromatin modifiers, NAC WITH TRANSMEMBRANE MOTIF 1-LIKE 8 (NTL8), and CCA1/LHY act as positive regulators of *VIN3* during the vernalization process (Kim et al., 2010; Finnegan et al., 2011; Zhao et al., 2020; Kyung et al., 2022a). However, little is known about the upstream regulators of *COOLAIR* required for cold-induction.

Recent reports have shown that an NAC domain-containing protein, NTL8, and the WRKY transcription factor, WRKY63, can bind to the promoter of *COOLAIR* and activate its expression (Zhao et al., 2021; Hung et al., 2022). Despite the lack of these factors, however, *COOLAIR* is still induced to a certain extent upon long-term cold treatment. Therefore, there is no doubt there will be other unknown factors that trigger the *COOLAIR* expression during the vernalization period.

This study aims to reveal novel cold-signal transducers primarily governing the cold-induced expression of *COOLAIR*. To this end, I isolate the cis-element in the *COOLAIR* promoter required for its vernalization response and identify the transcription factors binding to this element. The molecular mechanism of how these cold-signal transducers activate *COOLAIR* expression is also described.

Chapter 2

Materials and Methods

FLC$_{\Delta COOLAIR}$ lines were generated by Yupeng Yang at Chinese Academy of Sciences and Xiao Luo at Peking University. RNA-seq data analysis was carried out by Daesong Jeong at Seoul National University.

2.1. Plant materials and treatments

A. thaliana Columbia-0 (Col-0), Wassilewskija-2 (Ws-2), and Col *FRI*^{Sf2} (*FRI* Col) were used as the wild types in this study. “Wild type” in this thesis mainly refers to *FRI* Col unless otherwise specified. *FRI* Col (Lee et al., 1994), *cbfs-1*, *pCBF3:CBF3-myc* (Jia et al., 2016), *pSuper:CBF3-myc* (Liu et al., 2017), *FLC*$_{\Delta COOLAIR\text{-}1}$ (Luo et al., 2019), *35S:CBF1*, *35S:CBF2*, and *35S:CBF3* (Gilmour et al., 2004) have been previously described. *FRI cbfs-1* was generated by crossing the *FRI* Col with *cbfs-1* stated above. *FRI FLC*$_{\Delta COOLAIR\text{-}1}$ was generated by crossing *FRI* Col with *FLC*$_{\Delta COOLAIR\text{-}1}$ in the Col-0 background. *pSuper:CBF3-myc FLC*$_{\Delta COOLAIR\text{-}1}$ was generated by crossing *pSuper:CBF3-myc* with *FLC*$_{\Delta COOLAIR\text{-}1}$.

For all experiments using plant materials, seeds were sown on half-strength Murashige and Skoog (MS) medium (Duchefa, Haarlem, Netherlands) containing 1% sucrose and 1% plant agar (Duchefa) and stratified at 4°C for 3 days. Plants were germinated and grown at 22°C under a short-day (SD) photoperiod (8-h light/16-h dark) with cool white fluorescent lights (100 μmol·m^{-2}·s^{-1}).

For the vernalization treatment, the plants were grown at 22°C for the prescribed period and then transferred to a 4°C growth chamber under an SD cycle. To adjust the developmental stage, the plants vernalized for 40 days (40V), 30 days (30V), 20 days (20V), 10 days (10V), 4 days (4V), and 1 day (1V) were transferred to 4°C after being grown at 22°C for 10, 12, 14, 15, 15, and 16 days, respectively. Non-vernalized (NV) plants were grown at 22°C for 16 days. For 0.5, 1, 1.5, 2, 3, 6, and 24 h of cold treatment, the plants were grown at 22°C for 16 days before the 4°C treatment. For the freezing treatment, NV, 10V, and 20V plants were transferred to −1°C under dark condition for 8 h (F). To measure flowering time of vernalized plants, plants were transferred to 22°C under a long-day (LD) cycle (16-h light/8-h dark) directly after the vernalization treatment.

2.2. Generation of *FLC*$_{\Delta COOLAIR}$ lines by CRISPR-Cas9

The construction of *FLC*$_{\Delta COOLAIR\text{-}3}$ and *FLC*$_{\Delta COOLAIR\text{-}4}$ were as previously described (Luo et al., 2019). Briefly, two pairs of sgRNAs were designed for the deletion of *COOLAIR* promoter regions (5′-CTTCACAGTGAAGAAGCCTA-3′ and 5′-AAATGCACTCTTACGTAACG-3′ for *FLC*$_{\Delta COOLAIR\text{-}3}$; 5′-TTATCCTAAACGCGTATGGT-3′ and 5′-CGTAGTTCCGTCATCCATGA-3′ for *FLC*$_{\Delta COOLAIR\text{-}4}$), and sgRNA-Cas9 cassettes were introduced into Arabidopsis by floral dipping. Homozygous deletion mutants were screened in T_2 generation, and sgRNA-Cas9 free mutants were further isolated in T_3 generation.

2.3. Plasmid construction

To generate the *35S:CBF3-HA* construct, the entire coding sequence of CBF3 was amplified using polymerase chain reaction (PCR) and cloned into the *HBT-HA-NOS* plasmid (Yoo et al., 2007). For *pCOOLAIR*$_{DRE}$*:LUC* and *pCOOLAIR*$_{DRE}^{m}$*:LUC* construction, the 1-kb sequence containing the *COOLAIR* promoter, the 3′-UTR, and the last exon of *FLC* was amplified by PCR and cloned into the *LUC-NOS* plasmid (Hwang and Sheen, 2001). To generate *pCOOLAIR*$_{DRE}^{m}$*:LUC*, two CRT/DREs in the *COOLAIR* promoter, 5′-AGGTCGGT-3′ and 5′-ACCGACAT-3′, were replaced with 5′-CGAGGTGT-3′ and 5′-TGAACCCA-3′, respectively. For *pFLC:LUC* construction, the 1-kb sequence containing the promoter, 5′-UTR, and the first exon of *FLC* was amplified by PCR and was cloned into the *LUC-NOS* plasmid. Primers used for plasmid construction are listed in **Table 1**.

Table 1. Primers used for plasmid construction.

Construct	Primer	Sequence* (5′→3′)
35S:CBF3-HA	F	CGCCTGCAGATAAAATTAGATAAAGAAGAAATTGG
	R	CGCCCATGGCATCGCCGGAGGAGAA
pCOOLAIR:LUC	F	CGCCTGCAGAGTAACTAGAATGTGAAATAGAG
	R	CGCCCATGGGGAGAATAATCATCATGTGG
	DRE^{m}	CGCACGCGTGCGCGGTGTGGGGGGGTCGGGGGGCCTGGGTTCACACATTCGGCCC
pFLC:LUC	F	CGGGATCCATGAACTCATTTTCTGCTTTTTC
	R	CGCAGGCCTATAACTCCATAACGATACGTC

* Underlining indicates a restriction enzyme recognition site.

2.4. EMSA

Maltose-binding protein (MBP) and MBP-CBF3 recombinant fusion proteins were induced by 500 μM IPTG in the *Escherichia coli* BL21 (DE3) strain. Cell extracts were isolated with a buffer containing 20 mM Tris-HCl (pH 7.4), 1 mM EDTA, 200 mM NaCl, 10% glycerol, 1 mM DTT, and 1 mM PMSF. Proteins were purified from cell extracts using MBPTrap™ HP column (GE Healthcare, Chicago, IL, USA) with ÄKTA FPLC system (Amersham Biosciences, Amersham, UK). The Cy5-labeled probes and unlabeled competitors were generated by annealing 25 bp-length oligonucleotides.

Electrophoretic mobility shift assay (EMSA) was performed as previously described with a few modifications (Seo et al., 2012). For each EMSA reaction, 5 μM of protein and 100 nM of Cy5-labeled probe were incubated at room temperature in a binding buffer containing 10 mM Tris-HCl (pH 7.5), 1 mM EDTA, 50 mM NaCl, 5% glycerol, and 5 mM DTT. For the competition assay, the reaction mixtures were incubated in the presence of 100-fold molar excess of each competitor. The reaction mixtures were electrophoresed at 100 V after incubation. The Cy5 signals were detected using WSE-6200H LuminoGraph II (ATTO, Amherst, NY, USA). Probes and competitors used for EMSA are listed in **Table 2**.

Table 2. Probes and competitors used for EMSA

Target	**P/C***	**Sequence** (5′→3′)
DRE1	P	Cy5-CCGAATGTGACCGACATAGGCCCAA
	C	CCGAATGTGACCGACATAGGCCCAA
DRE2	P	Cy5-TATGGAAGAGGTCGGTCACGTTAAC
	C	TATGGAAGAGGTCGGTCACGTTAAC
DRE1^{m}	C	CCGAATGTGTGAACCCAAGGCCCAA
DRE2^{m}	C	TATGGAAGCGAGGTGTCACGTTAAC
DREa	C	TTGAACTCTTCCGACTTCTCAAAAC
DREb	C	AATATCTGGCCCGACGAAGAAAAAG
DREc	C	ACAAAAGTAGCCGACAAGTCACCTT
DREd	C	GGACAAATCTCCGACAATCTTCCGG

* P, Cy5-labeled probe; C, unlabeled competitor.

2.5. ChIP assay

Approximately 4 g of seedlings grown on MS plates were collected and cross-linked using 1% (v/v) formaldehyde. Nuclei were isolated from seedlings using a buffer containing 20 mM PIPES-KOH (pH 7.6), 1 M hexylene glycol, 10 mM $MgCl_2$, 0.1 mM EGTA, 15 mM NaCl, 60 mM KCl, 0.5% Triton X-100, 5 mM β-mercaptoethanol, and 1× cOmplete™ EDTA-free Protease Inhibitor Cocktail (Roche, Basel, Switzerland) as described previously with a few modifications (Shu et al., 2014). Isolated nuclei were lysed with a buffer containing 50 mM Tris-HCl (pH 7.4), 150 mM NaCl, 1% (v/v) Triton X-100, and 1% SDS (w/v), and were subsequently sonicated using a Digital Sonifier® (Branson, Danbury, CT, USA). Sheared chromatin was diluted with a buffer containing 50 mM Tris-HCl (pH 7.4), 150 mM NaCl, 1% (v/v) Triton X-100, and 1 mM EDTA.

Chromatin immunoprecipitation (ChIP) was performed by incubating sheared chromatin with Protein G Sepharose™ 4 Fast Flow beads (GE Healthcare) and antibodies. Anti-myc (MBL, Woburn, MA, USA; #M192-3) and normal mouse IgG_1 (Santa Cruz Biotechnology, Santa Cruz, CA, USA; #sc-3877) were used to detect CBF3 protein enrichment at the *FLC* locus, and anti-H3K36me3 (Abcam, Cambridge, UK; #Ab9050), H3K4me3 (Millipore, Bedford, MA, USA; #07-473), and anti-H3K27me3 (Millipore; #07-449) were used to detect histone modifications on the *FLC* chromatin. DNA was extracted with phenol:chloroform:isoamyl alcohol (25:24:1, v/v) or Chelex® 100 Resin according to the manufacturer's instruction. Primers used for ChIP-quantitative PCR (qPCR) are listed in **Table 3**.

Table 3. Primers used for ChIP assay

Target	Primer	Sequence (5′→3′)
FLC −2,320–2,267	F	ATCCAGAAAAGGGCAAGGAG
	R	CGAATCGATTGGGTGAATG
FLC −1,599–1,530	F	TGGAGGGAACAACCTAATGC
	R	TCATTGGACCAAACCAAACC
FLC −392–272	F	ACTATGTAGGCACGACTTTGGTAAC
	R	TGCAGAAAGAACCTCCACTCTAC
FLC −49–+53	F	GCCCGACGAAGAAAAAGTAG
	R	TCCTCAGGTTTGGGTTCAAG
FLC +157–314*†	F	CGACAAGTCACCTTCTCCAAA
	R	AGGGGGAACAAATGAAAACC
FLC +416–502†	F	GGCGGATCTCTTGTTGTTTC
	R	CTTCTTCACGACATTGTTCTTCC
FLC +652–809	F	CGTGCTCGATGTTGTTGAGT
	R	TCCCGTAAGTGCATTGCATA
FLC +1,144–1,257	F	CCTTTTGCTGTACATAAACTGGTC
	R	CCAAACTTCTTGATCCTTTTTACC
FLC +1,533–1,670	F	TTGACAATCCACAACCTCAATC
	R	TCAATTTCCTAGAGGCACCAA
FLC +1,933–2,171	F	AGCCTTTTAGAACGTGGAACC
	R	TCTTCCATAGAAGGAAGCGACT
FLC +2,465–2,560*	F	AGTTTGGCTTCCTCATACTTATGG
	R	CAATGAACCTTGAGGACAAGG
FLC +3,197–3,333	F	GGGGCTGCGTTTACATTTTA
	R	GTGATAGCGCTGGCTTTGAT
FLC +3,998–4,178	F	CTTTTTCATGGGCAGGATCA
	R	TGACATTTGATCCCACAAGC
FLC +4,322–4,469	F	AGAACAACCGTGCTGCTTTT
	R	TGTGTGCAAGCTCGTTAAGC
FLC +5,139–5,244	F	CCGGTTGTTGGACATAACTAGG
	R	CCAAACCCAGACTTAACCAGAC
FLC +5,643–5,758	F	TGGTTGTTATTTGGTGGTGTG
	R	ATCTCCATCTCAGCTTCTGCTC
FLC +6,057–6,175*	F	CGTGTGAGAATTGCATCGAG
	R	AAAAACGCGCAGAGAGAGAG
FLC +6,877–6,947	F	TTGTAAAGTCCGATGGAGACG
	R	ACTCGGCGAGAAAGTTTGTG

pTUB2	F	ACAAACACAGAGAGGAGTGAGCA
	R	ACGCATCTTCGGTTGGATGAGTGA
ACT7	F	TCGTTTCGCTTTCCTTAGTGT
	R	CGAAATCGGCATAGAGAATCA
FUS3	F	GTGGCAAGTGTTGATCATGG
	R	AGTTGGCACGTGGGAAATAG

* These primers were also used for the ChIP analysis shown in **Figure 11**. *FLC* +157–314, +2,465–2,560, +6,057–6,175 correspond to P1, P2, and P3, respectively.

† These primers, amplifying the nucleation region of *FLC*, were used for the statistical test of **Figure 35**.

2.6. Gene expression analysis

Total RNA was isolated from –100 mg of seedlings grown on MS agar plate using TRI Reagent® (Sigma-Aldrich, St Louis, MO, USA) or TS™ Plant Mini Kit (Taeshin Bio Science, Gyeonggi-do, Korea). cDNA was generated using 4 μg of total RNA, 5 units of recombinant DNase I (TaKaRa, Kyoto, Japan), 200 units of RevertAid™ reverse transcriptase (Thermo Scientific, Waltham, MA, USA), and buffer containing 0.25 mM dNTP and 0.1 μg oligo(dT)$_{18}$. qPCR analysis was performed using iQ™ SYBR® Green Supermix (Bio-Rad, Hercules, CA, USA) and a CFX96 Real-Time PCR system (Bio-Rad). Primers used for quantitative reverse transcription PCR (RT-qPCR) are listed in **Table 4**.

To examine *COOLAIR* expression in the *COOLAIR* promoter deletion lines, Total RNAs were extracted using the RNeasy® Plus Mini Kit (Qiagen, Hilden, Germany) according to the manufacturer's instructions, followed by the digestion of residual genomic DNA by the gDNA wiper (Vazyme, Nanjing, China). 1.0-μg RNA from each sample was taken for cDNA synthesis using the HiScript® III 1st Strand cDNA Synthesis Kit (Vazyme) with the transcript-specific primers (5′-TGGTTGTTATTTGGTGGTGTGAA-3′ for *COOLAIR* class I and 5′-GCCCGACGAAGAAAAAGTAG-3′ for class II; Zhao et al., 2021). Semi-quantitative PCR amplifications were performed, followed by agarose gel separation of PCR products.

Table 4. Primers used for gene expression analysis.

Target	Primer	Sequence (5′→3′)
Total *COOLAIR*	F1	TGTATGTGTTCTTCACTTCTGTCAA
	R1	GCCGTAGGCTTCTTCACTGT
	F2	TCGTGTGAGAATTGCATCGAG
	R2	AGCCACGTCCCTGTTGCAAA
COOLAIR class I.i	F1	GACAAATCTCCGACAATCTTCC
	R1	CTCACACGAATAAGGTGGCTAAT
	F2	TCATCATGTGGGAGCAGAAG
	R2	TCTCACACGAATAAGGTGGCTA
	F3*	TCACACGAATAAGGTGGCTAATTAAG
	R3*	TCCTTGGATAGAAGACAAAAAGAGA
COOLAIR class II.i	F1	CTCCTCCGGCGATAAGTA
	R1	CTCACACGAATAAGAAAAGTAAAA
	F2*	TGCAATTCTCACACGAATAAGAAAAGT
	R2*	TAGCCGACAAGTCACCTTCTCCAA
COOLAIR class II.ii	F1	CTCCTCCGGCGATAAGTA
	R1	ACGATAATCATAGAAAAGTAAAAGAGC
	F2*	TAGTGGGAGAGTCACCGGAAG
	R2*	TTCTCCTCCGGCGATAAGTAC
FLC mRNA	F	AGCCAAGAAGACCGAACTCA
	R	TTTGTCCAGCAGGTGACATC
Unspliced *FLC*	F	CGCAATTTTCATAGCCCTTG
	R	CTTTGTAATCAAAGGTGGAGAGC
CAS	F	ATCTCATGTATCTATCATGGTCGCAGA
	R	TTCTCCTCCGGCGATAAGTAC
CBF1	F	GGAGACAATGTTTGGGATGC
	R	CGACTATCGAATATTAGTAACTCC
CBF2	F	CGACGGATGCTCATGGTCTT
	R	TCTTCATCCATATAAAACGCATCTTG
CBF3	F	TTCCGTCCGTACAGTGGAAT
	R	AACTCCATAACGATACGTCGTC
COR15A	F	CTTACCTAATCAGTTAATTTCAAGCA
	R	TTAAACATGAAGAGAGAGGATATGG
RD29A	F	ATGGATCAAACAGAGGAACCACCA
	R	CTTAGTCGCACCATTCTCATGATG
PP2A	F	TATCGGATGACGATTCTTCGTGCAG
	R	GCTTGGTCGACTATCGGAATGAGAG

UBC	F	TTGTGCCATTGAATTGAACCC
	R	CATCCTAATGTTCATTTCAAGACAG

* These primers were used for the *COOLAIR* amplifications shown in **Figure 30**.

2.7. Immunoblotting

Total protein was isolated from –100 mg of seedlings using a buffer containing 50 mM Tris-HCl (pH 7.5), 100 mM NaCl, 10 mM $MgCl_2$, 1 mM EDTA, 10% glycerol, 1 mM PMSF, 1 mM DTT and 1× cOmplete™ EDTA-free Protease Inhibitor Cocktail (Roche). Fifty micrograms of total protein were loaded onto SDS-PAGE gels and separated by electrophoresis. The proteins were transferred to PVDF membranes (Amersham Biosciences) and probed with an anti-myc (MBL; #M192-3; 1:10,000 dilution) antibody overnight at 4°C. The samples were then probed with horseradish peroxidase (HRP)-conjugated anti-mouse IgG (Cell Signaling, Danvers, MA, USA; #7076; 1:10,000 dilution) antibody at room temperature. The signals were detected with ImageQuant™ LAS 4000 (GE Healthcare) using WesternBright™ Sirius ECL solution (Advansta, San Jose, CA, USA).

2.8. RNA-seq data analysis

Two sets of RNA-seq data deposited in the National Center for Biotechnology Information (NCBI) under BioProject accession codes PRJNA416120 and PRJNA732005 were retrieved. PRJNA416120 contains raw reads from NV, 1V, and 14-days vernalized (14V) wild-type and *cbfs* plants in an SW background (Park et al., 2018b). PRJNA732005 contains reads from 0-, 3-, and 24-h cold-treated wild-type and *cbfs* plants in a Col-0 background (Song et al., 2021). The reads were aligned to the Arabidopsis TAIR 10 reference genome and annotated in ARAPORT 11 using STAR version 2.7.10a. Isoform estimation was performed using Salmon version 1.6.0.

2.9. Luciferase assay using Arabidopsis protoplast

Protoplast isolation and transfection were performed as previously described with some modifications (Yoo et al., 2007). Protoplasts were isolated from leaves of SD-grown wild-type plant (Col-0) using a buffer containing 150 mg Cellulase Onozuka™ R-10 (Yakult, Tokyo, Japan), 50 mg Maceroenzyme™ R-10 (Yakult), 20 mM KCl, 20 mM MES-KOH (pH 5.6), 0.4 M D-mannitol, 10 mM $CaCl_2$, 5 mM β-mercaptoethanol, and 0.1 g bovine serum albumin. For protoplast transfection, 200 μg of plasmid DNA and isolated protoplasts were incubated in a buffer containing 0.1 M D-mannitol, 50 mM $CaCl_2$, and 20% (w/v) PEG. Luciferase activity in the protoplasts was measured using the Luciferase Assay System (Promega, Madison, WI, USA) and MicroLumat Plus LB96V microplate luminometer (Berthold Technologies, Bad Wildbad, Germany).

2.10. Statistical analysis

Statistical analyses were performed using unpaired Student's *t* test, one- or two-way analysis of variance (ANOVA) followed by a post hoc multiple comparison test.

Chapter 3

Results

Gene expression analysis and flowering time measurement on $FLC_{\Delta COOLAIR\text{-}3}$ and $FLC_{\Delta COOLAIR\text{-}4}$ were carried out by Yupeng Yang and Xiao Luo. RNA-seq data were analyzed by Daesong Jeong.

3.1. A CRT/DRE-binding factor, CBF3, directly binds to CRT/DREs at the 3′-end of the *FLC*

The proximal promoter region of *COOLAIR* is highly conserved among *FLC* orthologs from *A. thaliana* relatives (Castaings et al., 2014). Thus, I assumed that the cis-element conferring a long-term cold response would exist within that block. A comparison of the region near the TSS of *COOLAIR* revealed the conservation of two CRT/DREs among six *FLC* orthologs from five related species of the Brassicaceae family (**Figure 6**). CRT/DRE, the core sequence of which is CCGAC, is a regulatory element that imparts cold- or drought-responsive gene expression (Baker et al., 1994). *CBF1*, *2*, and *3* encode APETALA 2 (AP2) domain-containing proteins that can bind to CRT/DRE and are usually present in the promoters of cold- and drought-responsive genes (Stockinger et al., 1997; Medina et al., 1999). Consistent with this, the Arabidopsis cistrome database and the genome-wide ChIP sequencing (ChIP-seq) results from a previous study suggested that CBFs bind to the 3′-end sequence of *FLC* containing CRT/DREs (**Figure 7**; O'Malley et al., 2016; Song et al., 2021).

I performed an EMSA to confirm this binding using probes harboring CRT/DREs (named DRE1 or 2) from the *COOLAIR* promoter (**Figure 8**). The mobility of these two Cy5-labeled probes was retarded by MBP-fused CBF3 (**Figure 9**). The band shift was competed out by adding an excess amount of unlabeled DRE1 or 2 oligonucleotides. In contrast, competitors containing mutant forms of DRE1 or 2 (DRE1^{m} or 2^{m}, respectively) failed to compete (**Figure 9**). I also tested the binding of other CRT/DRE-like sequences in the *FLC* locus. Two (DREa and b) were present in the *FLC* promoter, while the other two (DREc and d), were present in the first and last exons, respectively (**Figure 8**). Only DREc competed with the band shift caused by the CBF3-DRE1 interaction (**Figures 9 and 10**). The presence or absence of bases

that determine the binding affinity between CBFs and CRT/DRE could explain the differences in CBF3-binding patterns among CRT/DRE-like sequences at the *FLC* locus (Maruyama et al., 2004).

Subsequently, a ChIP assay using a *CBF3*-overexpressing transgenic plant, *pSuper:CBF3-myc* (Liu et al., 2017), was conducted to determine whether CBF3 is associated with the *FLC* region containing CRT/DREs *in vivo*. Consistent with the *in vitro* results, CBF3-myc protein was enriched at the 3′-end of *FLC* and the first exon where DREc was located (**Figure 11**). Without vernalization (NV), CBF3-myc was highly enriched at both the 5′- and 3′-ends of *FLC* (P1 and P3), indicating that CBF3 protein can activate *FLC* under warm conditions, as previously reported (Seo et al., 2009). However, enrichment in the P1 region rapidly disappeared during the vernalization period. In contrast, enrichment on P3 was maintained until 10V and was subsequently reduced. This is coincident with the expression pattern of *COOLAIR*, which declines during the late phase of vernalization (Csorba et al., 2014).

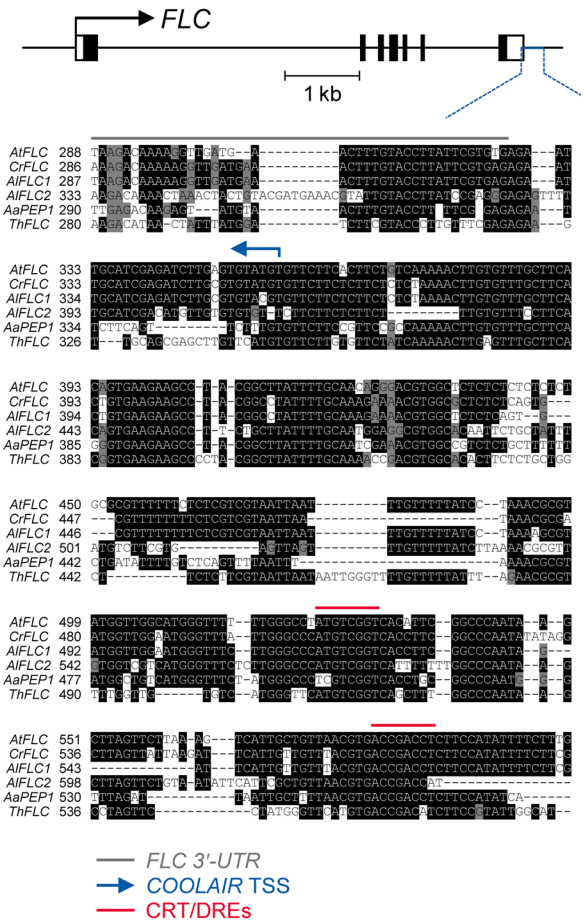

Figure 6. Comparison of sequences around the 3′-end of the *FLC* orthologs from Arabidopsis relatives.

The upper graphic presents the gene structure of *AtFLC*. The black bars, black lines, and white bars indicate exons, introns, and UTRs, respectively. The blue line presents the region used for sequence comparison among six orthologous genes from five plant species. In the sequence alignment below, the grey line indicates the 3′-UTR of *FLC* orthologs, the blue arrow indicates the transcriptional start site of *AtCOOLAIR*, and the red lines indicate CRT/DREs. At, *Arabidopsis thaliana*; Cr, *Capsella rubella*; Al, *Arabidopsis lyrata*; Aa, *Arabis alpina*; Th, *Thellungiella halophila*.

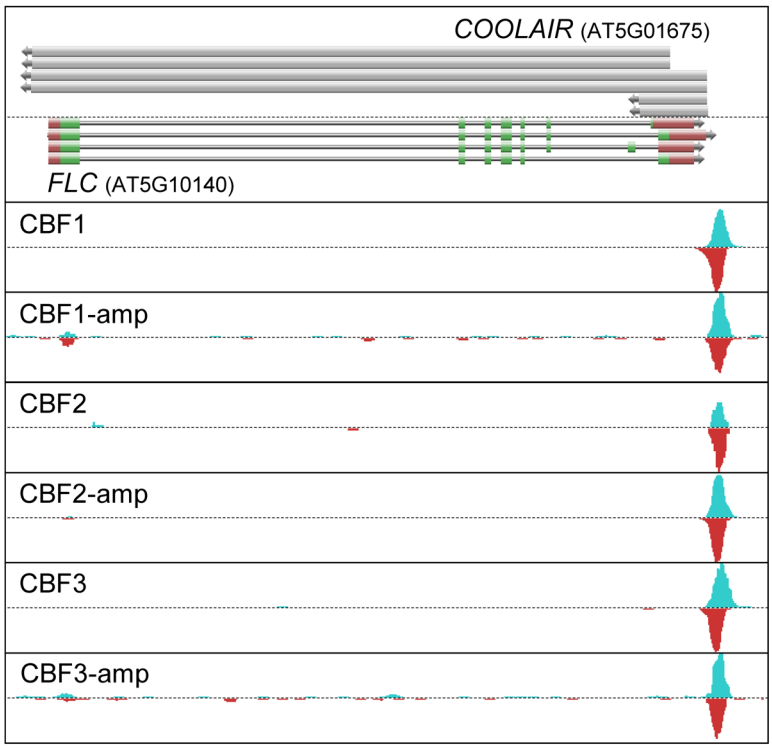

Figure 7. DAP-seq results showing the binding of CBF proteins to the 3′-end region of *FLC*.

DNA affinity purification sequencing (DAP-seq) results showed enrichment of CBF proteins at the *AtFLC* locus obtained from the Plant Cistrome Database (http://neomorph.salk.edu/dev/pages/shhuang/dap_web/pages/index.php; O'Malley et al., 2016). The top bars represent the transcribed regions of each *AtCOOLAIR* variant. The bars below represent the structures of the alternatively spliced forms of the *AtFLC* transcript. The green, grey, and red bars indicate the exons, introns, and UTRs of *AtFLC*, respectively. The peaks below represent the positions of CBF enrichment. CBF-amp, the results of ampDAP-seq using PCR-amplified DNA library.

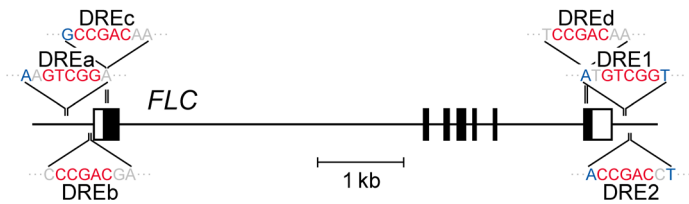

Figure 8. Schematic showing the positions of six CRT/DRE-like sequences distributed on the *FLC* locus.

CRT/DRE sequences have been labeled as DRE1 and 2, and CRT/DRE-like sequences have been labeled as DREa, b, c, and d. The black bars, black lines, and white bars represent exons, introns, and UTRs of *AtFLC*, respectively. The red bases indicate the core sequence (CCGAC) of CRT/DRE. The blue-colored bases represent bases known to determine the binding affinity of CBF3 to CRT/DRE (Maruyama et al., 2004).

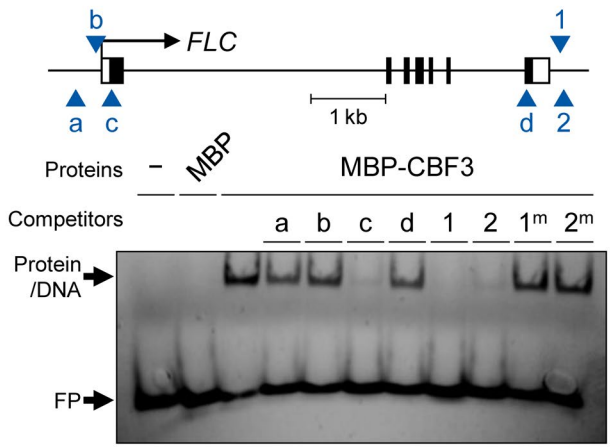

Figure 9. *In vitro* binding of CBF3 protein to the CRT/DREs at the *FLC*'s 3′-end.

EMSA using one of the CRT/DREs located at the *AtCOOLAIR* promoter, DRE1, as a probe. In the upper graphic showing *AtFLC* gene structure, CRT/DRE and CRT/DRE-like sequences are marked as blue arrows. CRT/DRE-like sequences have been labeled as a, b, c, and d, and CRT/DRE sequences have been labeled as 1 and 2. For the competition assay, DREa, b, c, and d, and mutant forms of DRE1 and DRE2 (1^m and 2^m) were used as competitors. A 100-fold molar excess of unlabeled competitors was added. No protein (−) or maltose binding protein (MBP) were used as controls. FP, free probe.

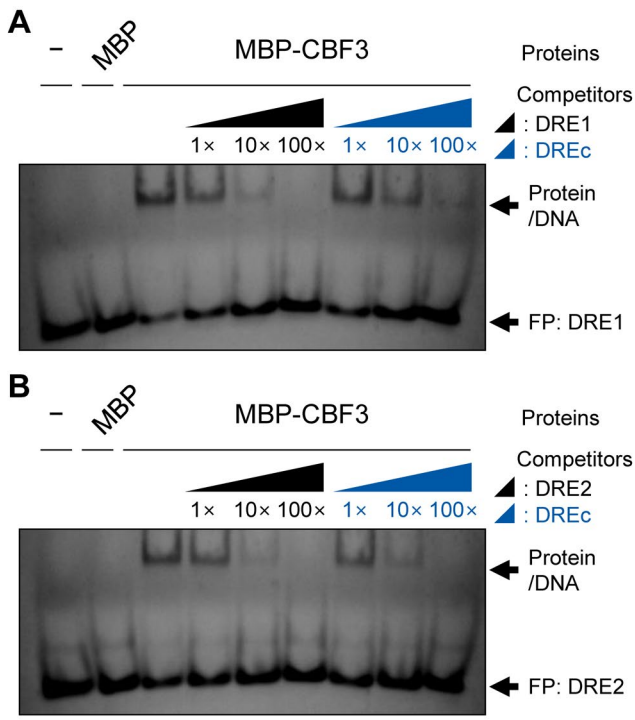

Figure 10. Comparison of CBF3-binding affinity between the CRT/DREs at the 3′-end and first exon of *FLC*.

(A–B) EMSA using DRE1 (A) or DRE2 (B) as probes. For competition assay, DRE1, DRE2, and DREc were used as competitors. Molar excess (1-, 10-, and 100-fold) of unlabeled competitors was added. FP, free probe.

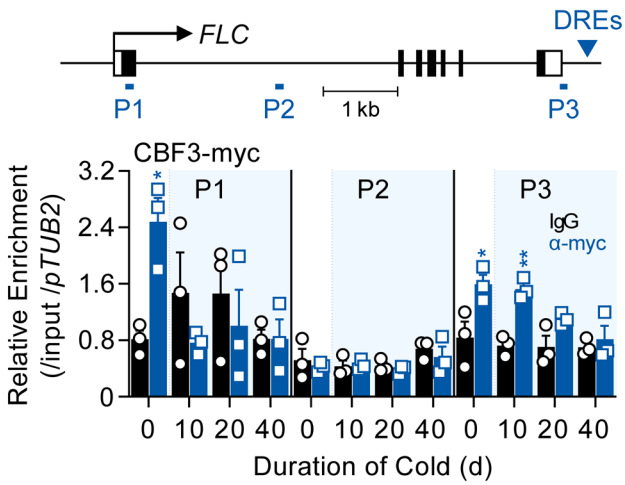

Figure 11. *In vivo* enrichment of CBF3 protein at the *FLC* locus during vernalization.

ChIP assay result showing the enrichment of CBF3-myc protein on the *AtFLC* locus. Samples of NV, 10V, 20V, and 40V *pSuper:CBF3-myc* plants were collected at ZT4 in an SD cycle. The CBF3-chromatin complex was immunoprecipitated (IP) with anti-myc antibodies (blue bars), and mouse IgG (black bars) was used as a control. Positions of qPCR amplicons used for ChIP-qPCR analysis are illustrated as P1, P2, and P3 in the upper graphic. The blue arrow in the graphic denotes the position of CRT/DREs located on the *AtCOOLAIR* promoter. ChIP-qPCR results have been represented as mean ± standard error of the mean (SEM) of the three biological replicates in the lower panel. Open circles and squares represent each data point. Relative enrichments of the IP/5% input were normalized to that of *pTUB2*. The blue shadings indicate cold periods. Asterisks indicate a significant difference between IgG and anti-myc ChIP-qPCR results at each vernalization time point (*$P < 0.05$; **$P < 0.01$; unpaired Student's *t*-test).

3.2. *COOLAIR* is one of the CBF regulons in Arabidopsis

CBF genes are rapidly and transiently induced upon exposure to cold (Medina et al., 1999). CBF regulons, which are CBF-targeted genes, are correspondingly up- or down-regulated after cold intervals of a few hours (Gilmour et al., 1998; Liu et al., 1998; Fowler and Thomashow, 2002). As *COOLAIR* contains CBF3-binding sites in its promoter (**Figures 6–11**), I analyzed whether *COOLAIR* shows CBF regulon-like expression. The expression of genes assigned to the CBF regulon is up- or down-regulated by *CBF* overexpression under warm conditions (Park et al., 2015). Similarly, I found that the total transcript level of *COOLAIR* increased in *CBF3*-overexpressing transgenic plants (*pSuper:CBF3-myc*) grown at room temperature (22°C) compared to that in the wild type, Col-0 (**Figure 12**). Such upregulation was mainly due to the type I.i or type II.i *COOLAIR* isoforms. As the levels of both proximal (type I) and distal (type II) variants of *COOLAIR* were higher in the *CBF3* overexpressor than in the wild type, it is likely that *COOLAIR* transcription, instead of the 3′-processing events, is affected by CBF3 (**Figure 12**; *Liu et al., 2010; Marquardt et al., 2014*). It has been reported that the targets of CBF1 or 2 are not entirely identical to those of CBF3, although CBF genes show high sequence similarity (Novillo et al., 2007). Thus, I compared the expression levels of all *COOLAIR* isoforms in transgenic plants overexpressing *CBF1*, *2*, or *3* (Seo et al., 2009). Overall, all *CBF*-overexpressing plants showed increased levels of *COOLAIR* (**Figure 13**). However, each *CBF*-overexpressing plant showed a subtly different effect on *COOLAIR* expression. The *CBF2* overexpressor showed the highest level of the proximal *COOLAIR* isoform, whereas the *CBF3* overexpressor showed the highest level of distal *COOLAIR*. In contrast, the *CBF1*-overexpressing plants showed a slightly smaller increase in proximal *COOLAIR* levels and a negligible increase in distal *COOLAIR*, compared to those in the wild type, Ws-2. Such results

imply that the three CBFs regulate *COOLAIR* transcription subtly differently.

Another characteristic of CBF regulons is that their expression is activated by a day of cold exposure (Park et al., 2015). Thus, I analyzed if *COOLAIR* is also induced by short-term cold exposure. I treated wild-type (*FRI* Col) plants with 0, 0.5, 1, 1.5, 2, 3, 6, and 24 h of cold (4°C), then measured the levels of total *COOLAIR*. The results showed that cold treatment for less than 3 h failed to induce *COOLAIR* expression, although *CBF* transcripts reached a peak at 3 h of cold exposure (**Figures 14 and 16**; *Gilmour et al., 1998*). However, after 6 h of cold treatment, when CBF3 protein levels peaked, *COOLAIR* was strongly induced (**Figures 14 and 20**). Thus, short-term cold-triggered *COOLAIR* expression dynamics were similar to those of other CBF-targeted genes; that is, the expression was highly increased after *CBF* transcript levels reached a peak upon cold exposure (Gilmour et al., 1998; Fowler and Thomashow, 2002). To confirm whether *CBFs* are responsible for the rapid cold response of *COOLAIR*, I examined *COOLAIR* induction after a day of cold treatment in the wild type and *cbfs-1* mutant, in which all three *CBFs* were knocked out (**Figure 15**; Jia et al., 2016). All isoforms, as well as total *COOLAIR*, failed to be induced by short-term cold exposure in the *cbfs* mutant, although a drastic increase was observed in the wild type. Thus, these results strongly suggest that *CBFs* are required for *COOLAIR* induction, even under a short period of cold exposure.

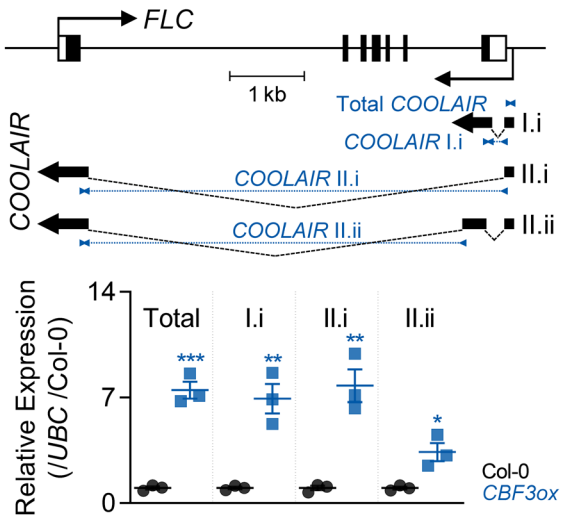

Figure 12. Increased *COOLAIR* expression levels in *CBF3*-overexpressing plant. Expression levels of total *COOLAIR* and *COOLAIR* isoforms in the wild-type (Col-0) and *CBF3*-overexpressing plants (*pSuper:CBF3-myc* [*CBF3ox*]). The gene structures of *FLC* and *COOLAIR* variants are illustrated in the upper panel. The thin black arrows indicate the TSSs of *FLC* and *COOLAIR*. The thick black arrows indicate the exons of each *COOLAIR* isoform. The structures of proximal (I.i) and distal (II.i and II.ii) *COOLAIR* isoforms are shown. The positions of qPCR amplicons used for detecting proximal (I.i), and distal (II.i, II.ii) *COOLAIR*s are marked using blue arrow heads. Relative transcript levels of total *COOLAIR* and *COOLAIR* variants were normalized to that of *UBC* and have been rep resented as mean ± SEM of three biological replicates. Dots and squares represent each data point. Asterisks indicate a significant difference as compared to the wild type (*$P < 0.05$; **$P < 0.01$; ***$P < 0.001$; unpaired Student's *t*-test).

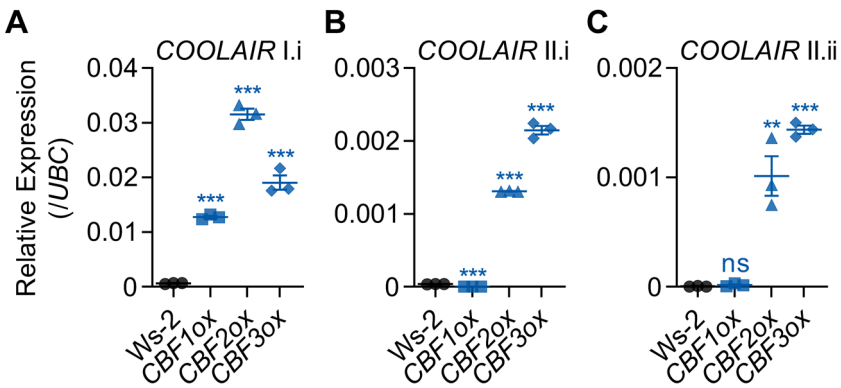

Figure 13. Different effects of *CBF1*-, *2*-, and *3*-overexpressions on *COOLAIR* variants.

(A–C) Transcript levels of *COOLAIR* variants in the wild type (Ws-2) and *CBF1*-, *2*-, and *3*-overexpressing transgenic plants (*35S:CBF1* [*CBF1ox*], *35S:CBF2* [*CBF2ox*], and *35S:CBF3* [*CBF3ox*], respectively; Seo et al., 2009). Relative levels of type I.i (A), type II.i (B), and type II.ii (C) *COOLAIR* were normalized to that of *UBC*. Values have been represented as mean ± SEM of three biological replicates. Dots, squares, triangles, and polygons represent each data point. Asterisks indicate a significant difference, as compared to the wild type (**$P < 0.01$; ***$P < 0.001$; unpaired Student's *t*-test). ns, not significant ($P \geq 0.05$).

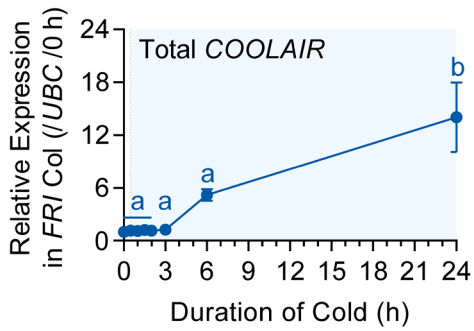

Figure 14. Expression dynamics of total *COOLAIR* after short-term cold treatment.

Wild types (*FRI* Col) were subjected to 4°C cold and harvested at each time point (0, 0.5, 1, 1.5, 2, 3, 6, and 24 h after cold). Relative transcript levels of total *COOLAIR* to *UBC* were normalized to that of non-cold treated wild type. The values have been represented as mean ± SEM of three biological replicates. The blue shading indicates periods under cold treatment. Significant differences have been marked using different letters (a, b; $P < 0.05$; one-way ANOVA followed by Tukey's post hoc test).

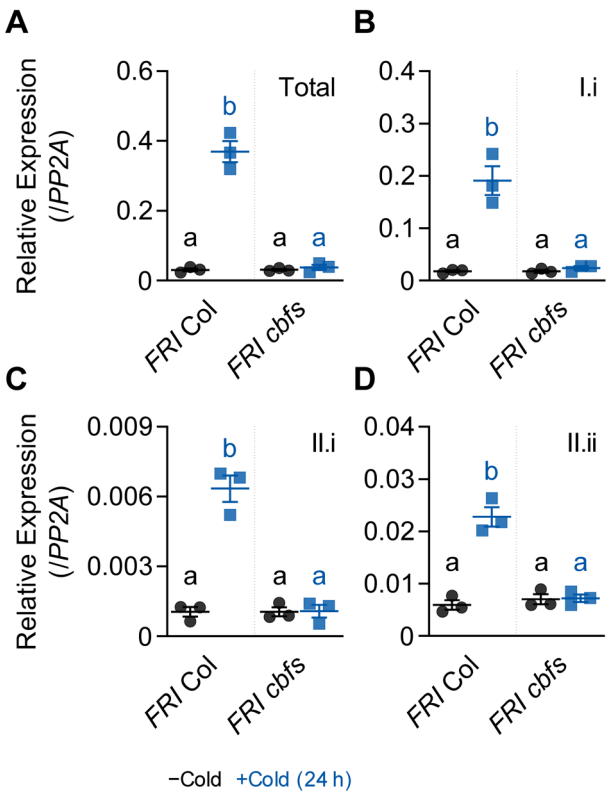

Figure 15. Transcript levels of total *COOLAIR* and *COOLAIR* isoforms in the wild type and *cbfs* mutant before and after a day of cold treatment.

(A–D) The wild-type and *cbfs-1* mutant seedlings were treated with (+Cold) or without (−Cold) a day of 4°C cold. Relative levels of total *COOLAIR* (A) and *COOLAIR* variants (B, class I.i; C, class II.i; D, class II.ii) were normalized to that of *PP2A*. Values have been represented as mean ± SEM of three biological replicates. Dots and squares indicate each data point. Significant differences have been marked using different letters (a, b; $P < 0.05$; two-way ANOVA followed by Tukey's post hoc test).

3.3. CBFs accumulate during vernalization

I subsequently investigated whether *CBFs* are also responsible for vernalization-induced *COOLAIR* activation. It has been reported that *COOLAIR* is gradually upregulated as the cold period persists and peaks after 2–3 weeks of vernalization (Csorba et al., 2014). However, most studies on *CBF* expression have been performed within a few days since the function of *CBFs* has been analyzed only in the context of short-term cold (Gilmour et al., 1998; Liu et al., 1998; Medina et al., 1999; McKhann et al., 2008). Therefore, I investigated the expression patterns of *CBFs* before and after long-term cold exposure to determine the correlation between the expression of *CBFs* and *COOLAIR* during vernalization. As previously shown, the levels of all three *CBFs* peaked within 3 h of cold exposure and then decreased rapidly (**Figure 16**). However, *CBF* levels increased again as the cold period was prolonged (> 20V), suggesting that both short-term and vernalizing cold treatments upregulated *CBF* expression (**Figure 17**).

Because *CBFs* exhibit rhythmic oscillations (Dong et al., 2011), I also investigated whether the rhythmic expression of *CBFs* is affected by vernalization. Wild-type (Col-0) plants were collected every 4 h under an SD photoperiod (8-h light/16-h dark) under both NV and 40V conditions. As shown in **Figure 18**, although the rhythmic pattern of each *CBF* was variable, the overall transcript levels of all three *CBFs* were much higher at 40V than under NV. Consistent with the transcript level, the level of CBF3 protein in vernalized plants was higher than that in NV plants during all circadian cycles (**Figure 19**).

To verify whether the increased transcription of *CBF3* led to protein accumulation, I measured the level of CBF3 at each time point of cold treatment using the *pCBF3:CBF3-myc* plant (Jia et al., 2016). Following the rapid and transient induction of *CBF3* under short-term cold conditions (**Figure 16**; Medina et al., 1999),

CBF3-myc protein levels peaked within 6 h of cold exposure and then decreased (**Figure 20**). Thus, the peak of the *CBF3* transcript and that of the CBF3 protein showed a gap of few hours. Notably, the peak of the CBF3 protein correlated with the time when *COOLAIR* was rapidly induced (**Figures 14 and 20**). During vernalization, the level of CBF3-myc protein was increased by 1 d of cold (1V), then declined until 10V (**Figure 21**). It increased again as the cold period was prolonged; thus, the level at 40V is similar to that at 1V. The protein level rapidly decreased when the plants were transferred to room temperature for 4 d after 40V (40VT4). These results suggest that CBFs are responsible for the progressive upregulation of *COOLAIR*, at least during the early phase of vernalization (Csorba et al., 2014).

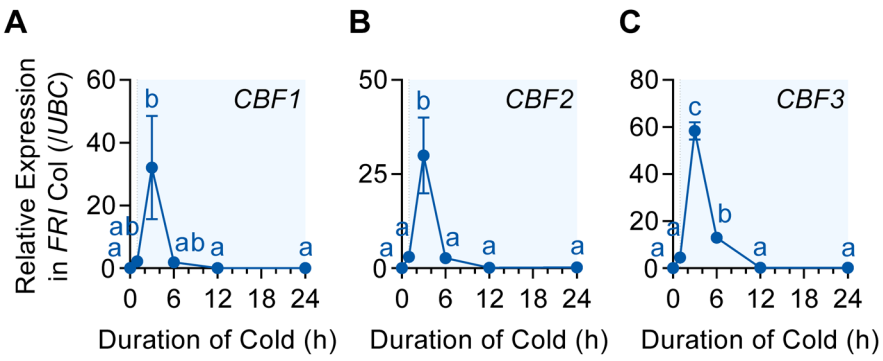

Figure 16. Transcript levels of *CBF1*, *2*, and *3* under short-term cold exposure. **(A–C)** Wild-type plants were subjected to 0, 1, 3, 6, 12, and 24 h of 4°C cold treatment. Relative levels of *CBF1* (A), *2* (B), and *3* (C) were normalized to that of *UBC*. Values have been represented as mean ± SEM of three biological replicates. The blue shadings indicate cold periods. Significant differences have been marked using different letters (a–c; $P < 0.05$; one-way ANOVA followed by Tukey's post hoc test).

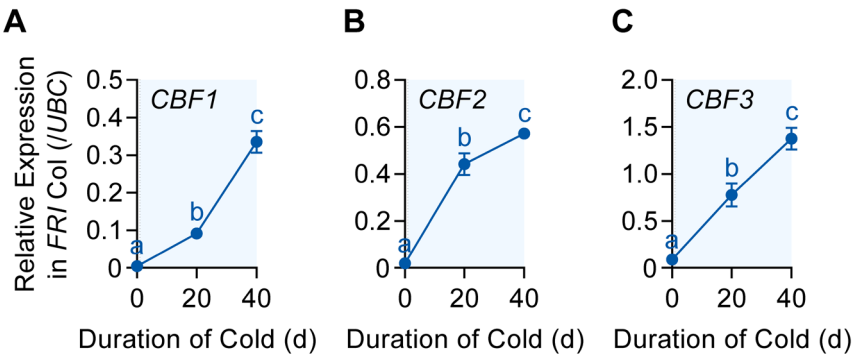

Figure 17. Transcript levels of *CBF1*, *2*, and *3* during vernalization.

(A–C) Wild-type plants were treated with 4°C vernalization (20 and 40 days) under an SD cycle and collected at ZT4. Relative levels of *CBF1* (A), *2* (B), and *3* (C) were normalized to that of *UBC*. Values have been represented as mean ± SEM of three biological replicates. The blue shadings denote periods under cold. Significant differences have been marked using different letters (a–c; $P < 0.05$; one-way ANOVA followed by Tukey's post hoc test).

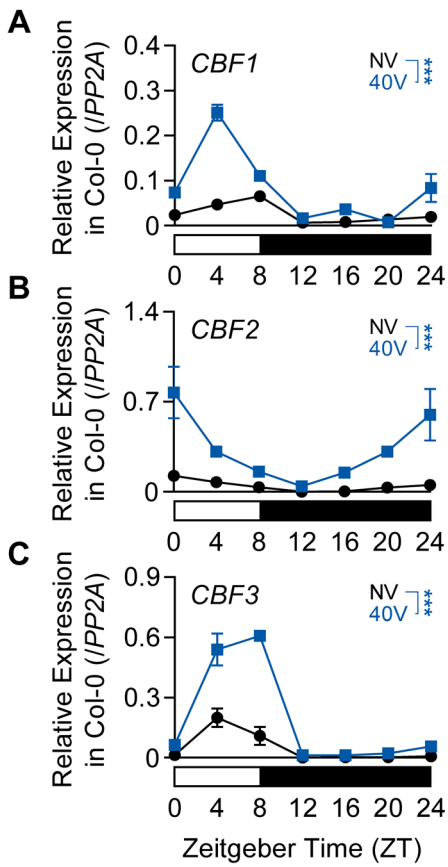

Figure 18. Daily rhythms of *CBF1*, *2*, and *3* transcript levels in non-vernalized or vernalized plants.

(A–C) NV or 40V Col-0 plants grown under an SD cycle were collected every 4 h between ZT0 and ZT24. Relative transcript levels of *CBF1* (A), *2* (B), and *3* (C) were normalized to that of *PP2A*. Values have been represented as mean ± SEM of three biological replicates. The white and black bars represent light and dark periods, respectively. Asterisks indicate a significant difference between NV and 40V (***$P < 0.001$; two-way ANOVA).

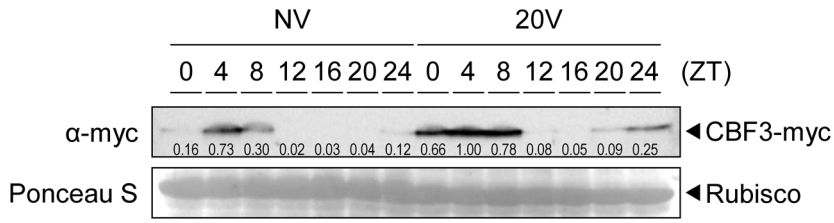

Figure 19. Daily rhythms of CBF3 protein levels in non-vernalized or vernalized plants.

The NV or 20V *pCBF3:CBF3-myc* transgenic plants, subjected to 4°C vernalization, were collected every 4 h between ZT0 and ZT24. CBF3 protein was detected using anti-myc antibodies. Rubisco was used as loading control. The numbers below each band indicate the relative signal intensity compared to 20V ZT4. The mean values of three biological replicates are presented.

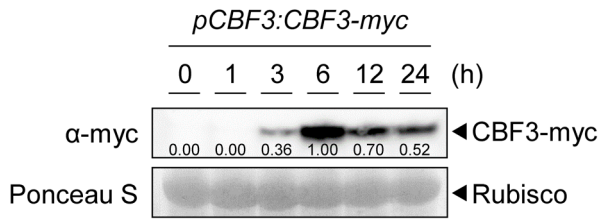

Figure 20. Dynamics of CBF3 protein abundance under short-term cold exposure.

The *pCBF3:CBF3-myc* transgenic plants were subjected to 0, 1, 3, 6, 12, and 24 h of 4°C cold treatment. CBF3 proteins were detected using anti-myc antibodies. Rubisco was considered the loading control. Numbers below each band indicate relative signal intensity compared to 6 h. The mean values of two biological replicates are presented.

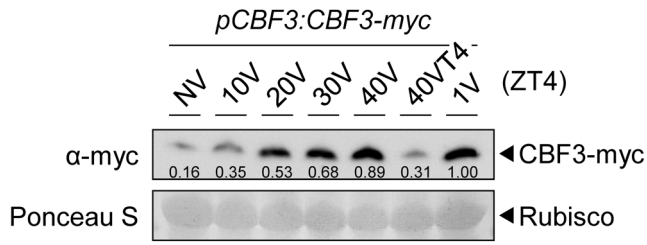

Figure 21. Increase in CBF3 protein level during the vernalization process.

The *pCBF3:CBF3-myc* transgenic plants, subjected to 4°C vernalization, were collected at ZT4 of the indicated time point. CBF3 proteins were detected using anti-myc antibodies. Rubisco was considered the loading control. Numbers below each band indicate relative signal intensity compared to 1V. The mean values of three biological replicates are presented.

3.4. *CBFs* are involved in vernalization-induced *COOLAIR* expression

To clarify whether *CBFs* are responsible for long-term cold-mediated *COOLAIR* induction, I quantified *COOLAIR* levels in wild type and *cbfs* mutant during vernalization. As shown in **Figures 14 and 15**, the *COOLAIR* level was considerably increased by a day of low-temperature treatment in the wild type but quickly declined afterward (**Figure 22**). The *COOLAIR* level increased again after 4V and reached a secondary peak at approximately 10V to 20V. It then decreased during the remaining vernalization period, as similar to previous results (Csorba et al., 2014). The expression dynamics of *COOLAIR* were similar to those of two well-known CBF targets, *COR15A* and *RESPONSIVE TO DESICCATION 29A* (*RD29A*), although their levels remained high until the end of the vernalization period (**Figure 23**). In contrast to the wild-type plants, the *cbfs* mutant showed severely reduced *COOLAIR* expression, as well as *COR15A* and *RD29A* levels, during all the period of vernalization (**Figures 22 and 23**). Analysis of RNA sequencing (RNA-seq) data from previous studies also revealed that the levels of total *COOLAIR,* and proximal and distal *COOLAIR* variants were reduced in the *cbfs* mutant in Col-0 or SW ecotype background when exposed to either short-term (3 and 24 h) or long-term (14V) cold, which supports my results (**Figures 24 and 25**; Park et al., 2018b; Song et al., 2021). All of these data support that *CBFs* are necessary to fully induce *COOLAIR* in the early phase of vernalization.

Consistent with the reduced *COOLAIR* levels in *cbfs* mutants, the *CBF3* overexpressor, *pSuper:CBF3-myc*, showed a much higher *COOLAIR* level than the wild type (Col-0), throughout the vernalization period (**Figure 26**). It is noteworthy that *COOLAIR* expression in *pSuper:CBF3-myc* was further upregulated by cold, especially during the early vernalization phase (10V), and then suppressed during

the late phase. This result implies that both the transcriptional and post-transcriptional regulations of CBFs are involved in the long-term cold response of *COOLAIR*.

A recent study showed that the first seasonal frost (< 0°C) during the winter season strongly induces *COOLAIR* expression (Zhao et al., 2021). Therefore, I tested whether *CBFs* are also required for the strong induction of *COOLAIR* triggered by freezing temperatures. Wild-type and *cbfs* plants were subjected to NV, 10V, and 20V, with or without an additional 8 h of −1°C freezing treatment. Irrespective of the pre-treatment with non-freezing cold, the freezing temperature increased the levels of both *COOLAIR* and *CBF* in the wild type (**Figures 27 and 28**). However, the *cbfs* mutants showed a much smaller increase in the *COOLAIR* level than the wild type when exposed to 8 h of sub-zero cold after 10V and 20V (**Figure 27**). In particular, *COOLAIR* levels were not elevated by freezing treatment in NV *cbfs*. Thus, *CBFs* seem responsible for both the gradual increase of *COOLAIR* during vernalization and the strong *COOLAIR* induction triggered by freezing temperatures.

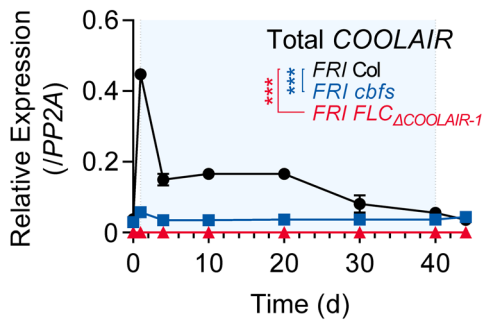

Figure 22. Expression dynamics of total *COOLAIR* in wild-type, *cbfs*, and $FLC_{\Delta COOLAIR\text{-}1}$ plants during vernalization.

Transcript level of total *COOLAIR* in wild-type, *cbfs-1*, and $FLC_{\Delta COOLAIR\text{-}1}$ plants during vernalization was determined by RT-qPCR. Relative transcript levels of total *COOLAIR* were normalized to that of *PP2A*. Values have been represented as mean ± SEM of three biological replicates. Blue shading denotes cold periods. Asterisks indicate a significant difference compared to the wild type (***$P < 0.001$; two-way ANOVA followed by Tukey's post hoc test).

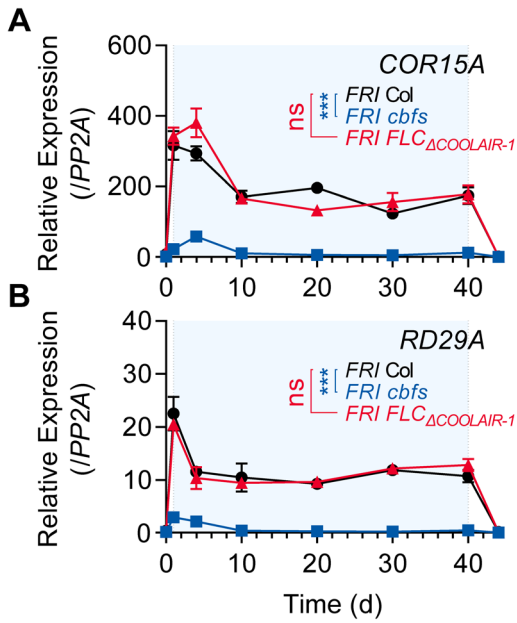

Figure 23. Expression dynamics of CBF regulons in wild-type, *cbfs*, and *FLC*$_{\Delta COOLAIR\text{-}1}$ plants during vernalization.

(A–B) Relative transcript levels of *COR15A* (A) and *RD29A* (B) in wild-type, *cbfs-1*, and *FLC*$_{\Delta COOLAIR\text{-}1}$ plants during vernalization were normalized to that of *PP2A*. Values have been represented as mean ± SEM of three biological replicates. Blue shadings denote cold periods. Asterisks indicate a significant difference compared to the wild type (***$P < 0.001$; two-way ANOVA followed by Tukey's post hoc test). ns, not significant ($P \geq 0.05$).

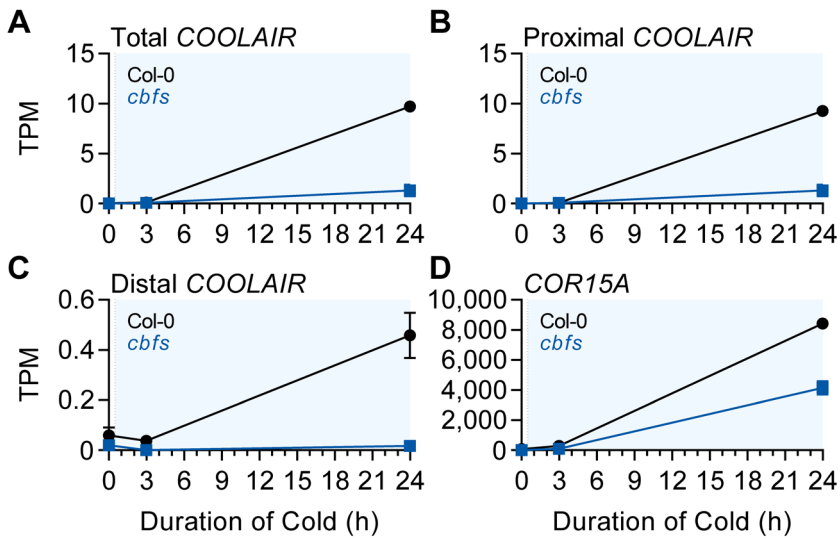

Figure 24. Expression dynamics of total, proximal, and distal *COOLAIR* in the wild type and *cbfs* mutant upon short-term cold exposure, as determined by RNA-seq.

(A–D) Transcript levels of total (A), proximal (B), distal (C) *COOLAIR* and *COR15A* (D) in the wild type (Col-0) and *cbfs* mutant upon 0, 3, 24 h of cold exposure. The data were obtained from the analysis using RNA-seq data reported (Song et al., 2021). The mean values of transcript per million (TPM) of each gene obtained from three experimental replicates are shown. Error bars denote SEM.

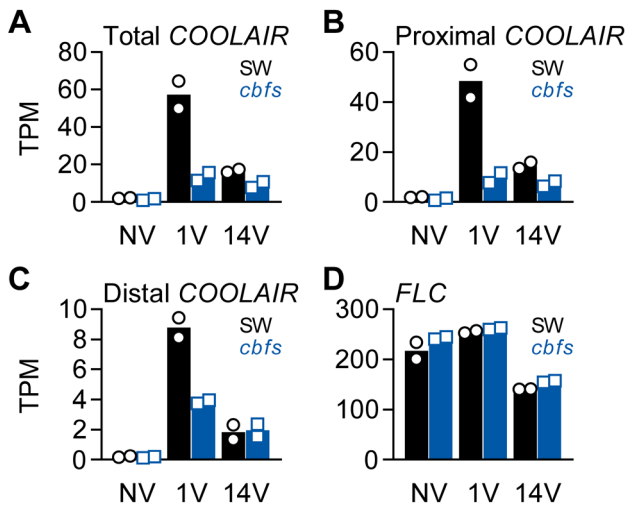

Figure 25. Expression dynamics of total, proximal, and distal *COOLAIR* in the wild type and *cbfs* mutant during vernalization, as determined by RNA-seq.

(A–D) Transcript levels of total (A), proximal (B), distal (C) *COOLAIR* and *FLC* (D) in NV, 1V, and 14V wild type (SW) and *cbfs* mutant. The data were obtained from the analysis using RNA-seq data reported (Park et al., 2018b). SW, an Arabidopsis ecotype collected from Sweden. The mean values of the TPM of each gene obtained from two experimental replicates are shown. Open circles and squares represent each data point.

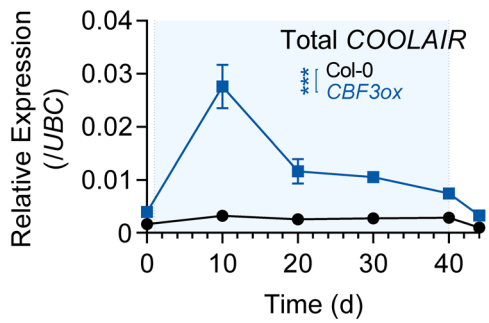

Figure 26. Expression dynamics of total *COOLAIR* in wild-type and *CBF3*-overexpressing plants during vernalization.

Transcript level of total *COOLAIR* in wild-type (Col-0) and *CBF3*-overexpressing transgenic plants (*pSuper:CBF3-myc* [*CBF3ox*]) during vernalization was determined by RT-qPCR. Relative levels of total *COOLAIR* were normalized to that of *PP2A*. Values have been represented as mean ± SEM of three biological replicates. Blue shading denotes cold periods. Asterisks indicate a significant difference between the wild type and *CBF3* overexpressor (***$P < 0.001$; two-way ANOVA).

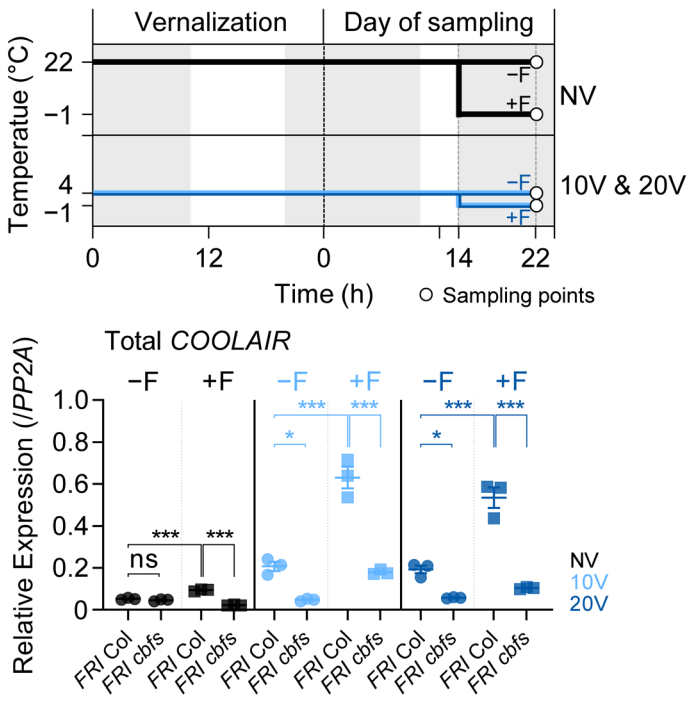

Figure 27. Effect of the first frost-mimicking treatment on the level of total *COOLAIR* in non-vernalized or vernalized wild type and *cbfs*.

The upper panel shows a schematic of the experimental procedure. The non-frost treated (−F) wild type and *cbfs-1* were collected at ZT22 after an 8 h of dark treatment at 22°C (NV) or 4°C (10V and 20V). For the first frost treatment, wild type and *cbfs-1* mutant were treated with an additional 8 h of −1°C (+F) under dark, and then the whole seedlings were collected at ZT22 for analysis. All the plants were grown under an SD cycle. The grey shadings denote dark periods. Total *COOLAIR* levels have been represented as mean ± SEM of three biological replicates in the lower panel. Dots and squares indicate each data point. Relative levels of total *COOLAIR* were normalized to that of *PP2A*. Asterisks indicate a significant difference (*$P < 0.05$; ***$P < 0.001$; two-way ANOVA followed by Tukey's post hoc test). ns, not significant ($P \geq 0.05$).

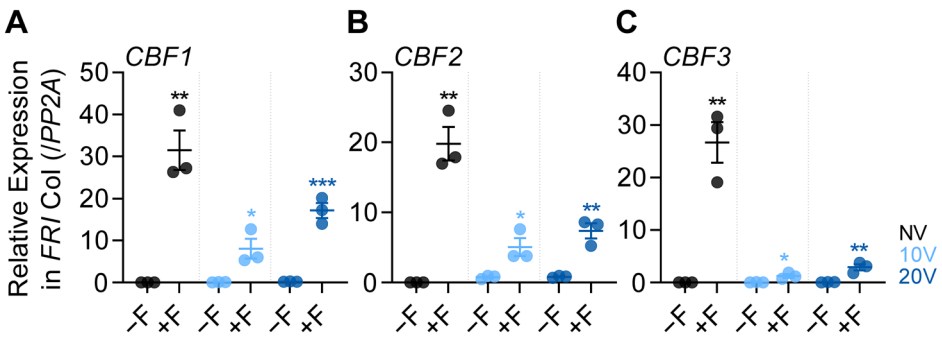

Figure 28. Effect of the first frost-mimicking treatment on the levels of *CBFs*.

(A–C) Transcript levels of *CBF1* (A), *2* (B), and *3* (C) in the wild type after the first frost-mimicking treatment. NV, 10V, 20V, NV+F, 10V+F, and 20V+F plants were subjected to the treatments described in **Figure 27**. Relative *CBF* levels were normalized to that of *PP2A*. Values have been represented as mean ± SEM of three biological replicates. Dots represent each data point. Asterisks indicate a significant difference (*$P < 0.05$; **$P < 0.01$; ***$P < 0.001$; unpaired Student's *t*-test).

3.5. CRT/DREs at the 3′-end of *FLC* are necessary for CBFs-mediated induction of *COOLAIR* during vernalization

Since CBF3 could bind to the CRT/DREs in the first exon (DREc) and the 3′-end of *FLC* (DRE1 and 2) (**Figures 9–11**), I investigated whether CRT/DRE is responsible for the CBF-mediated long-term cold response of *COOLAIR*. To address this, I performed an *A. thaliana* protoplast transfection assay using the *35S:CBF3-HA* effector construct and the *pCOOLAIR$_{DRE}$:LUC* reporter construct, in which the 1-kb wild-type *COOLAIR* promoter was fused to the luciferase reporter gene. The luciferase activity assay showed that CBF3-HA protein activated the transcription of the *COOLAIR* promoter (**Figure 29**). In contrast, CBF3-HA failed to increase luciferase activity when the mutant version of the *COOLAIR* promoter with mutations in the DRE1 and 2 sequences (*pCOOLAIR$_{DRE}^{m}$:LUC*) was used as a reporter. Additionally, co-transfection of the *35S:CBF3-HA* effector and *pFLC:LUC* reporter construct, which harbors the 1-kb sequence with the promoter and first exon of *FLC*, did not show increased luciferase activity. These results strongly indicate that CBF3 can activate *COOLAIR* transcription through DRE1 and 2 located in the *COOLAIR* promoter, but not via the first exon of *FLC*.

To further determine whether the 3′-end sequence of *FLC* is required for cold-induction of *COOLAIR* expression, *COOLAIR* levels in the *FLC$_{\Delta COOLAIR}$* mutant (*FLC$_{\Delta COOLAIR\text{-}1}$*) that lacks a 324-bp portion of the *COOLAIR* promoter region (Luo et al., 2019), were measured before and after vernalization. Reverse transcription PCR (RT-PCR) analysis showed that neither proximal nor distal *COOLAIR* variants were detected in this mutant, and the levels did not increase after 14-d cold exposure (**Figure 30**). Using the CRISPR-Cas9 system, additional *FLC$_{\Delta COOLAIR}$* mutant lines, *FLC$_{\Delta COOLAIR\text{-}3}$*, and *FLC$_{\Delta COOLAIR\text{-}4}$* were generated (**Figure 31**). *FLC$_{\Delta COOLAIR\text{-}3}$* has a 685-bp deletion in the *COOLAIR* promoter region where both CRT/DREs are located.

As expected, this mutant failed to express *COOLAIR* even after 14V, which is similar to the $FLC_{\Delta COOLAIR\text{-}1}$ mutant. In contrast, the $FLC_{\Delta COOLAIR\text{-}4}$ mutant, which bears a 301-bp deletion in the distal *COOLAIR* promoter region (upstream of CRT/DREs) and a 13-bp sequence replacement downstream of CRT/DREs, showed a normal vernalization-induced increase in all *COOLAIR* variants, similar to the wild type. This strongly suggests that CRT/DREs located at the *COOLAIR* promoter are critical for CBF-mediated *COOLAIR* induction during vernalization. Notably, the low-abundance convergent antisense transcripts (*CAS*; Zhao et al., 2021) were similarly reduced by 14V in all genotypes, *i.e.*, the wild type and $FLC_{\Delta COOLAIR}$ mutants (**Figures 30 and 32**), suggesting their regulation is independent of *COOLAIR*.

Although the common *COOLAIR* TSS was eliminated in $FLC_{\Delta COOLAIR\text{-}1}$ (**Figure 30**), the proximal *COOLAIR* isoform (type I.i) was still slightly detected by quantitative PCR (qPCR), probably due to alternative TSSs (**Figure 33**). However, the expression of the proximal *COOLAIR* variant in the $FLC_{\Delta COOLAIR\text{-}1}$ mutant was not induced throughout the vernalization period, while the wild type showed type I.i *COOLAIR* peaks at 1V and 20V (**Figure 33**). Furthermore, *CBF3* overexpression did not significantly increase type I.i *COOLAIR* levels in the $FLC_{\Delta COOLAIR\text{-}1}$ mutant, while it caused a strong increase in proximal *COOLAIR* in the wild-type background (Col-0) (**Figure 34**). Taken together, the results strongly suggest that the *COOLAIR* promoter region containing the two CRT/DREs is necessary for the long-term cold response of *COOLAIR*.

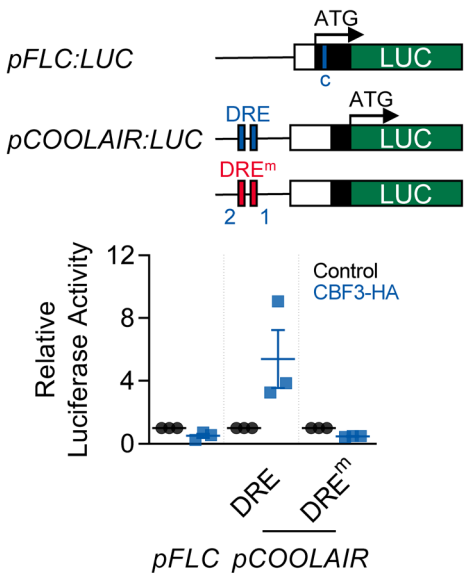

Figure 29. Arabidopsis protoplast transfection assay showing that CBF3 activates *COOLAIR* promoter through CRT/DREs.

A schematic of the reporter constructs used for the luciferase assay is presented in the upper panel. *pFLC:LUC* contains 1 kb of the promoter, the 5′-UTR, and the first exon of *FLC*. The blue line in the *pFLC:LUC* graphic indicates the location of DREc. Wild-type and mutant forms of *pCOOLAIR:LUC* include 1 kb of the *COOLAIR* promoter with the 3′-UTR and the last exon of *FLC*. The blue and red lines mark the positions of the wild-type (DRE) and mutant (DRE^{m}) forms of DRE1 and DRE2, respectively. Each reporter construct was co-transfected into Arabidopsis protoplast together with the *35S:CBF3-HA* effector construct. In parallel, *35S-NOS* plasmid was transfected as a control. The result is shown below. Relative luciferase activities were normalized to that of the *35S-NOS* control. Values have been represented as mean ± SEM of three biological replicates. Dots and squares represent each data point.

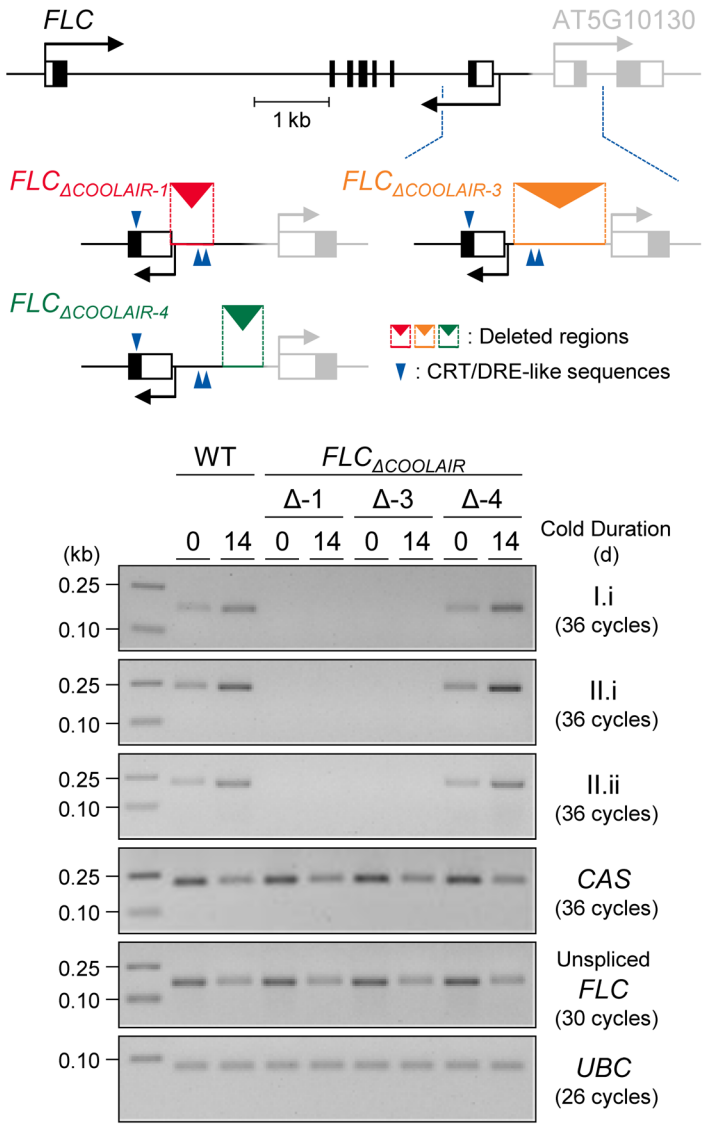

Figure 30. Transcript levels of total *COOLAIR* and *COOLAIR* variants in *FLC*$_{\Delta COOLAIR}$ lines.

Transcript levels of proximal (I.i) and distal (II.i and II.ii) *COOLAIR* isoforms, *CAS*, unspliced *FLC*, and *UBC* in wild-type, *FLC*$_{\Delta COOLAIR\text{-}1}$, *FLC*$_{\Delta COOLAIR\text{-}3}$, and *FLC*$_{\Delta COOLAIR\text{-}4}$ plants before and after 14 days of vernalization, as determined by RT-PCR. *FLC*$_{\Delta COOLAIR\text{-}1}$ and *FLC*$_{\Delta COOLAIR\text{-}3}$ have a 324- and 685-bp deletion of the

COOLAIR promoter region, respectively, where DRE1 and 2 are located. $FLC_{\Delta COOLAIR\text{-}4}$ has a 301-bp deletion in the *COOLAIR* promoter region outside of DRE1 and 2 location. The positions of the deleted region are marked in red, green, and orange lines with reversed triangle in the upper graphic. Blue arrows denote CRT/DRE-like sequences. Black and grey bars denote exons, thin lines denote introns, and white bars denote UTRs of *FLC* and its neighboring gene (AT5G10130). RT-PCR analysis results are shown below. *UBC* was used as a quantitative control.

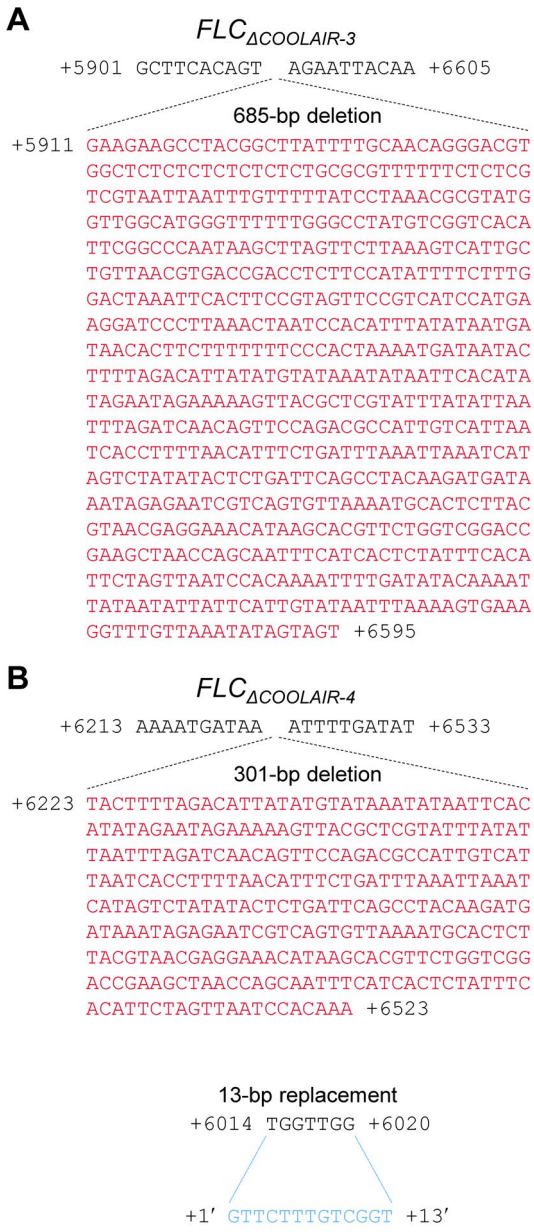

Figure 31. Genomic sequences near the deleted regions in two *COOLAIR* promoter deletion lines, *FLC*$_{\Delta COOLAIR\text{-}3}$ and *FLC*$_{\Delta COOLAIR\text{-}4}$.

(A–B) Genomic sequences around the deleted regions in newly generated *COOLAIR* promoter deletion lines, *FLC*$_{\Delta COOLAIR\text{-}3}$ (A) and *FLC*$_{\Delta COOLAIR\text{-}4}$ (B). Deleted or

replaced sequences are marked in red and cyan, respectively.

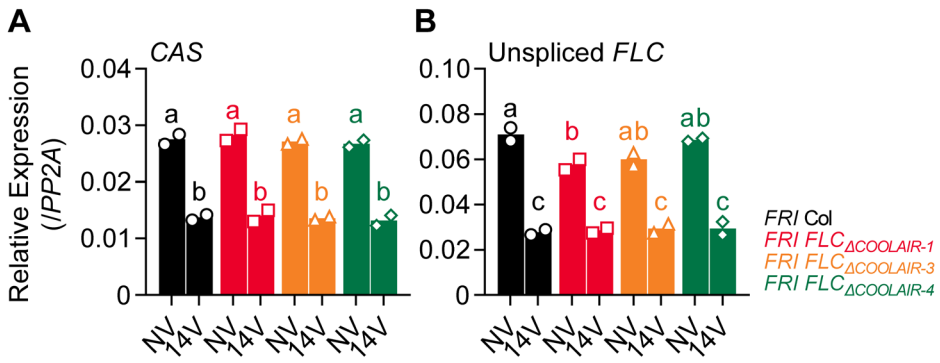

Figure 32. Transcript levels of *CAS* and unspliced *FLC* in *FLC*$_{\Delta COOLAIR}$ lines.

(A–B) Expression levels of *CAS* (A) and unspliced *FLC* (B) in NV or 14V wild-type, *FLC*$_{\Delta COOLAIR\text{-}1}$, *FLC*$_{\Delta COOLAIR\text{-}3}$, and *FLC*$_{\Delta COOLAIR\text{-}4}$ plants, as determined by RT-qPCR. Relative levels were normalized to that of *PP2A*. The mean values obtained from two biological replicates are shown. Open circles, squares, triangles, and polygons represent each data point. Significant differences have been marked using different letters (a–c; $P < 0.05$; two-way ANOVA followed by Tukey's post hoc test).

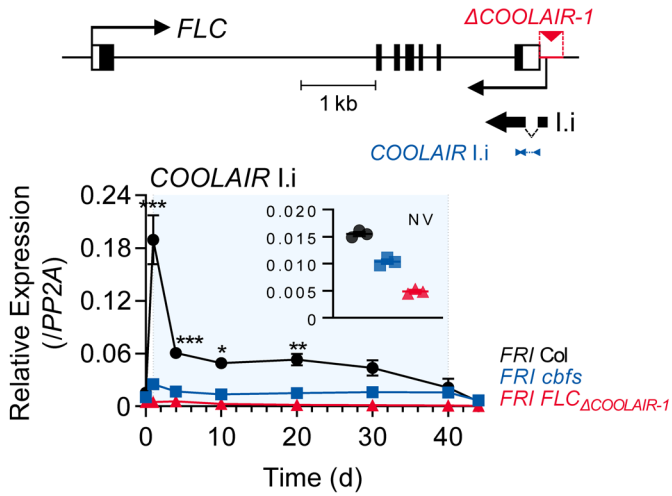

Figure 33. Transcript levels of proximal *COOLAIR* isoform in wild-type, *cbfs*, and $FLC_{\Delta COOLAIR\text{-}1}$ plants during vernalization.

The position of the deleted region in $FLC_{\Delta COOLAIR\text{-}1}$ is marked in red lines with a reversed triangle in the upper graphic. Black bars denote exons, thin lines denote introns, and white bars denote UTRs of *FLC*. The thin black arrow below the gene structure indicates the TSS of *COOLAIR*. The thick black arrow below denotes exons of the type I.i *COOLAIR* variant. The position of the amplicon used for the qPCR analysis is marked with blue arrows. The result of RT-qPCR analysis is presented in the lower panel. Relative transcript levels of type I.i *COOLAIR* in the wild type, *cbfs-1*, and $FLC_{\Delta COOLAIR\text{-}1}$ were normalized to that of *PP2A*. Values have been represented as mean ± SEM of three biological replicates. The blue shading indicates periods under cold treatment. Asterisks indicate a significant difference, as compared to NV (*$P < 0.05$; **$P < 0.01$; ***$P < 0.001$; two-way ANOVA followed by Tukey's post hoc test). Transcript levels of type I.i *COOLAIR* in non-cold treated plants have been re-plotted into the smaller graph with the smaller scale y-axis. Values have been represented as mean ± SEM of three biological replicates. Dots, squares, and triangles represent each data point.

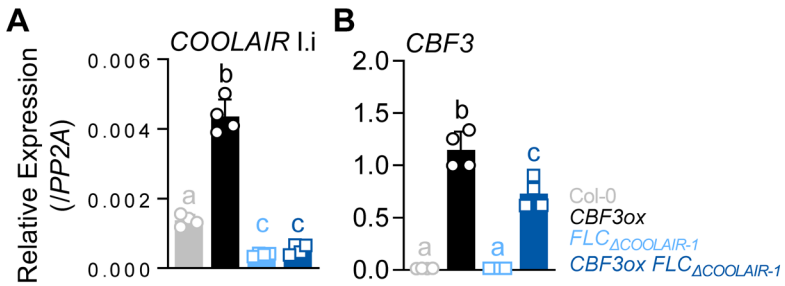

Figure 34. Effect of *CBF3*-overexpression on proximal *COOLAIR* expression in wild-type or *FLC*$_{\Delta COOLAIR}$ background.

(A–B) Expression levels of proximal *COOLAIR* variant I.i (A) and *CBF*3 (B) in NV wild type (Col-0), *pSuper:CBF3-myc* (*CBF3ox*), *FLC*$_{\Delta COOLAIR-1}$, and *pSuper:CBF3-myc FLC*$_{\Delta COOLAIR-1}$ (*CBF3ox FLC*$_{\Delta COOLAIR-1}$). The whole seedlings were collected at 16 days after germination under an SD cycle. Relative levels were normalized to that of *PP2A*. Values have been represented as mean ± SD of four technical replicates from two biological replicates. Open circles and squares represent each data point. Significant differences have been marked using different letters (a–c; $P < 0.05$; one-way ANOVA followed by Tukey's post hoc test).

3.6. CBFs-mediated *COOLAIR* induction during vernalization is not required for *FLC* silencing

Finally, I investigated the role of *COOLAIR* induced by CBFs in the vernalization-triggered *FLC* silencing process. *COOLAIR* was reported to facilitate the removal of H3K36me3 from *FLC* chromatin during vernalization, whereas the other lncRNAs, *COLDAIR* and *COLDWRAP*, are required for H3K27me3 deposition (Csorba et al., 2014; Berry and Dean, 2015; Kim and Sung, 2017b; Zhu et al., 2021). Therefore, I compared the enrichment of H3K4me3, H3K36me3, and H3K27me3 on *FLC* chromatin in non-vernalized or vernalized wild-type and *cbfs* plants. As reported (Bastow et al., 2004; Sung and Amasino, 2004b; Yang et al., 2014), the enrichments of H3K4me3 and H3K36me3 were reduced, but that of H3K27me3 was increased in *FLC* chromatin at 40V in the wild type (**Figure 35**). However, although *COOLAIR* levels were significantly reduced in the *cbfs* mutant (**Figure 22**), vernalization-mediated reductions in H3K4me3 and H3K36me3 levels and an increase in H3K27me3 levels in the *cbfs* mutant were comparable to those in the wild type (**Figure 35**). This result suggests that CBF-mediated *COOLAIR* induction is not required for vernalization-induced epigenetic changes on *FLC* chromatin.

Consistent with the epigenetic changes, the *FLC* level in the *cbfs* mutant was gradually suppressed during the vernalization process, and the suppression was maintained after 40VT4 similar to that observed in the wild type (**Figure 36**). Such result is consistent with the RNA-seq data previously reported using *cbfs* mutants in a SW ecotype (Park et al., 2018b). RNA-seq data analysis showed that the *cbfs* mutant in the SW background exhibited reduced *FLC* levels after 14V, similar to the wild type (**Figure 25**).

Because the results indicate that *COOLAIR* induction is not required for *FLC* silencing and the function of *COOLAIR* in vernalization-induced *FLC* silencing is

still debated (Helliwell et al., 2011; Csorba et al., 2014; Zhao et al., 2021; Zhu et al., 2021), I analyzed whether the loss-of-function mutations $FLC_{\Delta COOLAIR\text{-}1}$ and $FLC_{\Delta COOLAIR\text{-}3}$ result in any defect in the vernalization response. In contrast to the transgenic lines used in previous reports, $FLC_{\Delta COOLAIR\text{-}1}$ and $FLC_{\Delta COOLAIR\text{-}3}$, which have small deletions in the *COOLAIR* promoter region, are unlikely to cause any unexpected effects on *FLC* chromatin. $FLC_{\Delta COOLAIR\text{-}4}$, which has a deletion outside of the CRT/DRE region, exhibited a gradual decrease and eventual silencing of *FLC* by long-term cold, similar to the wild type (**Figure 36**). Interestingly, both $FLC_{\Delta COOLAIR\text{-}1}$ and $FLC_{\Delta COOLAIR\text{-}3}$ mutants exhibited similar decreases and silencing of *FLC* by vernalization (**Figure 36**). These results show that *FLC* is normally silenced by vernalization regardless of *COOLAIR* induction by cold.

Consistent with this, the *cbfs* mutant, compared to the wild type, did not show any difference in the reduction of *FLC* levels upon exposure to a freezing cold for 8 h after NV, 10V, and 20V (**Figure 37**). However, the same freezing cold treatment caused the failure of strong induction of *COOLAIR* in the *cbfs* (**Figure 27**). These results also support that CBF-mediated *COOLAIR* induction is not required for *FLC* silencing by vernalization.

As expected from the *FLC* levels, vernalization-mediated promotion of flowering was comparable in the wild type and *cbfs* (**Figure 38**), indicating that *cbfs* exhibits a normal vernalization response. Consistently, the flowering time of $FLC_{\Delta COOLAIR\text{-}1}$and $FLC_{\Delta COOLAIR\text{-}3}$ was accelerated by vernalization, similar to that of the wild type (**Figures 38 and 39**). These results show that *FLC* silencing occurs regardless of whether *COOLAIR* is induced during a cold exposure that results in vernalization. In summary, the data strongly support that CBFs, upregulated by long-term cold exposure, induce *COOLAIR* expression (**Figure 40**), however, cold-mediated *COOLAIR* induction is not required for *FLC* silencing during vernalization.

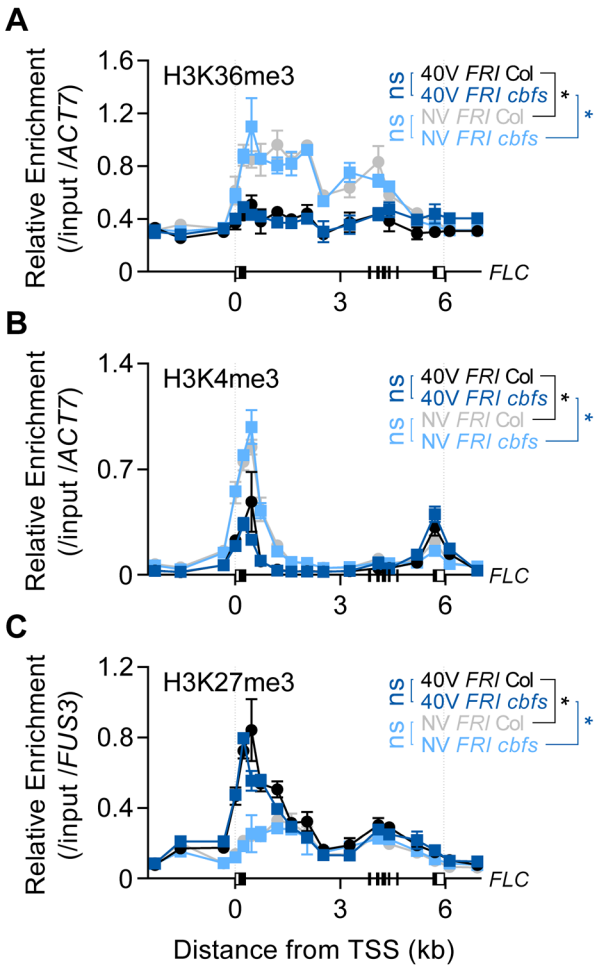

Figure 35. Histone modifications at the *FLC* chromatin in non-vernalized or vernalized wild type and *cbfs* mutant.

(A–C) Enrichments of H3K36me3 (A), H3K4me3 (B), and H3K27me3 (C) on the *FLC* locus in NV or 40V wild-type and *cbfs-1* plants. The whole seedlings were collected at ZT4 under an SD cycle. Modified histones were immunoprecipitated with anti-H3K36me3, anti-H3K4me3, or anti-H3K27me3 antibodies. H3K36me3, H3K4me3, and H3K27me3 enrichments of the IP/5% input were normalized to those of *ACT7* or *FUS3*. Relative enrichments have been represented as mean ± SEM of three biological replicates. One-way ANOVA and Tukey's post hoc test were

performed on the ChIP results obtained using two primer pairs corresponding to the *FLC* nucleation region (Yang et al., 2017). Asterisks indicate a significant difference (*$P < 0.05$). ns, not significant ($P \geq 0.05$).

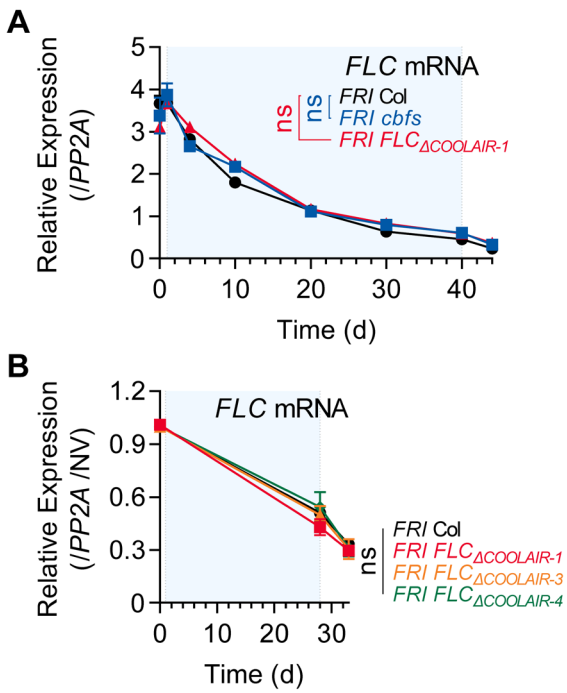

Figure 36. Expression dynamics of *FLC* mRNA in the wild type, *cbfs*, and *FLC*$_{\Delta COOLAIR}$ lines during vernalization.

(A) *FLC* mRNA levels in wild-type, *cbfs-1* and *FLC*$_{\Delta COOLAIR-1}$ plants during and after vernalization. Blue shading denotes cold periods. Relative levels were normalized to that of *PP2A*. Values have been represented as mean ± SEM of three biological replicates. ns, not significant between wild type and mutants, as assessed using two-way ANOVA followed by Tukey's post hoc test ($P \geq 0.05$).

(B) *FLC* mRNA levels in wild-type, *FLC*$_{\Delta COOLAIR-1}$, *FLC*$_{\Delta COOLAIR-3}$, and *FLC*$_{\Delta COOLAIR-4}$ plants during and after vernalization. Blue shading denotes cold periods. Relative levels were normalized to that of *PP2A*, and then normalized to NV of each genotype. Values have been represented as mean ± SEM of three biological replicates. ns, not significant between wild type and mutants, as assessed using two-way ANOVA followed by Tukey's post hoc test ($P \geq 0.05$).

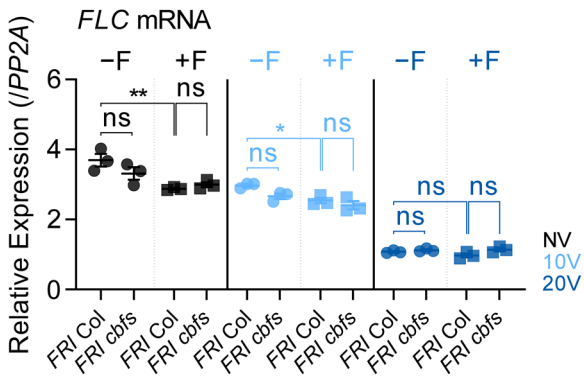

Figure 37. Effect of the first frost-mimicking treatment on the *FLC* mRNA level in the wild type and *cbfs* after vernalization.

NV, 10V, 20V, NV+F, 10V+F, and 20V+F plants were subjected to the treatments described in **Figure 27**. Relative *FLC* mRNA levels in the wild type and *cbfs-1* mutant were normalized to that of *PP2A*. Values have been represented as mean ± SEM of three biological replicates. Dots and squares represent each data point. Asterisks indicate a significant difference (*$P < 0.05$; **$P < 0.01$; two-way ANOVA followed by Tukey's post hoc test). ns, not significant ($P \geq 0.05$).

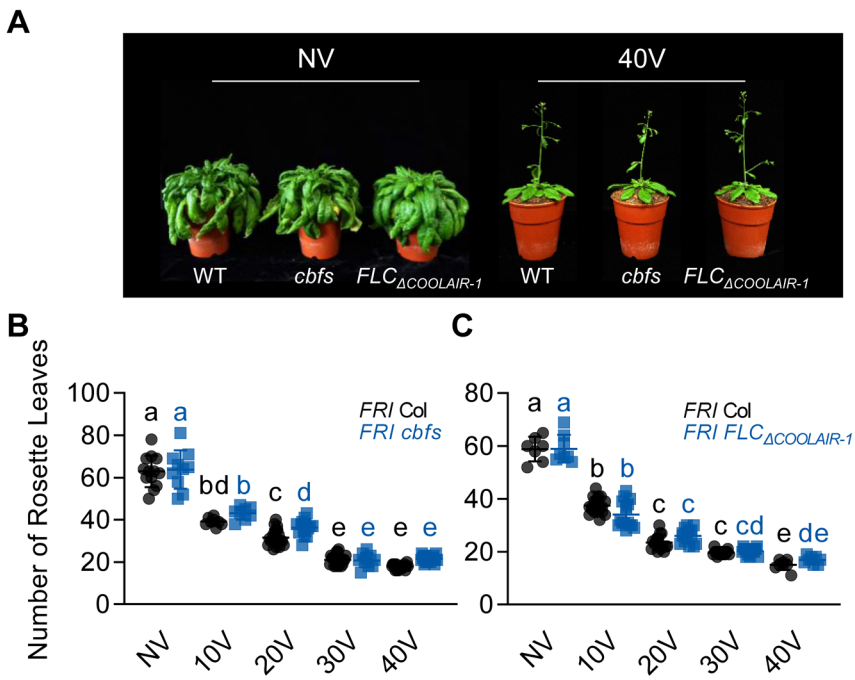

Figure 38. Flowering times of non-vernalized or vernalized wild-type, *cbfs*, and *FLC*$_{\Delta COOLAIR\text{-}1}$ plants.

(A) Photographs of NV and 40V wild type, *cbfs-1*, and *FLC*$_{\Delta COOLAIR\text{-}1}$. NV plants were grown at 22°C under LD and 40V plants were grown at 22°C under LD after being treated for 40V under SD. The photos were taken when the NV plants started to bolt and the 40V plants showed the first open flower.

(B–C) Flowering times of NV and vernalized (10V–40V) wild type and *cbfs-1* (B), and *FLC*$_{\Delta COOLAIR\text{-}1}$ plants (C). Flowering time was measured in terms of the number of rosette leaves produced when bolting. Plants were grown under LD after vernalization treatment. Bars and error bars represent the mean ± SD. Each dot and square indicates individual flowering time. Significant differences have been marked using different letters (a–e; two-way ANOVA followed by Tukey's post hoc test; $P < 0.05$).

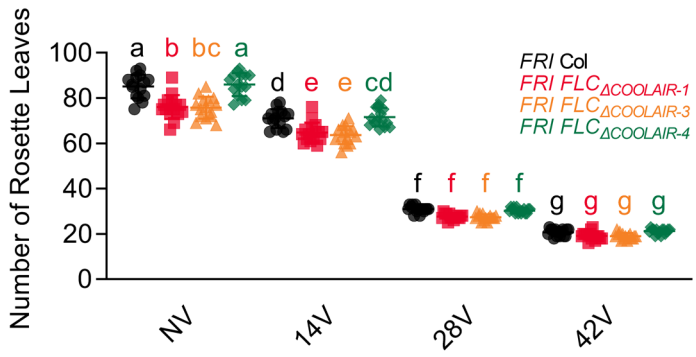

Figure 39. Flowering times of non-vernalized or vernalized wild type and *FLC*$_{\Delta COOLAIR}$ lines.

Flowering times of NV and vernalized (14V–42V) wild-type, *FLC*$_{\Delta COOLAIR\text{-}1}$, *FLC*$_{\Delta COOLAIR\text{-}3}$, and *FLC*$_{\Delta COOLAIR\text{-}4}$ plants. Flowering time was measured in terms of the number of rosette leaves produced when bolting. Plants were grown under LD after vernalization. Bars and error bars indicate the mean ± SD. Each dot, square, triangle, and polygon represents the individual flowering time. Significant differences have been indicated using different letters (a–g; two-way ANOVA followed by Tukey's post hoc test; $P < 0.05$).

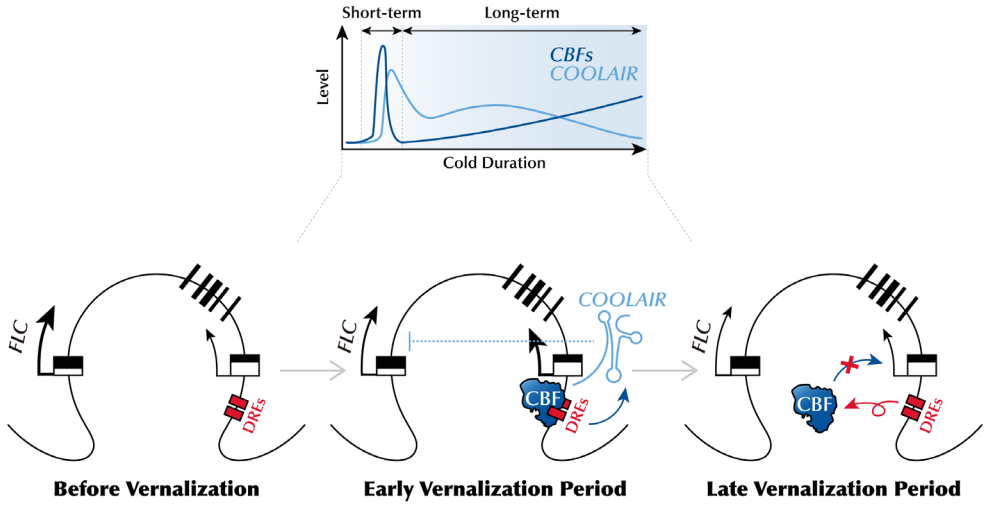

Figure 40. Schematic model describing the regulatory mechanism *COOLAIR* mediated by CBFs during vernalization.

During the early phase of vernalization, increased CBFs upregulate *COOLAIR* expression by binding to CRT/DREs at the 3′-end of *FLC*. In the late phase of vernalization, owing to the silencing of *FLC* chromatin, CBF proteins are released from the CRT/DREs in the *COOLAIR* promoter, which leads to a reduction in *COOLAIR* levels.

Chapter 4

Discussion

4.1. Molecular mechanisms behind the CBFs-mediated regulation of *COOLAIR* expression

Based on the data presented here, I propose a working model (**Figure 40**) in which a prolonged low-temperature environment gradually increases the levels of CBF proteins, which activate *COOLAIR* transcription in the early phase of vernalization by binding to CRT/DREs at the 3′-end of *FLC*.

However, as cold period is extended, CBF proteins are excluded from the *COOLAIR* promoter, probably because silencing of *FLC* chromatin occurs regardless of CBFs level. This may account for a decrease in *COOLAIR* levels during the later phase of vernalization. Consistent with this, a previous report showed a continuous increase in the *COOLAIR* level throughout the vernalization period in the *vin3* mutant, which has a defect in the maintenance of *FLC* silencing (Swiezewski et al., 2009). Thus, VIN3-dependent Polycomb silencing is at least partially involved in the release of CBF proteins from the *COOLAIR* promoter.

Although CBFs are upregulated by cold to trigger *COOLAIR* expression, CBF-mediated *COOLAIR* induction during vernalization is not solely due to increased CBF levels because the *CBF3* overexpression lines still showed *COOLAIR* induction by vernalization (**Figure 26**). This may indicate that additional factors participate in the regulation of CBFs function. As aforementioned, it has previously been reported that low temperatures cause functional activation of CBFs through the degradation of HD2C which maintains an epigenetically inactive state of downstream targets at warm temperatures (Park et al., 2018a). Moreover, cold triggers the monomerization or stabilization of CBF proteins, thereby promoting their functions (Ding et al., 2018; Lee et al., 2021). Similarly, such an additional regulatory mechanism of CBF function may be enhanced by long-term winter cold to fine-tune *COOLAIR* expression.

4.2. Relationship among *COOLAIR*-activating thermosensors

In addition, other thermosensors are likely to facilitate *COOLAIR* induction by vernalization. Recently, it was suggested that NTL8, an NAC domain-containing transcription factor, acts as an upstream regulator of *COOLAIR* (Zhao et al., 2021). NTL8 also binds to the *COOLAIR* promoter region and *COOLAIR* is highly expressed in both dominant mutant alleles, *ntl8-Ds*, and *NTL8*-overexpressing transgenic plants at warm temperatures (O'Malley et al., 2016; Zhao et al., 2021). Thus, it has been proposed that slow accumulation of the NTL8 protein, due to reduced dilution during slower growth at low temperatures, causes *COOLAIR* induction during vernalization.

A WRKY transcription factor, WRKY63, has also been suggested as another inducer of *COOLAIR* transcription during vernalization (Hung et al., 2022). WRKY63 is enriched in the *COOLAIR* promoter region, and *COOLAIR* expression is reduced in the *wrky63* mutant, suggesting that WRKY63 functions as a *COOLAIR* activator. Unlike NTL8, both transcript and protein levels of *WRKY63* are upregulated by vernalization, which may lead to an increase in *COOLAIR* expression.

The binding sites of CBFs, NTL8, and WRKY63 are not much far from each other (O'Malley et al., 2016; Zhao et al., 2021; Hung et al., 2022), perhaps they are mutually interdependent. Hence, it would be worthwhile to elucidate whether NTL8, WRKY63, and CBFs synergistically activate *COOLAIR* transcription during vernalization. The reason why vernalization-triggered *COOLAIR* induction requires more than one thermosensor is unclear. Presumably, multiple thermosensory modules ensure precise and robust *COOLAIR* expression during winter, when the temperature fluctuates.

4.3. Function of *COOLAIR* in vernalization

Transcription of *COOLAIR* has been proposed to govern the *FLC* chromatin environment in both warm and cold temperatures (Csorba et al., 2014; Fang et al., 2020; Xu et al., 2021b). Previous studies have inferred that *COOLAIR* is required to remove H3K36me3 from *FLC* chromatin, especially under low-temperature conditions. This argument is supported by the delayed H3K36me3 removal in vernalized *FLC-TEX* transgenic plants, where the *COOLAIR* promoter is substituted by the *rbcs3B* terminator sequence (Csorba et al., 2014; Marquardt et al., 2014; Wang et al., 2014). In addition, *COOLAIR* is reported to promote condensation of FRI upon cold exposure (Zhu et al., 2021). Thus, FRI is sequestered from the *FLC* promoter as a nuclear condensate, which causes the transcriptional repression of *FLC*. Therefore, it has been suggested that vernalization-induced *COOLAIR* prevents the activation of *FLC* by the FRI complex and causes epigenetic silencing of *FLC* chromatin through a decrease of H3K36me3 during the vernalization process.

However, there is some controversy as to whether *COOLAIR* is required for vernalization and the associated *FLC* silencing. In contrast to the *FLC-TEX* lines, some T-DNA insertion lines which lack *COOLAIR* induction by long-term cold exposure show a normal vernalization response (Helliwell et al., 2011). Likewise, the results from this study show that *COOLAIR* transcription is not required for the epigenetic silencing of *FLC*. The *cbfs* mutant, which exhibits severely reduced *COOLAIR* induction, shows relatively normal vernalization responses such that flowering time is fairly well accelerated and active histone marks, H3K36me3 and H3K4me3, are reduced in *FLC* chromatin while the repressive histone mark, H3K27me3, is increased in *FLC* chromatin, similar to the wild type (**Figures 22, 35–38**). Consistently, $FLC_{\Delta COOLAIR\text{-}1}$, and $FLC_{\Delta COOLAIR\text{-}3}$ mutants, which have almost undetectable levels of *COOLAIR*, exhibit both *FLC* suppression and flowering

acceleration by vernalization similar to that seen in the wild type (**Figures 36, 38, and 39**). Moreover, the freezing treatment mimicking the first frost did not affect *FLC* suppression in the *cbfs*, although the mutant showed defects in CBF-mediated *COOLAIR* induction (**Figures 27 and 37**). It is noteworthy that my finding that vernalization and the associated *FLC* silencing do not require *COOLAIR* expression was obtained using mutant lines, *cbfs* and $FLC_{\Delta COOLAIR}$, rather than the transgenic lines used in previous studies. Thus, I can exclude the possibility that transgenes somehow provide cryptic promoters or cause unexpected epigenetic effects.

COOLAIR is highly conserved among Arabidopsis relatives (Castaings et al., 2014), thus, my finding that *COOLAIR* is not required for vernalization-induced *FLC* silencing is surprising. There are several caveats in the studies of *COOLAIR* function. First, different experimental schemes may affect the vernalization response differently. A recent study of plants grown in conditions with fluctuating temperatures designed to mimic natural environments may indicate a role for *COOLAIR* in vernalization-mediated *FLC* repression (Zhao et al., 2021), and perhaps fluctuating temperatures that mimic field conditions may have different effects on the vernalization response of *cbfs* or $FLC_{\Delta COOLAIR}$ mutants as well. However, the experiments in most studies that claimed a role for *COOLAIR* in vernalization were performed in laboratory conditions with controlled temperatures as in this study. If indeed *COOLAIR* does have a role in vernalization in specific environmental conditions, the lack of a role for *COOLAIR* in vernalization in other conditions such as those in this study may be due to functional redundancy between *COOLAIR* and other *FLC* repressors such that other repressors, such as *COLDAIR*, obscure the effect of *COOLAIR* on *FLC* silencing, as has been proposed before (Castaings et al., 2014). This issue should be addressed in future studies.

Chapter 5

Conclusion

Winter is challenging for sessile plants: cold weather makes reproduction difficult, and frost threatens survival. Cold acclimation and vernalization, the two types of low-temperature memories, allow plants to overcome this harsh season by making them more viable during winter or flowering in the subsequent warm spring (Thomashow, 1999; Michaels and Amasino, 2000). Although it is well understood how plants recognize and remember short-term cold exposure to increase frost hardiness, there is still much to know about the long-term cold sensing mechanism that establishes the ability to flower.

FLC orthologs from a range of *A. thaliana* relatives express the vernalization-induced antisense lncRNA, *COOLAIR* (Castaings et al., 2014). As the proximal sequence blocks within the *COOLAIR* promoters are conserved, they are likely targets of cold sensor modules. This study shows that CBF proteins act as cold sensors binding to the CRT/DREs in the conserved promoter region, thereby activating the transcription of *COOLAIR*.

Although short-term and long-term cold memories elicit different developmental responses, both are triggered by the same physical environment. Therefore, it is not surprising that a common signaling network governs both processes. *CBF* genes have been highlighted for their roles in cold acclimation (Gilmour et al., 1998; Liu et al., 1998; Jia et al., 2016; Zhao et al., 2016). CBFs rapidly accumulate upon short-term cold exposure, thereby activating the transcription of cold-responsive genes, such as *COR15A* and *RD29A* (Stockinger et al., 1997; Liu et al., 1998). Interestingly, CBFs are also highly accumulated during vernalization and mediate long-term cold-induced *COOLAIR* expression. Hence, my results indicate that the cold signaling pathways that establish the short-term and long-term cold responses are not sharply distinguishable, as suggested previously (Sung and Amasino, 2004a; Seo et al., 2009).

References

Angel A, Song J, Dean C, Howard M (2011) A Polycomb-based switch underlying quantitative epigenetic memory. *Nature* **476:** 105-108. doi: 10.1038/nature10241

Baker SS, Wilhelm KS, Thomashow MF (1994) The 5'-region of *Arabidopsis thaliana cor15a* has *cis*-acting elements that confer cold-, drought- and ABA-regulated gene expression. *Plant Mol Biol* **24:** 701-713. doi: 10.1007/BF00029852

Bastow R, Mylne JS, Lister C, Lippman Z, Martienssen RA, Dean C (2004) Vernalization requires epigenetic silencing of *FLC* by histone methylation. *Nature* **427:** 164-167. doi: 10.1038/nature02269

Berry S, Dean C (2015) Environmental perception and epigenetic memory: Mechanistic insight through *FLC*. *Plant J* **83:** 133-148. doi: 10.1111/tpj.12869

Castaings L, Bergonzi S, Albani MC, Kemi U, Savolainen O, Coupland G (2014) Evolutionary conservation of cold-induced antisense RNAs of *FLOWERING LOCUS C* in *Arabidopsis thaliana* perennial relatives. *Nat Commun* **5:** 4457. doi: 10.1038/ncomms5457

Chinnusamy V, Zhu J, Zhu JK (2007) Cold stress regulation of gene expression in plants. *Trends Plant Sci* **12:** 444-451. doi: 10.1016/j.tplants.2007.07.002

Choi K, Kim J, Hwang HJ, Kim S, Park C, Kim SY, Lee I (2011) The FRIGIDA complex activates transcription of *FLC*, a strong flowering repressor in *Arabidopsis*, by recruiting chromatin modification factors. *Plant Cell* **23:** 289-303. doi: 10.1105/tpc.110.075911

Chouard P (1960) Vernalization and its relations to dormancy. *Annu Rev Plant Phys* **11:** 191-238. doi: 10.1146/annurev.pp.11.060160.001203

Csorba T, Questa JI, Sun Q, Dean C (2014) Antisense *COOLAIR* mediates the coordinated switching of chromatin states at *FLC* during vernalization. *Proc Natl Acad Sci U S A* **111:** 16160-16165. doi: 10.1073/pnas.1419030111

De Lucia F, Crevillen P, Jones AM, Greb T, Dean C (2008) A PHD-Polycomb

Repressive Complex 2 triggers the epigenetic silencing of *FLC* during vernalization. *Proc Natl Acad Sci U S A* **105:** 16831-16836. doi: 10.1073/pnas.0808687105

Ding Y, Jia Y, Shi Y, Zhang X, Song C, Gong Z, Yang S (2018) OST1-mediated BTF3L phosphorylation positively regulates CBFs during plant cold responses. *EMBO J* **37**. doi: 10.15252/embj.201798228

Ding Y, Shi Y, Yang S (2019) Advances and challenges in uncovering cold tolerance regulatory mechanisms in plants. *New Phytol* **222:** 1690-1704. doi: 10.1111/nph.15696

Ding Y, Yang S (2022) Surviving and thriving: How plants perceive and respond to temperature stress. *Dev Cell* **57:** 947-958. doi: 10.1016/j.devcel.2022.03.010

Doherty CJ, Van Buskirk HA, Myers SJ, Thomashow MF (2009) Roles for *Arabidopsis* CAMTA transcription factors in cold-regulated gene expression and freezing tolerance. *Plant Cell* **21:** 972-984. doi: 10.1105/tpc.108.063958

Dong MA, Farré EM, Thomashow MF (2011) CIRCADIAN CLOCK-ASSOCIATED 1 and LATE ELONGATED HYPOCOTYL regulate expression of the C-REPEAT BINDING FACTOR (CBF) pathway in *Arabidopsis*. *Proc Natl Acad Sci U S A* **108:** 7241-7246. doi: 10.1073/pnas.1103741108

Eremina M, Unterholzner SJ, Rathnayake AI, Castellanos M, Khan M, Kugler KG, May ST, Mayer KF, Rozhon W, Poppenberger B (2016) Brassinosteroids participate in the control of basal and acquired freezing tolerance of plants. *Proc Natl Acad Sci U S A* **113:** E5982-E5991. doi: 10.1073/pnas.1611477113

Fang X, Wang L, Ishikawa R, Li Y, Fiedler M, Liu F, Calder G, Rowan B, Weigel D, Li P, Dean C (2019) *Arabidopsis* FLL2 promotes liquid-liquid phase separation of polyadenylation complexes. *Nature* **569:** 265-269. doi: 10.1038/s41586-019-1165-8

Fang X, Wu Z, Raitskin O, Webb K, Voigt P, Lu T, Howard M, Dean C (2020) The 3' processing of antisense RNAs physically links to chromatin-based transcriptional control. *Proc Natl Acad Sci U S A* **117:** 15316-15321. doi:

10.1073/pnas.2007268117

Finnegan EJ, Bond DM, Buzas DM, Goodrich J, Helliwell CA, Tamada Y, Yun JY, Amasino RM, Dennis ES (2011) Polycomb proteins regulate the quantitative induction of *VERNALIZATION INSENSITIVE 3* in response to low temperatures. *Plant J* **65:** 382-391. doi: 10.1111/j.1365-313X.2010.04428.x

Fowler S, Thomashow MF (2002) Arabidopsis transcriptome profiling indicates that multiple regulatory pathways are activated during cold acclimation in addition to the CBF cold response pathway. *Plant Cell* **14:** 1675-1690. doi: 10.1105/tpc.003483

Gilmour SJ, Fowler SG, Thomashow MF (2004) Arabidopsis transcriptional activators CBF1, CBF2, and CBF3 have matching functional activities. *Plant Mol Biol* **54:** 767-781. doi: 10.1023/B:PLAN.0000040902.06881.d4

Gilmour SJ, Hajela RK, Thomashow MF (1988) Cold acclimation in *Arabidopsis thaliana*. *Plant Physiol* **87:** 745-750. doi: 10.1104/pp.87.3.745

Gilmour SJ, Zarka DG, Stockinger EJ, Salazar MP, Houghton JM, Thomashow MF (1998) Low temperature regulation of the *Arabidopsis* CBF family of AP2 transcriptional activators as an early step in cold-induced *COR* gene expression. *Plant J* **16:** 433-442. doi: 10.1046/j.1365-313x.1998.00310.x

Guy CL (1990) Cold acclimation and freezing stress tolerance: Role of protein metabolism. *Annu Rev Plant Physiol Plant Mol Biol* **41:** 187-223. doi: 10.1146/annurev.pp.41.060190.001155

Hajela RK, Horvath DP, Gilmour SJ, Thomashow MF (1990) Molecular cloning and expression of *cor* (*co*ld-*r*egulated) genes in *Arabidopsis thaliana*. *Plant Physiol* **93:** 1246-1252. doi: 10.1104/pp.93.3.1246

Helliwell CA, Robertson M, Finnegan EJ, Buzas DM, Dennis ES (2011) Vernalization-repression of Arabidopsis *FLC* requires promoter sequences but not antisense transcripts. *PLoS One* **6:** e21513. doi: 10.1371/journal.pone.0021513

Helliwell CA, Wood CC, Robertson M, James Peacock W, Dennis ES (2006) The Arabidopsis FLC protein interacts directly *in vivo* with *SOC1* and *FT*

chromatin and is part of a high-molecular-weight protein complex. *Plant J* **46:** 183-192. doi: 10.1111/j.1365-313X.2006.02686.x

Heo JB, Sung S (2011) Vernalization-mediated epigenetic silencing by a long intronic noncoding RNA. *Science* **331:** 76-79. doi: 10.1126/science.1197349

Hung FY, Shih YH, Lin PY, Feng YR, Li C, Wu K (2022) WRKY63 transcriptional activation of *COOLAIR* and *COLDAIR* regulates vernalization-induced flowering. *Plant Physiol*. doi: 10.1093/plphys/kiac295

Hwang I, Sheen J (2001) Two-component circuitry in *Arabidopsis* cytokinin signal transduction. *Nature* **413:** 383-389. doi: 10.1038/35096500

Jia Y, Ding Y, Shi Y, Zhang X, Gong Z, Yang S (2016) The *cbfs* triple mutants reveal the essential functions of *CBFs* in cold acclimation and allow the definition of CBF regulons in *Arabidopsis*. *New Phytol* **212:** 345-353. doi: 10.1111/nph.14088

Johanson U, West J, Lister C, Michaels S, Amasino R, Dean C (2000) Molecular analysis of *FRIGIDA*, a major determinant of natural variation in *Arabidopsis* flowering time. *Science* **290:** 344-347. doi: 10.1126/science.290.5490.344

Kidokoro S, Yoneda K, Takasaki H, Takahashi F, Shinozaki K, Yamaguchi-Shinozaki K (2017) Different cold-signaling pathways function in the responses to rapid and gradual decreases in temperature. *Plant Cell* **29:** 760-774. doi: 10.1105/tpc.16.00669

Kim DH, Sung S (2013) Coordination of the vernalization response through a *VIN3* and *FLC* gene family regulatory network in *Arabidopsis*. *Plant Cell* **25:** 454-469. doi: 10.1105/tpc.112.104760

Kim DH, Sung S (2017a) The binding specificity of the PHD-finger domain of VIN3 moderates vernalization response. *Plant Physiol* **173:** 1258-1268. doi: 10.1104/pp.16.01320

Kim DH, Sung S (2017b) Vernalization-triggered intragenic chromatin loop formation by long noncoding RNAs. *Dev Cell* **40:** 302-312 e304. doi: 10.1016/j.devcel.2016.12.021

Kim DH, Zografos BR, Sung S (2010) Mechanisms underlying vernalization-mediated *VIN3* induction in Arabidopsis. *Plant Signal Behav* **5:** 1457-1459. doi: 10.4161/psb.5.11.13465

Kim Y, Park S, Gilmour SJ, Thomashow MF (2013) Roles of CAMTA transcription factors and salicylic acid in configuring the low-temperature transcriptome and freezing tolerance of Arabidopsis. *Plant J* **75:** 364-376. doi: 10.1111/tpj.12205

Kyung J, Jeon M, Jeong G, Shin Y, Seo E, Yu J, Kim H, Park CM, Hwang D, Lee I (2022a) The two clock proteins CCA1 and LHY activate *VIN3* transcription during vernalization through the vernalization-responsive cis-element. *Plant Cell* **34:** 1020-1037. doi: 10.1093/plcell/koab304

Kyung J, Jeon M, Lee I (2022b) Recent advances in the chromatin-based mechanism of *FLOWERING LOCUS C* repression through autonomous pathway genes. *Front Plant Sci* **13:** 964931. doi: 10.3389/fpls.2022.964931

Lang A (1952) Physiology of Flowering. *Annu Rev Plant Phys* **3:** 265-306. doi: DOI 10.1146/annurev.pp.03.060152.001405

Lee ES, Park JH, Wi SD, Kang CH, Chi YH, Chae HB, Paeng SK, Ji MG, Kim WY, Kim MG, Yun DJ, Stacey G, Lee SY (2021) Redox-dependent structural switch and CBF activation confer freezing tolerance in plants. *Nat Plants* **7:** 914-922. doi: 10.1038/s41477-021-00944-8

Lee H, Suh SS, Park E, Cho E, Ahn JH, Kim SG, Lee JS, Kwon YM, Lee I (2000) The AGAMOUS-LIKE 20 MADS domain protein integrates floral inductive pathways in *Arabidopsis*. *Genes Dev* **14:** 2366-2376. doi: 10.1101/gad.813600

Lee I, Bleecker A, Amasino R (1993) Analysis of naturally occurring late flowering in *Arabidopsis thaliana*. *Mol Gen Genet* **237:** 171-176. doi: 10.1007/BF00282798

Lee I, Michaels SD, Masshardt AS, Amasino RM (1994) The late-flowering phenotype of *FRIGIDA* and mutations in *LUMINIDEPENDENS* is suppressed in the Landsberg *erecta* strain of *Arabidopsis*. *Plant J* **6:** 903-909. doi: 10.1046/j.1365-313X.1994.6060903.x

Li H, Ye K, Shi Y, Cheng J, Zhang X, Yang S (2017) BZR1 positively regulates freezing tolerance via CBF-dependent and CBF-independent pathways in *Arabidopsis*. *Mol Plant* **10:** 545-559. doi: 10.1016/j.molp.2017.01.004

Li Z, Jiang D, He Y (2018) FRIGIDA establishes a local chromosomal environment for *FLOWERING LOCUS C* mRNA production. *Nat Plants* **4:** 836-846. doi: 10.1038/s41477-018-0250-6

Liu F, Marquardt S, Lister C, Swiezewski S, Dean C (2010) Targeted 3' processing of antisense transcripts triggers *Arabidopsis FLC* chromatin silencing. *Science* **327:** 94-97. doi: 10.1126/science.1180278

Liu F, Quesada V, Crevillén P, Bäurle I, Swiezewski S, Dean C (2007) The *Arabidopsis* RNA-binding protein FCA requires a lysine-specific demethylase 1 homolog to downregulate *FLC*. *Mol Cell* **28:** 398-407. doi: 10.1016/j.molcel.2007.10.018

Liu Q, Kasuga M, Sakuma Y, Abe H, Miura S, Yamaguchi-Shinozaki K, Shinozaki K (1998) Two transcription factors, DREB1 and DREB2, with an EREBP/AP2 DNA binding domain separate two cellular signal transduction pathways in drought- and low-temperature-responsive gene expression, respectively, in Arabidopsis. *Plant Cell* **10:** 1391-1406. doi: 10.1105/tpc.10.8.1391

Liu Z, Jia Y, Ding Y, Shi Y, Li Z, Guo Y, Gong Z, Yang S (2017) Plasma membrane CRPK1-mediated phosphorylation of 14-3-3 proteins induces their nuclear import to fine-tune CBF signaling during cold response. *Mol Cell* **66:** 117-128 e115. doi: 10.1016/j.molcel.2017.02.016

Luo X, Chen T, Zeng X, He D, He Y (2019) Feedback regulation of *FLC* by *FLOWERING LOCUS T* (*FT*) and *FD* through a 5' *FLC* promoter region in *Arabidopsis*. *Mol Plant* **12:** 285-288. doi: 10.1016/j.molp.2019.01.013

Marquardt S, Raitskin O, Wu Z, Liu F, Sun Q, Dean C (2014) Functional consequences of splicing of the antisense transcript *COOLAIR* on *FLC* transcription. *Mol Cell* **54:** 156-165. doi: 10.1016/j.molcel.2014.03.026

Maruyama K, Sakuma Y, Kasuga M, Ito Y, Seki M, Goda H, Shimada Y, Yoshida S, Shinozaki K, Yamaguchi-Shinozaki K (2004) Identification of

cold-inducible downstream genes of the *Arabidopsis* DREB1A/CBF3 transcriptional factor using two microarray systems. *Plant J* **38:** 982-993. doi: 10.1111/j.1365-313X.2004.02100.x

McKhann HI, Gery C, Bérard A, Lévêque S, Zuther E, Hincha DK, De Mita S, Brunel D, Téoulé E (2008) Natural variation in CBF gene sequence, gene expression and freezing tolerance in the Versailles core collection of Arabidopsis thaliana. *BMC Plant Biol* **8:** 105. doi: 10.1186/1471-2229-8-105

Medina J, Bargues M, Terol J, Pérez-Alonso M, Salinas J (1999) The Arabidopsis *CBF* gene family is composed of three genes encoding AP2 domain-containing proteins whose expression Is regulated by low temperature but not by abscisic acid or dehydration. *Plant Physiol* **119:** 463-470. doi: 10.1104/pp.119.2.463

Michaels SD, Amasino RM (1999) *FLOWERING LOCUS C* encodes a novel MADS domain protein that acts as a repressor of flowering. *Plant Cell* **11:** 949-956. doi: 10.1105/tpc.11.5.949

Michaels SD, Amasino RM (2000) Memories of winter: Vernalization and the competence to flower. *Plant Cell Environ* **23:** 1145-1153. doi: 10.1046/j.1365-3040.2000.00643.x

Michaels SD, Amasino RM (2001) Loss of *FLOWERING LOCUS C* activity eliminates the late-flowering phenotype of *FRIGIDA* and autonomous pathway mutations but not responsiveness to vernalization. *Plant Cell* **13:** 935-941. doi: 10.1105/tpc.13.4.935

Michaels SD, Himelblau E, Kim SY, Schomburg FM, Amasino RM (2005) Integration of flowering signals in winter-annual Arabidopsis. *Plant Physiol* **137:** 149-156. doi: 10.1104/pp.104.052811

Mylne JS, Barrett L, Tessadori F, Mesnage S, Johnson L, Bernatavichute YV, Jacobsen SE, Fransz P, Dean C (2006) LHP1, the *Arabidopsis* homologue of HETEROCHROMATIN PROTEIN1, is required for epigenetic silencing of *FLC*. *Proc Natl Acad Sci U S A* **103:** 5012-5017. doi: 10.1073/pnas.0507427103

Napp-Zinn K (1955) Genetische grundlagen des Kältebedürfnisses bei *Arabidopsis thaliana* (L.) Heynh. *Naturwissenschaften* **42:** 650-650. doi: 10.1007/Bf00622395

Nishio H, Buzas DM, Nagano AJ, Suzuki Y, Sugano S, Ito M, Morinaga S, Kudoh H (2016) From the laboratory to the field: assaying histone methylation at *FLOWERING LOCUS C* in naturally growing *Arabidopsis halleri*. *Genes Genet Syst* **91:** 15-26. doi: 10.1266/ggs.15-00071

Novillo F, Medina J, Salinas J (2007) *Arabidopsis* CBF1 and CBF3 have a different function than CBF2 in cold acclimation and define different gene classes in the CBF regulon. *Proc Natl Acad Sci U S A* **104:** 21002-21007. doi: 10.1073/pnas.0705639105

O'Malley RC, Huang SC, Song L, Lewsey MG, Bartlett A, Nery JR, Galli M, Gallavotti A, Ecker JR (2016) Cistrome and epicistrome features shape the regulatory DNA landscape. *Cell* **165:** 1280-1292. doi: 10.1016/j.cell.2016.04.038

Park J, Lim CJ, Shen M, Park HJ, Cha JY, Iniesto E, Rubio V, Mengiste T, Zhu JK, Bressan RA, Lee SY, Lee BH, Jin JB, Pardo JM, Kim WY, Yun DJ (2018a) Epigenetic switch from repressive to permissive chromatin in response to cold stress. *Proc Natl Acad Sci U S A* **115:** E5400-E5409. doi: 10.1073/pnas.1721241115

Park S, Gilmour SJ, Grumet R, Thomashow MF (2018b) CBF-dependent and CBF-independent regulatory pathways contribute to the differences in freezing tolerance and cold-regulated gene expression of two Arabidopsis ecotypes locally adapted to sites in Sweden and Italy. *PLoS One* **13:** e0207723. doi: 10.1371/journal.pone.0207723

Park S, Lee CM, Doherty CJ, Gilmour SJ, Kim Y, Thomashow MF (2015) Regulation of the Arabidopsis CBF regulon by a complex low-temperature regulatory network. *Plant J* **82:** 193-207. doi: 10.1111/tpj.12796

Penfield S (2008) Temperature perception and signal transduction in plants. *New Phytol* **179:** 615-628. doi: 10.1111/j.1469-8137.2008.02478.x

Qüesta JI, Song J, Geraldo N, An H, Dean C (2016) *Arabidopsis* transcriptional

repressor VAL1 triggers Polycomb silencing at *FLC* during vernalization. *Science* **353:** 485-488. doi: 10.1126/science.aaf7354

Seo E, Lee H, Jeon J, Park H, Kim J, Noh YS, Lee I (2009) Crosstalk between cold response and flowering in *Arabidopsis* is mediated through the flowering-time gene *SOC1* and its upstream negative regulator *FLC*. *Plant Cell* **21:** 3185-3197. doi: 10.1105/tpc.108.063883

Seo PJ, Park MJ, Lim MH, Kim SG, Lee M, Baldwin IT, Park CM (2012) A self-regulatory circuit of CIRCADIAN CLOCK-ASSOCIATED1 underlies the circadian clock regulation of temperature responses in *Arabidopsis*. *Plant Cell* **24:** 2427-2442. doi: 10.1105/tpc.112.098723

Sheldon CC, Burn JE, Perez PP, Metzger J, Edwards JA, Peacock WJ, Dennis ES (1999) The *FLF* MADS box gene: A repressor of flowering in Arabidopsis regulated by vernalization and methylation. *Plant Cell* **11:** 445-458. doi: 10.1105/tpc.11.3.445

Sheldon CC, Rouse DT, Finnegan EJ, Peacock WJ, Dennis ES (2000) The molecular basis of vernalization: The central role of *FLOWERING LOCUS C* (*FLC*). *Proc Natl Acad Sci U S A* **97:** 3753-3758. doi: 10.1073/pnas.97.7.3753

Shi Y, Ding Y, Yang S (2018) Molecular regulation of CBF signaling in cold acclimation. *Trends Plant Sci* **23:** 623-637. doi: 10.1016/j.tplants.2018.04.002

Shindo C, Aranzana MJ, Lister C, Baxter C, Nicholls C, Nordborg M, Dean C (2005) Role of *FRIGIDA* and *FLOWERING LOCUS C* in determining variation in flowering time of Arabidopsis. *Plant Physiol* **138:** 1163-1173. doi: 10.1104/pp.105.061309

Shinozaki K, Yamaguchi-Shinozaki K, Seki M (2003) Regulatory network of gene expression in the drought and cold stress responses. *Curr Opin Plant Biol* **6:** 410-417. doi: 10.1016/s1369-5266(03)00092-x

Shu H, Nakamura M, Siretskiy A, Borghi L, Moraes I, Wildhaber T, Gruissem W, Hennig L (2014) *Arabidopsis* replacement histone variant H3.3 occupies promoters of regulated genes. *Genome Biol* **15:** R62. doi: 10.1186/gb-2014-

15-4-r62

Song Y, Zhang X, Li M, Yang H, Fu D, Lv J, Ding Y, Gong Z, Shi Y, Yang S (2021) The direct targets of CBFs: In cold stress response and beyond. *J Integr Plant Biol* **63:** 1874-1887. doi: 10.1111/jipb.13161

Srikanth A, Schmid M (2011) Regulation of flowering time: all roads lead to Rome. *Cell Mol Life Sci* **68:** 2013-2037. doi: 10.1007/s00018-011-0673-y

Stockinger EJ, Gilmour SJ, Thomashow MF (1997) *Arabidopsis thaliana CBF1* encodes an AP2 domain-containing transcriptional activator that binds to the C-repeat/DRE, a cis-acting DNA regulatory element that stimulates transcription in response to low temperature and water deficit. *Proc Natl Acad Sci U S A* **94:** 1035-1040. doi: 10.1073/pnas.94.3.1035

Sung S, Amasino RM (2004a) Vernalization and epigenetics: how plants remember winter. *Curr Opin Plant Biol* **7:** 4-10. doi: 10.1016/j.pbi.2003.11.010

Sung S, Amasino RM (2004b) Vernalization in *Arabidopsis thaliana* is mediated by the PHD finger protein VIN3. *Nature* **427:** 159-164. doi: 10.1038/nature02195

Sung S, He Y, Eshoo TW, Tamada Y, Johnson L, Nakahigashi K, Goto K, Jacobsen SE, Amasino RM (2006) Epigenetic maintenance of the vernalized state in Arabidopsis thaliana requires LIKE HETEROCHROMATIN PROTEIN 1. *Nat Genet* **38:** 706-710. doi: 10.1038/ng1795

Swiezewski S, Liu F, Magusin A, Dean C (2009) Cold-induced silencing by long antisense transcripts of an *Arabidopsis* Polycomb target. *Nature* **462:** 799-802. doi: 10.1038/nature08618

Thomashow MF (1999) PLANT COLD ACCLIMATION: Freezing tolerance genes and regulatory mechanisms. *Annu Rev Plant Physiol Plant Mol Biol* **50:** 571-599. doi: 10.1146/annurev.arplant.50.1.571

Thomashow MF (2010) Molecular basis of plant cold acclimation: Insights gained from studying the CBF cold response pathway. *Plant Physiol* **154:** 571-577. doi: 10.1104/pp.110.161794

Thomashow MF, Stockinger EJ, Jaglo-Ottosen KR, Gilmour SJ, Zarka DG

(1997) Function and regulation of *Arabidopsis thaliana COR* (cold-regulated) genes. *Acta Physiol Plant* **19:** 497-504. doi: 10.1007/s11738-997-0046-1

Wada KC, Takeno K (2010) Stress-induced flowering. *Plant Signal Behav* **5:** 944-947. doi: 10.4161/psb.5.8.11826

Wang ZW, Wu Z, Raitskin O, Sun Q, Dean C (2014) Antisense-mediated *FLC* transcriptional repression requires the P-TEFb transcription elongation factor. *Proc Natl Acad Sci U S A* **111:** 7468-7473. doi: 10.1073/pnas.1406635111

Weinig C, Schmitt J (2004) Environmental effects on the expression of quantitative trait loci and implications for phenotypic evolution. *Bioscience* **54:** 627-635. doi: 10.1641/0006-3568(2004)054[0627:EEOTEO]2.0.CO;2

Weiser CJ (1970) Cold resistance and injury in woody plants: Knowledge of hardy plant adaptations to freezing stress may help us to reduce winter damage. *Science* **169:** 1269-1278. doi: 10.1126/science.169.3952.1269

Went FW (1953) The effect of temperature on plant growth. *Annu Rev Plant Phys* **4:** 347-362. doi: 10.1146/annurev.pp.04.060153.002023

Wood CC, Robertson M, Tanner G, Peacock WJ, Dennis ES, Helliwell CA (2006) The *Arabidopsis thaliana* vernalization response requires a polycomb-like protein complex that also includes VERNALIZATION INSENSITIVE 3. *Proc Natl Acad Sci U S A* **103:** 14631-14636. doi: 10.1073/pnas.0606385103

Wu Z, Fang X, Zhu D, Dean C (2020) Autonomous pathway: *FLOWERING LOCUS C* repression through an antisense-mediated chromatin-silencing mechanism. *Plant Physiol* **182:** 27-37. doi: 10.1104/pp.19.01009

Xu C, Fang X, Lu T, Dean C (2021a) Antagonistic cotranscriptional regulation through ARGONAUTE1 and the THO/TREX complex orchestrates *FLC* transcriptional output. *Proc Natl Acad Sci U S A* **118**. doi: 10.1073/pnas.2113757118

Xu C, Wu Z, Duan HC, Fang X, Jia G, Dean C (2021b) R-loop resolution promotes co-transcriptional chromatin silencing. *Nat Commun* **12:** 1790. doi: 10.1038/s41467-021-22083-6

Yang H, Berry S, Olsson TSG, Hartley M, Howard M, Dean C (2017) Distinct phases of Polycomb silencing to hold epigenetic memory of cold in *Arabidopsis*. *Science* **357:** 1142-1145. doi: 10.1126/science.aan1121

Yang H, Howard M, Dean C (2014) Antagonistic roles for H3K36me3 and H3K27me3 in the cold-induced epigenetic switch at *Arabidopsis FLC*. *Curr Biol* **24:** 1793-1797. doi: 10.1016/j.cub.2014.06.047

Yoo SD, Cho YH, Sheen J (2007) *Arabidopsis* mesophyll protoplasts: a versatile cell system for transient gene expression analysis. *Nat Protoc* **2:** 1565-1572. doi: 10.1038/nprot.2007.199

Yuan W, Luo X, Li Z, Yang W, Wang Y, Liu R, Du J, He Y (2016) A *cis* cold memory element and a *trans* epigenome reader mediate Polycomb silencing of *FLC* by vernalization in *Arabidopsis*. *Nat Genet* **48:** 1527-1534. doi: 10.1038/ng.3712

Zhao C, Zhang Z, Xie S, Si T, Li Y, Zhu JK (2016) Mutational evidence for the critical role of CBF transcription factors in cold acclimation in Arabidopsis. *Plant Physiol* **171:** 2744-2759. doi: 10.1104/pp.16.00533

Zhao Y, Antoniou-Kourounioti RL, Calder G, Dean C, Howard M (2020) Temperature-dependent growth contributes to long-term cold sensing. *Nature* **583:** 825-829. doi: 10.1038/s41586-020-2485-4

Zhao Y, Zhu P, Hepworth J, Bloomer R, Antoniou-Kourounioti RL, Doughty J, Heckmann A, Xu C, Yang H, Dean C (2021) Natural temperature fluctuations promote *COOLAIR* regulation of *FLC*. *Genes Dev* **35:** 888-898. doi: 10.1101/gad.348362.121

Zhu P, Lister C, Dean C (2021) Cold-induced *Arabidopsis* FRIGIDA nuclear condensates for *FLC* repression. *Nature* **599:** 657-661. doi: 10.1038/s41586-021-04062-5

Appendix

Recent advances in the chromatin-based mechanism of *FLOWERING LOCUS C* repression through autonomous pathway genes

Jinseul Kyung[1,2†], Myeongjune Jeon[1,2†], and Ilha Lee[1,2*]

[1] School of Biological Sciences, Seoul National University, Seoul, Korea

[2] Research Center for Plant Plasticity, Seoul National University, Seoul, Korea

[†] These authors have contributed equally to this work

[*] Correspondence: Ilha Lee, ilhalee@snu.ac.kr

Abstract

Proper timing of flowering, a phase transition from vegetative to reproductive development, is crucial for plant fitness. The floral repressor *FLC* is the major determinant of flowering in *A. thaliana*. In rapid-cycling *A. thaliana* accessions, which bloom rapidly, *FLC* is constitutively repressed by autonomous pathway (AP) genes, regardless of photoperiod. Diverse AP genes have been identified over the past two decades, and most of them repress *FLC* through histone modifications. However, the detailed mechanism underlying such modifications remains unclear. Several recent studies have revealed novel mechanisms to control *FLC* repression in concert with histone modifications. This review summarizes the latest advances in understanding the novel mechanisms by which AP proteins regulate *FLC* repression, including changes in chromatin architecture, RNA polymerase pausing, and liquid–liquid phase separation- and ncRNA-mediated gene silencing. Furthermore, we discuss how each mechanism is coupled with histone modifications in *FLC* chromatin.

This section has been published at **Kyung J, Jeon M, Lee I** (2022) Recent advances in the chromatin-based mechanism of *FLOWERING LOCUS C* repression through autonomous pathway genes. *Front Plant Sci* **13:** 964931.

Introduction

Proper timing of flowering, a phase transition from vegetative to reproductive development, is crucial for plant survival. Consequently, plants have evolved and developed various mechanisms to control flowering time in response to variable environments. Many plants in temperate regions have adopted winter-annual flowering traits that require prolonged cold winter temperatures for flowering in spring when the environment is favorable (Chouard, 1960; Bernier et al., 1993). However, some plants complete their life cycle rapidly, either in spring or fall (Weinig and Schmitt, 2004). For example, *A. thaliana* accessions are classified into winter-annual and rapid-cycling types based on the requirement of long-term winter cold for rapid flowering (Michaels and Amasino, 2000). The underlying genetic difference in flowering traits between the two types is the presence or absence of the *FLC* and *FRI* genes (Gazzani et al., 2003). *FLC,* which encodes a MADS-box transcription factor, acts as a potent floral repressor which inhibits the transcription of floral promoters, including *FT* (encoding florigen) and *SOC1* (Lee et al., 2000; Michaels et al., 2005; Helliwell et al., 2006). FRI, a coiled-coil protein which forms part of a super protein complex, acts as a transcriptional activator of *FLC* (Michaels and Amasino, 1999; Choi et al., 2011; Li et al., 2018).

In rapid cyclers, the autonomous floral-promotion pathway (AP) induces early flowering by repressing *FLC* expression (Koornneef et al., 1998; Levy and Dean, 1998). Since *LUMINIDEPENDENS* (*LD*) was first isolated (Rédei, 1962; Lee et al., 1994), several genes, including *FCA*, *FLD*, *FLK*, *FPA*, *FVE*, and *FY*, have been cloned as AP genes (Macknight et al., 1997; Koornneef et al., 1998; Schomburg et al., 2001; He et al., 2003; Quesada et al., 2003; Simpson et al., 2003; Lim et al., 2004; Mockler et al., 2004). For the past two decades, researchers have investigated the biochemical functions of AP proteins. Reports suggest that a subset of AP proteins catalyze the epigenetic changes in *FLC* chromatin. Specifically, FVE and FLD constitute histone deacetylation or demethylation complexes, whereby the *FLC* chromatin turns into a repressive state (Liu et al., 2007; Yu et al., 2016). Additionally, several RNA-binding family proteins, such as FPA, FCA, and FY, indirectly repress *FLC* by mediating the 3′-end processing of *FLC* antisense transcript (Simpson et al., 2003; Liu et al., 2007; Hornyik et al., 2010; Liu et al., 2010). However, the function of AP proteins has yet to be completely understood.

Emerging evidence suggests that multiple layers of transcriptional processes determine transcript level (Gressel et al., 2019). In addition to well-known processes (*e.g.*, enhancer- and histone modification-mediated gene regulation), regulatory

mechanisms, such as RNA polymerase II (Pol II) pause–release control during transcriptional elongation and alternative polyadenylation during transcriptional termination, are critical gene regulatory processes (Tian and Manley, 2017; Chen et al., 2018). Notably, recent studies have consistently revealed that AP in floral promotion is also involved in such mechanisms. This review summarizes the latest findings on the molecular mechanisms of AP, including the control of chromatin architecture, Pol II pausing, and phase separation with ncRNA-mediated gene silencing.

Architecture of *FLC* chromatin and AP

The 3D property of chromatin plays a vital role in transcriptional regulation (Dileep and Tsai, 2021; Deng et al., 2022). Although histone modifications such as methylation and acetylation have been the main focus of the studies for transcriptional regulation over the past two decades, studies on how chromatin architecture, such as chromatin loops, R-loops, and DNA topology, controls gene expression have been actively conducted in recent years (Kadauke and Blobel, 2009; Kouzine et al., 2014; Al-Hadid and Yang, 2016). Accordingly, the AP-mediated repression of *FLC* has been re-examined based on its chromatin architecture.

Chromatin loops, defined as the intergenic or intragenic bending of chromatin, are observed genome-wide in Arabidopsis (Grob et al., 2013; Feng et al., 2014). The 5′-end region of the *FLC* locus is connected to either the first intron or 3′-end region to form chromatin loops (Crevillén et al., 2013; Kim and Sung, 2017; Li et al., 2018). Importantly, the loop linking the 5′- and 3′-ends of *FLC* may contribute to *FLC* activation, possibly through enhancing Pol II recycling (Crevillén et al., 2013; Li et al., 2018). A recent study has identified novel AP members, the GH1-HMGA family proteins, which are involved in regulating this loop (Zhao et al., 2021a). GH1-HMGA family proteins, also known as HIGH MOBILITY GROUP A4, 5 (HON4, 5), are homologs of human HMGA proteins which bend or unwind local chromatin structure (Ozturk et al., 2014). Similar to other AP mutant lines, the *honq* (*gh1-hmga quadruple*) mutant line exhibits increased *FLC* expression and delayed flowering (Zhao et al., 2021a). Given that the *FLC* gene loop in the *honq* mutant line is increased, it has been suggested that the disruption of gene looping by GH1-HMGA family proteins may repress *FLC* expression by altering chromatin structures required for effective transcription (**Figure 1A**; Zhao et al., 2021a). However, the causal relationship between the chromatin looping and the repression of *FLC* by GH1-HMGA family proteins should be validated in the future study. In contrast to

the GH1-HMGA family proteins, the histone variant H3.3 appears to stabilize *FLC* looping by binding at both ends of *FLC* gene (Zhao et al., 2021b). Importantly, *h3.3* knock-down mutants (*h3.3kd*) consistently show reduced *FLC* looping and decreased *FLC* level (Zhao et al., 2021b). Therefore, it is likely that the opposite effects of GH1-HMGA family proteins and H3.3 for the *FLC* looping may be associated with their antagonistic function on *FLC* expression. BAF60, a component of the Arabidopsis SWI/SNF (SWITCH/SUCROSE NON-FERMNETABLE)-type ATP-dependent chromatin remodeling complex, also participates in *FLC* repression by affecting *FLC* gene looping (Jégu et al., 2014). It has been shown that the RNA interference lines of *BAF60* (*BAF60 RNAi*) display an increased number of *FLC* gene loops and upregulated expression of *FLC,* thereby producing the late-flowering phenotype in long days. This finding suggests that *BAF60* plays a negative role in loop formation. Histone modifications including H3K27me3, H3K9Ac, and H2A.Z replacement, are also altered in the *BAF60 RNAi* lines; thus, the effect of BAF60 on *FLC* gene looping may be mediated through histone modifications. One caveat is that *BAF60* is not a typical AP gene because the *BAF60 RNAi* lines do not show delayed flowering in short days. The increased *FLC* level caused by *BAF60 RNAi* is probably masked by the additional targets of *BAF60*. Therefore, *BAF60* may also be an *FLC* repressor which acts on gene looping. The functional interdependency between GH1-HMGA family proteins and BAF60 needs further analysis.

R-loops are another type of chromatin architecture which are composed of a DNA:RNA hybrid and an associated non-template single-stranded DNA (Al-Hadid and Yang, 2016). R-loops play important roles in gene expression, genome stability, and epigenomic signatures (Gao et al., 2021). *FLC* chromatin has an R-loop around its 3′-end, where the antisense transcript *COOLAIR* is transcribed (Sun et al., 2013; Baxter et al., 2021; Xu et al., 2021b). NODULIN HOMEOBOX (NDX) is a potential AP member that reportedly stabilizes this R-loop by binding onto the non-template ssDNA region (Sun et al., 2013). The increased *COOLAIR* level and the reduction of FCA-*COOLAIR* interaction in the *ndx* mutant suggest that R-loop stabilizing processes likely inhibit further transcription of *COOLAIR* and enhance binding of FCA onto *COOLAIR* (Xu et al., 2021b). The *fca* and *fy* mutants show an increased level of R-loops, suggesting that FCA and its binding partner, FY, act to resolve the R-loops (**Figure 1B**). Thus, R-loop dynamics, involving the stabilization by NDX and resolution by FCA and FY, result in *FLC* repression. However, the detailed mechanism by which R-loops participate in *FLC* transcription warrants further investigation. Furthermore, the loss of m^6A methyltransferase (*mRNA ADENOSINE METHYLASE, MTA*) increases the level of R-loops, indicating that the N^6-

methyladenosine (m^6A) modification of RNA is involved in R-loop resolution (Xu et al., 2021b). MTA interacts with FCA and is a potential AP member, as evidenced by the increased *FLC* expression in the *mta* mutant line. Moreover, a follow-up study showed that the resolution of the R-loop by FCA or FY is required for the proper progression of DNA replication fork, suggesting an interplay between DNA replication and transcription (Baxter et al., 2021).

AP is also possibly involved in regulating DNA topology. During transcription, torsional stress generated by DNA supercoiling inhibits proper transcription (Liu and Wang, 1987). Thus, the proper release of supercoiling by topoisomerases is required for transcriptional activation (French et al., 2011). Consistently, DNA topoisomerase I, TOP1α, in Arabidopsis, which binds to *FLC* chromatin, promotes *FLC* expression (Gong et al., 2017). Thus, the modulation of DNA topology by TOP1α promotes *FLC* transcription, possibly through Pol II accommodation. In contrast, the AP protein, FLD, counteracts TOP1α (Inagaki et al., 2021). FLD acts antagonistically to TOP1α for *FLC* transcription, as evidenced by the partial suppression of the late-flowering phenotype of *fld* in the *top1α fld* double mutant line (Gong et al., 2017). In addition, enhanced Pol II enrichment on the *FLD*-target genes in the *fld* mutant line is suppressed by *top1α* (Inagaki et al., 2021). This result suggests that FLD antagonizes the function of TOP1α and FLD is involved in the control of torsional stress on *FLC* chromatin (**Figure 1C**). However, the detailed function of FLD needs further elucidation.

FLC repression by 3′-pausing of Pol II

During transcription in *Drosophila melanogaster*, or in mammalian cells, Pol II is transiently paused before it enters the elongation phase (Adelman and Lis, 2012; Chen et al., 2018). Controlling Pol II pause–release is possibly a core determinant of gene expression, considering that successful Pol II release into the productive elongation phase is required for the complete transcription (Core and Adelman, 2019). In most animal genes, Pol II pauses after transcribing short stretches (approximately 30–50 nts) of RNA from the TSS. Several pause-inducing factors, including DRB sensitivity-inducing factor (DSIF) and negative elongation factor (NELF), are known to stabilize the paused Pol II (Wu et al., 2003; Wu et al., 2005).

In contrast to animals, plants were thought to have different types of Pol II pausing, because they lack NELF proteins (Hetzel et al., 2016). However, Pol II pausing at the 5′-end is also observed in plants, although Pol II is usually stalled near the transcription termination site (TTS) of plant genes according to the studies using

Global Run-On sequencing (GRO-seq) and plant native elongating transcript sequencing (plaNET-seq) methods (Hetzel et al., 2016; Zhu et al., 2018; Kindgren et al., 2020). *FLC* appears to be one of the 3′-paused genes, as it shows the typical characteristics: it has a relatively long gene length, it expresses antisense RNAs, and it is relatively close to its neighbor gene with the same orientation (Yu et al., 2019; Inagaki et al., 2021).

Emerging evidence suggests that some AP genes act as pause-inducing factors which may govern *FLC* transcription (**Figure 2A**). For example, a recent study has identified novel AP members, called *BORDER* (*BDR*) family genes (Yu et al., 2021). Similar to other AP mutants, the *bdr123* triple mutant shows delayed flowering with elevated expression of *FLC*. In general, BDR proteins localize at the borders of genes close to their neighbor genes (Yu et al., 2019). They are likely to inhibit the progression of Pol II over the gene border, thereby preventing Pol II invasion into the promoters of downstream genes. However, the impediment of Pol II elongation by BDRs may result in decreased transcript accumulation. *FLC* may also be a target of such an inhibitory mechanism; however, further research is warranted for verification. Notably, the popular AP protein, FPA, is located at the borders of genes, especially at TTS (Yu et al., 2021). In addition, FPA physically interacts with BDR proteins and shares common targets. Therefore, it would be valuable to address whether FPA also promotes 3′ Pol II pausing in a similar manner to BDR, especially around the *FLC* locus. In addition, there is still uncertainty around whether 3′ Pol II pausing causes *FLC* gene silencing.

FLD, another major AP component, reportedly modulates Pol II pause–release (Inagaki et al., 2021). FLD is enriched at the TSS and TTS of genes rather than their gene body. Pol II is stalled around the TTS of FLD-targeted genes, and such 3′ Pol II pausing is conspicuously reduced in the *fld* mutant, indicating that FLD accelerates Pol II pausing. Since FLD occupies the 3′-end regions of *FLC* (Inagaki et al., 2021), *FLC* transcription is potentially repressed by FLD-promoted 3′ Pol II pausing. The physical interaction between FLD and LD proteins and similar transcriptome profiles between the *fld* and *ld* mutants suggest that FLD and LD cooperatively regulate the transcription (Fang et al., 2020; Inagaki et al., 2021). While the genome-wide function of FLD on 3′ Pol II pausing has been addressed (Inagaki et al., 2021), whether FLD also triggers 3′ Pol II pausing on the *FLC* locus is yet to be confirmed.

Accumulating evidence from studies using metazoans suggests an interplay between Pol II pausing and chromatin landscape. For instance, a rapid release of Pol II facilitates a broad distribution of active histone marks over the gene body, which

is tightly linked with the high expression of the gene (Chen et al., 2015; Tettey et al., 2019). In contrast, Polycomb-group (PcG) proteins that catalyze the deposition of repressive histone marks preferentially target paused promoters (Enderle et al., 2011). Similarly, AP-mediated 3′-pausing at *FLC* may switch the *FLC* chromatin state inactive, thus suppressing *FLC* transcription. Consistent with this idea, 3′ Pol II pausing events triggered by the BDRs and FPA are correlated with the removal of H3K4me3 and the deposition of H3K27me3 (Yu et al., 2021). Furthermore, FLD and LD are likely to remove H3K4me1 from the gene bodies of their targets, suggesting that the AP proteins coordinate transcriptional events with chromatin silencing (Fang et al., 2020; Inagaki et al., 2021). Future research should explore the mechanism by which Pol II pause–release is linked to histone modifications for *FLC* suppression.

Phase-separated AP proteins- and noncoding RNA-mediated gene silencing

ncRNAs are RNAs that are not translated into proteins. They function in transcriptional or post-transcriptional gene regulation, structural organization of nuclear bodies, and genome integrity control (Ponting et al., 2009; Statello et al., 2021). The *FLC* locus also produces multiple long noncoding RNAs, such as *COOLAIR*, *COLDAIR*, and *COLDWRAP* (Swiezewski et al., 2009; Heo and Sung, 2011; Kim and Sung, 2017), all of which reportedly control dynamic alterations of chromatin state in the *FLC* locus after long-term cold exposure (Csorba et al., 2014; Kim and Sung, 2017; Kim et al., 2017; Zhao et al., 2021c). Among these RNAs, *COOLAIR*, an antisense transcript produced from the 3′-end of *FLC,* has been proposed to play a role in the epigenetic control of *FLC* with the help of AP proteins (Whittaker and Dean, 2017; Wu et al., 2020).

Multiple studies suggest that several AP genes, especially those encoding RNA-processing factors, control the 3′-end processing of *COOLAIR* (Hornyik et al., 2010; Liu et al., 2010; Marquardt et al., 2014; Wang et al., 2014). Some RNA-processing factors, such as a core spliceosome subunit (PRE-MRNA PROCESSING 8 [PRP8]) and a transcriptional elongation factor (CYCLIN-DEPENDENT KINASE C;2 [CDKC;2]), have been identified as AP members (Marquardt et al., 2014; Wang et al., 2014). The functions of *PRP8* and *CDKC;2* in *FLC* repression are dependent on *COOLAIR*; *prp8* or *cdkc;2* does not upregulate *FLC* expression any further if the *COOLAIR* promoter is replaced with *rbcs3B* terminator sequence (*FLC-TEX* in Marquardt et al., 2014 and Wang et al., 2014). Consistent with this, previous studies reported that PRP8 and CDKC;2 indirectly affect the expression of *FLC* by

promoting the proximal polyadenylation of *COOLAIR* (Marquardt et al., 2014; Wang et al., 2014). The major AP genes, *FCA*, *FPA,* and *FY,* have also been proposed to control the processing of *COOLAIR.* FCA, FPA, and FY reportedly favor the usage of proximal poly(A) site in *COOLAIR* (Liu et al., 2010). Considering the epistatic interactions between *fca*, and *prp8* or *cdkc;2*, *FCA,* and *PRP8* or *CDKC;2* are thought to share the same genetic pathway to antagonize *FLC* expression (Marquardt et al., 2014; Wang et al., 2014).

Such *COOLAIR*-processing machinery is likely to be condensed into phase-separated nuclear bodies, and this process may be a mechanism behind *FLC* repression. FCA is clustered into nuclear condensates together with FPA, FY, and the subunits of polyadenylation machinery, including cleavage and polyadenylation factor 30 (CPSF30), CPSF100, and FH INTERACTING PROTEIN 1 (FIP1) (Fang et al., 2019). FCA is required for the condensation of the polyadenylation machinery and directly associates with *COOLAIR* transcripts; thus, it likely concentrates the polyadenylation machinery near the *COOLAIR* to promote the usage of the proximal poly(A) site (Fang et al., 2019; Tian et al., 2019; Xu et al., 2021b). This condensation is enhanced by the prion-like domain (PrLD)-containing protein FLX-LIKE 2 (FLL2), RNA slicer ARGONAUTE 1 (AGO1), and m^6A writer complex depositing m^6A onto *COOLAIR* (Fang et al., 2019; Xu et al., 2021a; Xu et al., 2021b).

The phase-separated *COOLAIR*-processing complex likely controls the *FLC* chromatin state through FLD. FLD assembles into a complex with LD and SET DOMAIN GROUP 26 (SDG26), which causes the removal of H3K4me1 deposited at *FLC* chromatin (Fang et al., 2020). This disables SDG8, which binds to H3K4me1 and facilitates the enrichment of H3K36me3, thereby suppressing *FLC* transcription (Fang et al., 2020). Recent results obtained using cross-linked nuclear immunoprecipitation and mass spectrometry (CLNIP-MS) suggest that a transient and dynamic interaction occurs between SDG26 and the components of the phase-separated poly(A) machinery, such as FCA, FPA, and FY (**Figure 2B**; Fang et al., 2019; Fang et al., 2020). In addition, AGO1, which is bound to *COOLAIR* at a proximal exon-intron junction region, also interacts with SDG26 (Xu et al., 2021a). Therefore, the *COOLAIR* 3′-processing event likely controls the *FLC* chromatin state through the physical interaction between components of the *COOLAIR* polyadenylation condensate and the FLD/LD/SDG26 protein complex. Moreover, this phase-separated polyadenylation complex, including FCA and FY, may resolve the *COOLAIR*-mediated R-loop at the 3′-end of *FLC* (Xu et al., 2021a; Xu et al., 2021b), as mentioned earlier. Given that this R-loop is also closely connected to the histone modifications in other organisms (Chédin, 2016), this connection may be a

missing link between co-transcriptional *COOLAIR* processing and *FLC* chromatin silencing. However, the causal relationship between *COOLAIR*-mediated R-loop processing and *FLC* chromatin silencing needs further verification (Xu et al., 2021b).

Recent studies have inferred that another clade of ncRNAs, small RNAs (sRNAs), could be associated with *FLC* repression. For example, AGO1 interacts with sRNA fragments that are complementary to *COOLAIR* (Xu et al., 2021a). Moreover, DICER-LIKE 1 (DCL1) and DCL3, required for sRNA production, are likely to suppress *FLC* independently of the FCA-mediated *FLC* silencing mechanism (Schmitz et al., 2007; Xu et al., 2021a).

Conclusion

This review summarizes the latest research progress in the autonomous pathway in Arabidopsis. Decades of studies have proposed unique mechanisms for *FLC* regulation, such as control of Pol II pause–release mechanism, modulation of chromatin architecture, and processing of ncRNA triggered by phase-separated machinery. The studies on such mechanisms are still in their infancy and heavily dependent on genome-wide transcriptome analyses. Thus, a large portion of the current models presented in this review has yet to be validated. Further verification of the proposed mechanisms through biochemical, genetic, and molecular work would be valuable to develop a better understanding of AP. In addition, this pathway has been closely linked with the epigenetic modification of *FLC* chromatin, particularly in relation to the changes in histone methylation patterns in the AP mutants. However, the detailed mechanism connecting the regulatory function of AP proteins described in this review and the epigenetic silencing of *FLC* remain largely unknown; thus, further studies are required.

The FRI complex strongly activates *FLC* expression even in the presence of AP proteins in winter-annual Arabidopsis (Johanson et al., 2000; Choi et al., 2011). This finding suggests that the *FLC* regulatory mechanisms of AP genes are counteracted by FRI complex. Therefore, there is a need for further studies elucidating the role of the FRI complex in the mechanisms of AP.

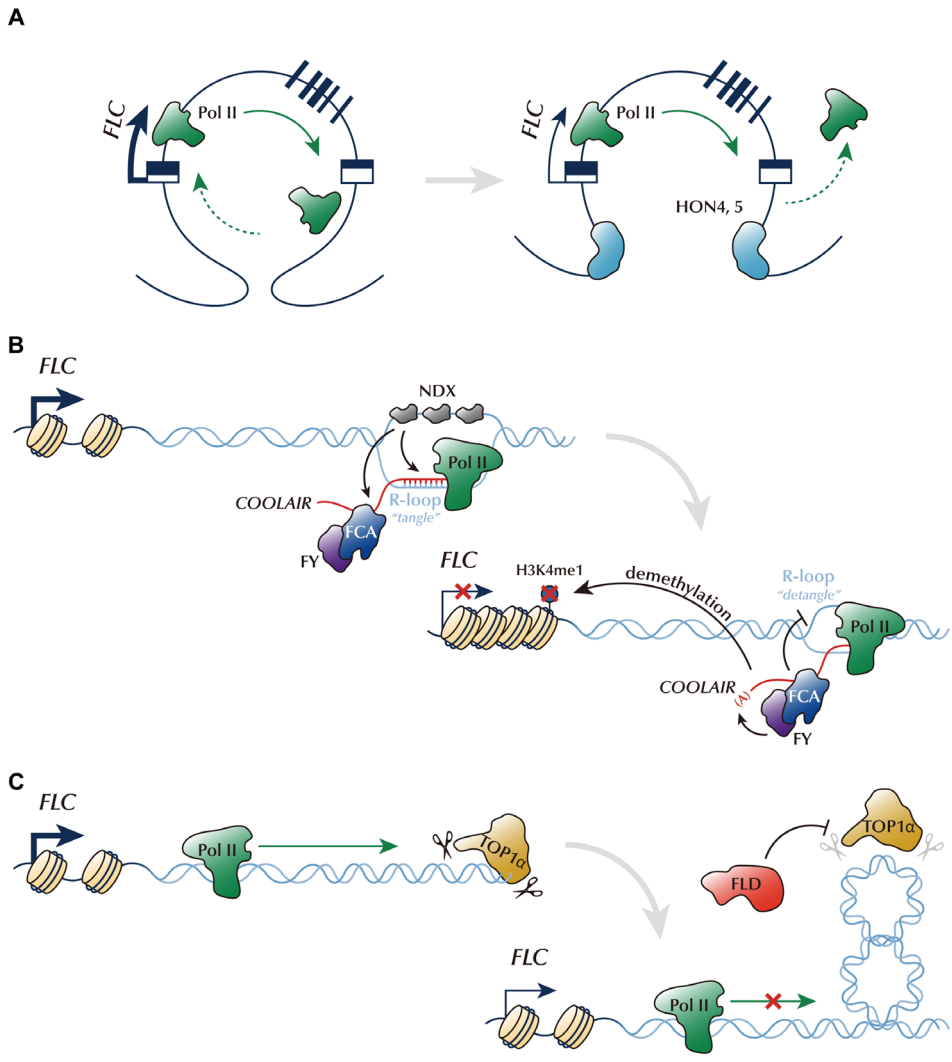

Figure 1. Control of *FLC* chromatin architecture by the autonomous pathway.
(A) Chromatin loop linking the 5′- and 3′-ends of *FLC* will likely intensify the *FLC* transcription by promoting Pol II recycling. GH1-HMGA family proteins, HON4 and HON5, disrupt this chromatin looping, and thus reduce *FLC* expression.
(B) NDX stabilizes the R-loop at the *FLC* 3′-end, where the antisense ncRNA, *COOLAIR*, is transcribed (tangled). This process probably enhances the binding of FCA/FY onto *COOLAIR* and inhibits Pol II progression. FCA/FY, in turn, represses *FLC* expression by promoting the proximal polyadenylation of *COOLAIR* and resolving the R-loop (detangled).

(C) Antagonized function of TOP1α and FLD controlling DNA topology. TOP1α enhances *FLC* transcription potentially by reducing the torsional stress generated by DNA supercoiling. FLD partially counteracts TOP1α activity.

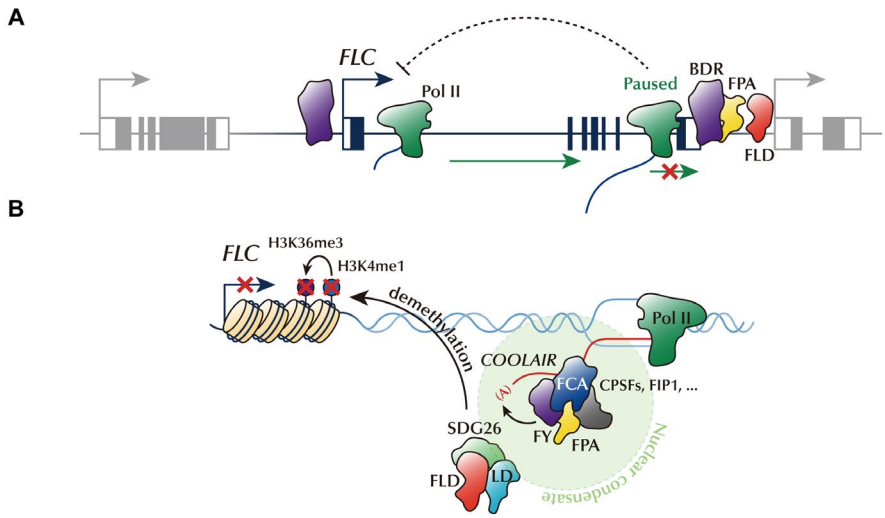

Figure 2. *FLC* repression by 3′-pausing, phase-separated AP proteins, and ncRNA.

(A) AP proteins, BDR, FPA, and FLD, localizing at the gene borders, trigger 3' Pol II pausing. Impediment of Pol II release into the elongation phase may reduce *FLC* transcript accumulation.

(B) AP proteins, including FCA, FPA, FY, and RNA-processing factors, are condensed into phase-separated nuclear condensates to promote the proximal polyadenylation of *COOLAIR*. This phase-separated ncRNA-processing machinery transiently interacts with FLD/LD/SDG26, H3K4me1 demethylase complex, thereby removing the active histone marks (H3K4me1 and H3K36me3) from *FLC* chromatin.

References

Adelman K, Lis JT (2012) Promoter-proximal pausing of RNA polymerase II: emerging roles in metazoans. *Nat Rev Genet* **13:** 720-731. doi: 10.1038/nrg3293

Al-Hadid Q, Yang Y (2016) R-loop: an emerging regulator of chromatin dynamics. *Acta Biochim Biophys Sin (Shanghai)* **48:** 623-631. doi: 10.1093/abbs/gmw052

Baxter CL, Šviković S, Sale JE, Dean C, Costa S (2021) The intersection of DNA replication with antisense 3' RNA processing in *Arabidopsis FLC* chromatin silencing. *Proc Natl Acad Sci U S A* **118**. doi: 10.1073/pnas.2107483118

Bernier G, Havelange A, Houssa C, Petitjean A, Lejeune P (1993) Physiological signals that induce flowering. *Plant Cell* **5:** 1147-1155. doi: 10.1105/tpc.5.10.1147

Chédin F (2016) Nascent connections: R-Loops and chromatin patterning. *Trends Genet* **32:** 828-838. doi: 10.1016/j.tig.2016.10.002

Chen FX, Smith ER, Shilatifard A (2018) Born to run: control of transcription elongation by RNA polymerase II. *Nat Rev Mol Cell Biol* **19:** 464-478. doi: 10.1038/s41580-018-0010-5

Chen K, Chen Z, Wu D, Zhang L, Lin X, Su J, Rodriguez B, Xi Y, Xia Z, Chen X, Shi X, Wang Q, Li W (2015) Broad H3K4me3 is associated with increased transcription elongation and enhancer activity at tumor-suppressor genes. *Nat Genet* **47:** 1149-1157. doi: 10.1038/ng.3385

Choi K, Kim J, Hwang HJ, Kim S, Park C, Kim SY, Lee I (2011) The FRIGIDA complex activates transcription of *FLC*, a strong flowering repressor in *Arabidopsis*, by recruiting chromatin modification factors. *Plant Cell* **23:** 289-303. doi: 10.1105/tpc.110.075911

Chouard P (1960) Vernalization and its relations to dormancy. *Annu Rev Plant Phys* **11:** 191-238. doi: 10.1146/annurev.pp.11.060160.001203

Core L, Adelman K (2019) Promoter-proximal pausing of RNA polymerase II: a nexus of gene regulation. *Genes Dev* **33:** 960-982. doi: 10.1101/gad.325142.119

Crevillén P, Sonmez C, Wu Z, Dean C (2013) A gene loop containing the floral repressor *FLC* is disrupted in the early phase of vernalization. *EMBO J* **32:** 140-148. doi: 10.1038/emboj.2012.324

Csorba T, Questa JI, Sun Q, Dean C (2014) Antisense *COOLAIR* mediates the coordinated switching of chromatin states at *FLC* during vernalization. *Proc*

Natl Acad Sci U S A **111:** 16160-16165. doi: 10.1073/pnas.1419030111

Deng S, Feng Y, Pauklin S (2022) 3D chromatin architecture and transcription regulation in cancer. *J Hematol Oncol* **15:** 49. doi: 10.1186/s13045-022-01271-x

Dileep V, Tsai LH (2021) Three-dimensional chromatin organization in brain function and dysfunction. *Curr Opin Neurobiol* **69:** 214-221. doi: 10.1016/j.conb.2021.04.006

Enderle D, Beisel C, Stadler MB, Gerstung M, Athri P, Paro R (2011) Polycomb preferentially targets stalled promoters of coding and noncoding transcripts. *Genome Res* **21:** 216-226. doi: 10.1101/gr.114348.110

Fang X, Wang L, Ishikawa R, Li Y, Fiedler M, Liu F, Calder G, Rowan B, Weigel D, Li P, Dean C (2019) *Arabidopsis* FLL2 promotes liquid-liquid phase separation of polyadenylation complexes. *Nature* **569:** 265-269. doi: 10.1038/s41586-019-1165-8

Fang X, Wu Z, Raitskin O, Webb K, Voigt P, Lu T, Howard M, Dean C (2020) The 3' processing of antisense RNAs physically links to chromatin-based transcriptional control. *Proc Natl Acad Sci U S A* **117:** 15316-15321. doi: 10.1073/pnas.2007268117

Feng S, Cokus SJ, Schubert V, Zhai J, Pellegrini M, Jacobsen SE (2014) Genome-wide Hi-C analyses in wild-type and mutants reveal high-resolution chromatin interactions in *Arabidopsis*. *Mol Cell* **55:** 694-707. doi: 10.1016/j.molcel.2014.07.008

French SL, Sikes ML, Hontz RD, Osheim YN, Lambert TE, El Hage A, Smith MM, Tollervey D, Smith JS, Beyer AL (2011) Distinguishing the roles of Topoisomerases I and II in relief of transcription-induced torsional stress in yeast rRNA genes. *Mol Cell Biol* **31:** 482-494. doi: 10.1128/MCB.00589-10

Gao J, Zhang P, Li X, Wu W, Wei H, Zhang W (2021) Toward an understanding of the detection and function of R-loops in plants. *J Exp Bot* **72:** 6110-6122. doi: 10.1093/jxb/erab280

Gazzani S, Gendall AR, Lister C, Dean C (2003) Analysis of the molecular basis of flowering time variation in Arabidopsis accessions. *Plant Physiol* **132:** 1107-1114. doi: 10.1104/pp.103.021212

Gong X, Shen L, Peng YZ, Gan Y, Yu H (2017) DNA Topoisomerase Iα affects the floral transition. *Plant Physiol* **173:** 642-654. doi: 10.1104/pp.16.01603

Gressel S, Schwalb B, Cramer P (2019) The pause-initiation limit restricts transcription activation in human cells. *Nat Commun* **10:** 3603. doi: 10.1038/s41467-019-11536-8

Grob S, Schmid MW, Luedtke NW, Wicker T, Grossniklaus U (2013) Characterization of chromosomal architecture in *Arabidopsis* by chromosome conformation capture. *Genome Biol* **14:** R129. doi: 10.1186/gb-2013-14-11-r129

He Y, Michaels SD, Amasino RM (2003) Regulation of flowering time by histone acetylation in *Arabidopsis*. *Science* **302:** 1751-1754. doi: 10.1126/science.1091109

Helliwell CA, Wood CC, Robertson M, James Peacock W, Dennis ES (2006) The Arabidopsis FLC protein interacts directly *in vivo* with *SOC1* and *FT* chromatin and is part of a high-molecular-weight protein complex. *Plant J* **46:** 183-192. doi: 10.1111/j.1365-313X.2006.02686.x

Heo JB, Sung S (2011) Vernalization-mediated epigenetic silencing by a long intronic noncoding RNA. *Science* **331:** 76-79. doi: 10.1126/science.1197349

Hetzel J, Duttke SH, Benner C, Chory J (2016) Nascent RNA sequencing reveals distinct features in plant transcription. *Proc Natl Acad Sci U S A* **113:** 12316-12321. doi: 10.1073/pnas.1603217113

Hornyik C, Terzi LC, Simpson GG (2010) The spen family protein FPA controls alternative cleavage and polyadenylation of RNA. *Dev Cell* **18:** 203-213. doi: 10.1016/j.devcel.2009.12.009

Inagaki S, Takahashi M, Takashima K, Oya S, Kakutani T (2021) Chromatin-based mechanisms to coordinate convergent overlapping transcription. *Nat Plants* **7:** 295-302. doi: 10.1038/s41477-021-00868-3

Jégu T, Latrasse D, Delarue M, Hirt H, Domenichini S, Ariel F, Crespi M, Bergounioux C, Raynaud C, Benhamed M (2014) The BAF60 subunit of the SWI/SNF chromatin-remodeling complex directly controls the formation of a gene loop at *FLOWERING LOCUS C* in *Arabidopsis*. *Plant Cell* **26:** 538-551. doi: 10.1105/tpc.113.114454

Johanson U, West J, Lister C, Michaels S, Amasino R, Dean C (2000) Molecular analysis of *FRIGIDA*, a major determinant of natural variation in *Arabidopsis* flowering time. *Science* **290:** 344-347. doi: 10.1126/science.290.5490.344

Kadauke S, Blobel GA (2009) Chromatin loops in gene regulation. *Biochim Biophys Acta* **1789:** 17-25. doi: 10.1016/j.bbagrm.2008.07.002

Kim DH, Sung S (2017) Vernalization-triggered intragenic chromatin loop formation by long noncoding RNAs. *Dev Cell* **40:** 302-312 e304. doi: 10.1016/j.devcel.2016.12.021

Kim DH, Xi Y, Sung S (2017) Modular function of long noncoding RNA,

COLDAIR, in the vernalization response. *PLoS Genet* **13:** e1006939. doi: 10.1371/journal.pgen.1006939

Kindgren P, Ivanov M, Marquardt S (2020) Native elongation transcript sequencing reveals temperature dependent dynamics of nascent RNAPII transcription in *Arabidopsis*. *Nucleic Acids Res* **48:** 2332-2347. doi: 10.1093/nar/gkz1189

Koornneef M, Alonso-Blanco C, Peeters AJ, Soppe W (1998) Genetic control of flowering time in Arabidopsis. *Annu Rev Plant Physiol Plant Mol Biol* **49:** 345-370. doi: 10.1146/annurev.arplant.49.1.345

Kouzine F, Levens D, Baranello L (2014) DNA topology and transcription. *Nucleus* **5:** 195-202. doi: 10.4161/nucl.28909

Lee H, Suh SS, Park E, Cho E, Ahn JH, Kim SG, Lee JS, Kwon YM, Lee I (2000) The AGAMOUS-LIKE 20 MADS domain protein integrates floral inductive pathways in *Arabidopsis*. *Genes Dev* **14:** 2366-2376. doi: 10.1101/gad.813600

Lee I, Aukerman MJ, Gore SL, Lohman KN, Michaels SD, Weaver LM, John MC, Feldmann KA, Amasino RM (1994) Isolation of *LUMINIDEPENDENS*: a gene involved in the control of flowering time in Arabidopsis. *Plant Cell* **6:** 75-83. doi: 10.1105/tpc.6.1.75

Levy YY, Dean C (1998) The transition to flowering. *Plant Cell* **10:** 1973-1990. doi: 10.1105/tpc.10.12.1973

Li Z, Jiang D, He Y (2018) FRIGIDA establishes a local chromosomal environment for *FLOWERING LOCUS C* mRNA production. *Nat Plants* **4:** 836-846. doi: 10.1038/s41477-018-0250-6

Lim MH, Kim J, Kim YS, Chung KS, Seo YH, Lee I, Kim J, Hong CB, Kim HJ, Park CM (2004) A new Arabidopsis gene, *FLK*, encodes an RNA binding protein with K homology motifs and regulates flowering time via *FLOWERING LOCUS C*. *Plant Cell* **16:** 731-740. doi: 10.1105/tpc.019331

Liu F, Marquardt S, Lister C, Swiezewski S, Dean C (2010) Targeted 3' processing of antisense transcripts triggers *Arabidopsis FLC* chromatin silencing. *Science* **327:** 94-97. doi: 10.1126/science.1180278

Liu F, Quesada V, Crevillén P, Bäurle I, Swiezewski S, Dean C (2007) The *Arabidopsis* RNA-binding protein FCA requires a lysine-specific demethylase 1 homolog to downregulate *FLC*. *Mol Cell* **28:** 398-407. doi: 10.1016/j.molcel.2007.10.018

Liu LF, Wang JC (1987) Supercoiling of the DNA template during transcription. *Proc Natl Acad Sci U S A* **84:** 7024-7027. doi: 10.1073/pnas.84.20.7024

Macknight R, Bancroft I, Page T, Lister C, Schmidt R, Love K, Westphal L, Murphy G, Sherson S, Cobbett C, Dean C (1997) *FCA*, a gene controlling flowering time in Arabidopsis, encodes a protein containing RNA-binding domains. *Cell* **89:** 737-745. doi: 10.1016/s0092-8674(00)80256-1

Marquardt S, Raitskin O, Wu Z, Liu F, Sun Q, Dean C (2014) Functional consequences of splicing of the antisense transcript *COOLAIR* on *FLC* transcription. *Mol Cell* **54:** 156-165. doi: 10.1016/j.molcel.2014.03.026

Michaels SD, Amasino RM (1999) *FLOWERING LOCUS C* encodes a novel MADS domain protein that acts as a repressor of flowering. *Plant Cell* **11:** 949-956. doi: 10.1105/tpc.11.5.949

Michaels SD, Amasino RM (2000) Memories of winter: Vernalization and the competence to flower. *Plant Cell Environ* **23:** 1145-1153. doi: 10.1046/j.1365-3040.2000.00643.x

Michaels SD, Himelblau E, Kim SY, Schomburg FM, Amasino RM (2005) Integration of flowering signals in winter-annual Arabidopsis. *Plant Physiol* **137:** 149-156. doi: 10.1104/pp.104.052811

Mockler TC, Yu X, Shalitin D, Parikh D, Michael TP, Liou J, Huang J, Smith Z, Alonso JM, Ecker JR, Chory J, Lin C (2004) Regulation of flowering time in *Arabidopsis* by K homology domain proteins. *Proc Natl Acad Sci U S A* **101:** 12759-12764. doi: 10.1073/pnas.0404552101

Ozturk N, Singh I, Mehta A, Braun T, Barreto G (2014) HMGA proteins as modulators of chromatin structure during transcriptional activation. *Front Cell Dev Biol* **2:** 5. doi: 10.3389/fcell.2014.00005

Ponting CP, Oliver PL, Reik W (2009) Evolution and functions of long noncoding RNAs. *Cell* **136:** 629-641. doi: 10.1016/j.cell.2009.02.006

Quesada V, Macknight R, Dean C, Simpson GG (2003) Autoregulation of *FCA* pre-mRNA processing controls *Arabidopsis* flowering time. *EMBO J* **22:** 3142-3152. doi: 10.1093/emboj/cdg305

Rédei GP (1962) Supervital mutants of Arabidopsis. *Genetics* **47:** 443-460. doi: 10.1093/genetics/47.4.443

Schmitz RJ, Hong L, Fitzpatrick KE, Amasino RM (2007) *DICER-LIKE 1* and *DICER-LIKE 3* redundantly act to promote flowering via repression of *FLOWERING LOCUS C* in *Arabidopsis thaliana*. *Genetics* **176:** 1359-1362. doi: 10.1534/genetics.107.070649

Schomburg FM, Patton DA, Meinke DW, Amasino RM (2001) *FPA*, a gene involved in floral induction in Arabidopsis, encodes a protein containing RNA-recognition motifs. *Plant Cell* **13:** 1427-1436. doi:

10.1105/tpc.13.6.1427

Simpson GG, Dijkwel PP, Quesada V, Henderson I, Dean C (2003) FY is an RNA 3' end-processing factor that interacts with FCA to control the *Arabidopsis* floral transition. *Cell* **113:** 777-787. doi: 10.1016/s0092-8674(03)00425-2

Statello L, Guo CJ, Chen LL, Huarte M (2021) Gene regulation by long non-coding RNAs and its biological functions. *Nat Rev Mol Cell Biol* **22:** 96-118. doi: 10.1038/s41580-020-00315-9

Sun Q, Csorba T, Skourti-Stathaki K, Proudfoot NJ, Dean C (2013) R-loop stabilization represses antisense transcription at the *Arabidopsis FLC* locus. *Science* **340:** 619-621. doi: 10.1126/science.1234848

Swiezewski S, Liu F, Magusin A, Dean C (2009) Cold-induced silencing by long antisense transcripts of an *Arabidopsis* Polycomb target. *Nature* **462:** 799-802. doi: 10.1038/nature08618

Tettey TT, Gao X, Shao W, Li H, Story BA, Chitsazan AD, Glaser RL, Goode ZH, Seidel CW, Conaway RC, Zeitlinger J, Blanchette M, Conaway JW (2019) A role for FACT in RNA Polymerase II promoter-proximal pausing. *Cell Rep* **27:** 3770-3779 e3777. doi: 10.1016/j.celrep.2019.05.099

Tian B, Manley JL (2017) Alternative polyadenylation of mRNA precursors. *Nat Rev Mol Cell Biol* **18:** 18-30. doi: 10.1038/nrm.2016.116

Tian Y, Zheng H, Zhang F, Wang S, Ji X, Xu C, He Y, Ding Y (2019) PRC2 recruitment and H3K27me3 deposition at *FLC* require FCA binding of *COOLAIR*. *Sci Adv* **5:** eaau7246. doi: 10.1126/sciadv.aau7246

Wang ZW, Wu Z, Raitskin O, Sun Q, Dean C (2014) Antisense-mediated *FLC* transcriptional repression requires the P-TEFb transcription elongation factor. *Proc Natl Acad Sci U S A* **111:** 7468-7473. doi: 10.1073/pnas.1406635111

Weinig C, Schmitt J (2004) Environmental effects on the expression of quantitative trait loci and implications for phenotypic evolution. *Bioscience* **54:** 627-635. doi: 10.1641/0006-3568(2004)054[0627:EEOTEO]2.0.CO;2

Whittaker C, Dean C (2017) The *FLC* locus: a platform for discoveries in epigenetics and adaptation. *Annu Rev Cell Dev Biol* **33:** 555-575. doi: 10.1146/annurev-cellbio-100616-060546

Wu CH, Lee C, Fan R, Smith MJ, Yamaguchi Y, Handa H, Gilmour DS (2005) Molecular characterization of *Drosophila* NELF. *Nucleic Acids Res* **33:** 1269-1279. doi: 10.1093/nar/gki274

Wu CH, Yamaguchi Y, Benjamin LR, Horvat-Gordon M, Washinsky J, Enerly E, Larsson J, Lambertsson A, Handa H, Gilmour D (2003) NELF and

DSIF cause promoter proximal pausing on the *hsp70* promoter in *Drosophila*. *Genes Dev* **17:** 1402-1414. doi: 10.1101/gad.1091403

Wu Z, Fang X, Zhu D, Dean C (2020) Autonomous pathway: *FLOWERING LOCUS C* repression through an antisense-mediated chromatin-silencing mechanism. *Plant Physiol* **182:** 27-37. doi: 10.1104/pp.19.01009

Xu C, Fang X, Lu T, Dean C (2021a) Antagonistic cotranscriptional regulation through ARGONAUTE1 and the THO/TREX complex orchestrates *FLC* transcriptional output. *Proc Natl Acad Sci U S A* **118**. doi: 10.1073/pnas.2113757118

Xu C, Wu Z, Duan HC, Fang X, Jia G, Dean C (2021b) R-loop resolution promotes co-transcriptional chromatin silencing. *Nat Commun* **12:** 1790. doi: 10.1038/s41467-021-22083-6

Yu CW, Chang KY, Wu K (2016) Genome-wide analysis of gene regulatory networks of the FVE-HDA6-FLD complex in *Arabidopsis*. *Front Plant Sci* **7:** 555. doi: 10.3389/fpls.2016.00555

Yu X, Martin PGP, Michaels SD (2019) BORDER proteins protect expression of neighboring genes by promoting 3' Pol II pausing in plants. *Nat Commun* **10:** 4359. doi: 10.1038/s41467-019-12328-w

Yu X, Martin PGP, Zhang Y, Trinidad JC, Xu F, Huang J, Thum KE, Li K, Zhao S, Gu Y, Wang X, Michaels SD (2021) The BORDER family of negative transcription elongation factors regulates flowering time in *Arabidopsis*. *Curr Biol* **31:** 5377-5384 e5375. doi: 10.1016/j.cub.2021.09.074

Zhao B, Xi Y, Kim J, Sung S (2021a) Chromatin architectural proteins regulate flowering time by precluding gene looping. *Sci Adv* **7**. doi: 10.1126/sciadv.abg3097

Zhao F, Zhang H, Zhao T, Li Z, Jiang D (2021b) The histone variant H3.3 promotes the active chromatin state to repress flowering in Arabidopsis. *Plant Physiol* **186:** 2051-2063. doi: 10.1093/plphys/kiab224

Zhao Y, Zhu P, Hepworth J, Bloomer R, Antoniou-Kourounioti RL, Doughty J, Heckmann A, Xu C, Yang H, Dean C (2021c) Natural temperature fluctuations promote *COOLAIR* regulation of *FLC*. *Genes Dev* **35:** 888-898. doi: 10.1101/gad.348362.121

Zhu J, Liu M, Liu X, Dong Z (2018) RNA polymerase II activity revealed by GRO-seq and pNET-seq in *Arabidopsis*. *Nat Plants* **4:** 1112-1123. doi: 10.1038/s41477-018-0280-0

Abstract in Korean

국문초록

온대 기후 지역에 서식하는 식물로서는 기후가 온화할 뿐 아니라 수분매개자들이 활발히 활동하는 봄에 한꺼번에 개화하는 것이 생식에 유리하다. 이 때문에 이 지역 식물종 중 다수는 겨우내 장기간 지속되는 저온에 감응하여 개화가 유도되는 춘화 현상을 겪는다. 모델식물인 애기장대에서는 개화 억제 유전자인 *FLOWERING LOCUS C* (*FLC*)가 후성유전학적으로 저해됨에 따라 춘화 현상이 일어난다. 장기간 지속되는 저온 환경에 의해 발현이 증가하는 인자들이 이 과정을 매개하는 것으로 알려져 있는데, *FLC* 좌위에서 발현하는 역배열 RNA인 *COOLAIR*가 대표적 예다. *COOLAIR*의 생화학적 기능은 비교적 상세히 규명되었지만 이들 발현이 어떻게 장기 저온 환경에 의해 유도되는지는 잘 알려져 있지 않다. 이에 본 연구에서는 *COOLAIR* 발현이 장기 저온 환경에 의해 유도될 수 있게끔 하는 데 필수적인 cis-regulatory element를 발굴하고, 이를 통해 *COOLAIR* 발현이 활성화되는 기전을 밝히는 데 주안점을 두었다.

COOLAIR 프로모터 부위에 해당하는 *FLC* 3′ 말단 구역에 진화적으로 보존된 C-repeat (CRT)/dehydration-responsive element (DRE)가 존재함을 확인하였다. 저온 내성 매개 단백질인 CRT/DRE-BINDING FACTOR 3 (CBF3)는 식물 체외, 체내 모두에서 *FLC* 3′ 말단 구역의 CRT/DRE에 결합했다. 세 종류의 CBF 단백질들이 모두 무력화된 *cbfs* 돌연변이체에서는 장기 저온 환경에도 불구, *COOLAIR* 발현이 정상적으로 유도되지 않는 반면, *CBF3* 과발현체는 상온에서도 높은 *COOLAIR* 발현량을 보였다. 이로 미루어 볼 때 CBF 단백질이 춘화 현상 동안 *COOLAIR*의 발현을

활성화시키는 인자임을 알 수 있었다. 장기 저온 환경에 노출되었을 때 CBF 메신저 RNA 와 단백질 양이 모두 점진적으로 증가한다는 사실을 감안하면 CBF 양 증가가 *COOLAIR* 발현 유도로 이어짐을 추론할 수 있다. 반면, 저온 환경이 더 오래 지속되면 CBF3 단백질이 *COOLAIR* 프로모터 부위로부터 분리되는데, 이 때문에 춘화 현상 말엽 *COOLAIR* 발현이 다시 감소하는 것으로 사료된다. *cbfs* 돌연변이체와, CRT/DRE 를 포함하는 *COOLAIR* 프로모터 구역이 결실된 $FLC_{\Delta COOLAIR}$ 돌연변이체에서는 *COOLAIR* 발현이 장기 저온 환경에 의해 활성화되지 못함에도 불구하고 *FLC* 의 후성유전학적 저해와 개화 유도가 야생형 식물과 다를 바 없이 일어났다. 이는 *COOLAIR* 가 춘화현상에 필수적인 인자는 아님을 시사한다.

결국, 본 연구는 지금까지 충분히 규명되지 않은, 춘화현상 동안의 장기 저온 신호 전달 경로를 새롭게 밝혔다는 점에서 그 의의가 크다. 이뿐 아니라 지금껏 논쟁의 대상이었던, 후성유전학적 *FLC* 저해 과정에서의 *COOLAIR* 의 기능과 관련해 신뢰성이 높으면서도 단순명료한 반박 증거를 새로이 제시했다.

주요어: 애기장대, 개화, 춘화현상, *COOLAIR*, *CBF*, *FLC*

학번: 2015-20445